Designing an In-Vitro Model of Uterine Myometrium to Study Intramural Uterine Fibroids

A Major Qualifying Project
Submitted to the Faculty of
Worcester Polytechnic Institute
In partial fulfillment for the
Degree of Bachelor of Science

Submitted by:
Elizabeth Hicks
Micah Wilde
Zara Alkaff

Advisors:
Dr. Catherine Whittington
Dr. Marsha Rolle

Submitted on 27 APR, 2023

Table of Contents

Authorship Table

Section	Writer
1.0 Introduction	Liz and Micah
2.0 Literature Review	Liz
2.1 Uterine Fibroids	Liz
2.1.1 Demographics	Liz
2.1.2 Location and Overall Structure	Liz
2.1.3 Growth and Development	Liz
2.1.4 Risk Factors	Liz
2.1.5 Treatment Options	Liz
2.2 Tissue Modeling Systems	Micah
2.2.1 Xenografts	Micah
2.2.2 Tumorspheres	Micah
2.2.3 Spheroids	Micah
2.2.4 Microfluidic Models (Organ-on-chip)	Micah
2.2.5 Tissue Rings	Micah and Zara
2.2.6 3D Bioprinting	Micah
3.0 Project Strategy	■■■■■■■■■■■■■■■■■■■■
3.1 Initial Client Statement	All
3.2 Technical Design Requirements	Zara
3.2.1 Design Objectives	All
3.2.2 Design Functions and Means	Zara
3.2.2.1 Functions to Accomplish Objective 1	Zara
3.2.2.2 Functions to Accomplish Objective 2	Zara and Liz

3.2.2.3 Functions to Accomplish Objective 3	Zara
3.2.2.4 Functions to Accomplish Objective 4	Zara and Liz
3.2.2.5 Functions to Accomplish Objective 5	Zara
3.3 Standard Design Requirements	Zara
3.4 Revised Client Statement	All
3.5 Management Approach	Micah and Zara
4.0 Design Process	
4.1 Needs Analysis	Micah and Zara
4.2 Alternative Designs	Zara
4.3 Final Design Selection	Micah and Zara
5.0 Design Verification	
5.1 Design of all Experiments and Tests	All
5.1.1 Spheroids	Liz
5.1.2 Rings	Zara
5.1.3 Alginate Beads	Micah
5.2 Experimental Methods to Test Designs	Zara
5.2.1 Spheroids	Liz
5.2.1.1 Hanging Drop Method	Liz
5.2.1.2 Agarose Method	Liz
5.2.2 Rings	Zara
5.2.3 Alginate Beads	Micah
5.3 Experimental Results	Zara
5.3.1 Spheroids	Liz
5.3.1.1 Hanging Drop Method	Liz

5.3.1.1.1 Hanging Drop Viability Assay	Liz
5.3.1.2 Agarose Mold Method	Liz
5.3.1.3 Spheroid Viability Testing	Liz
5.3.2 Rings	Zara
5.3.2.1 Rat Aortic Smooth Muscle Cells Rings	Zara
5.3.2.2 Uterine Smooth Muscle Cells (uSMCs) Rings.	Zara
5.3.2.3 Uterine Smooth Muscle Cells (uSMCs) Rings with Ficoll and Ascorbic Acid Crowder	Zara
5.3.2.4 Collagen Production Testing	Zara
5.3.3 Alginate Beads	Micah
5.3.3.1 Alginate Bead Cell Encapsulation and Degradation Study	Micah
6.0 Final Design and Validation	Zara and Liz
6.1 Ethics Statement	Liz and Micah
6.1.1 Environmental Impact	Micah
6.1.2 Societal Influence	Liz and Micah
6.1.3 Global Influence	Micah
6.1.4 Economics	Zara and Micah
7.0 Discussion	All
7.1 Spheroids	Liz
7.2 Rings	Zara
7.3 Alginate Beads	Micah
7.4 Limitations	All
8.0 Conclusions and Recommendations	Liz and Micah

| Appendices A-K | All |

List of Figures

List of Tables

Abstract

I. INTRODUCTION

Uterine fibroids (UF) are benign tumors found in the uterus that form from a single-cell clonal expansion. There are several types of fibroids in the uterus, the most common being intramural, subserosal, and submucosal (Stewart et al., 2016). They have a disorganized internal structure with a lot of extracellular matrix (ECM) and can range in size from 1 mm to 20 cm (Bulun, 2013). They are found in approximately 70% of people with uteruses at reproductive age and disappear after menopause. This number may be far greater because many cases go unreported due to a lack of symptoms, which can include pelvic pain, heavy bleeding, and infertility (McWilliams & Chennathukuzhi, 2017).

There is currently no curative treatment for UF. Many treatments have serious complications and high recurrence. The most common clinical models used for UF currently are animal models, and current in-vitro 3D models are limited and not independently representative of an in-vivo fibroid (Weiswald et al., 2015). This project focused on designing and assessing the feasibility of tissue model components to mimic features of intramural UFs within the myometrium (muscular wall).

II. DESIGN PROCESS OVERVIEW

A successful model for this purpose must replicate the structures and functions of UF. The design objectives for this project were to create an effective modeling system that replicated fibroid/tissue interface, replicated in situ tissue composition, was reproducible, ensured cell viability, and was affordable. A pairwise comparison chart determined the best of several modeling approaches to address these objectives and to prioritize the replication of the fibroid/tissue interface as the most important objective.

III. METHODOLOGY

Different alternative designs were tested to ensure the components of the model could accurately mimic the structures and properties of intramural uterine fibroids. The designs of 3D spheroids, 3D rings, and alginate beads with encapsulated cells were established and tested to identify the most promising model components. These designs were first used with rat smooth muscle cells (RaSMCs) to establish techniques before using uterine smooth muscle cells (uSMCs) to represent fibroids or myometrium.

A. Spheroid Formation

Spheroids were selected as a way to represent the intramural fibroids. They were formed via the agarose mold (AM) and hanging drop (HD) methods. In the AM method, two 2% (w/v) agarose molds of the same diameter but different volumes (190 μL and 75 μL) were used to form spheroids with different initial numbers of cells per well. In the HD method, 10 μL of a concentrated cell suspension was pipetted onto the top plate of a petri dish, then inverted to form the spheroid. Cell suspensions of different densities were tested via the hanging drop method to see if initial seeding density had an impact on circularity, spheroid size, and viability. Spheroid size and viability were measured for each method at Days 1, 3, and 5. The size was measured using ImageJ and the viability was measured using the CellTiter 96® AQ$_{ueous}$ One Solution Cell Proliferation Assay (MTS).

B. Ring Formation

The ring model was selected to represent the myometrial wall as they portray a similar structure and tissue composition. 2% (w/v) agarose ring molds were made and set to rest for a day in media (Gwyther et al., 2011). Both RaSMCs and uSMCs were seeded into each well of the molds and incubated for 8, 10, or 14

days in their respective culture media. For uSMCs, supplemented vascular basal media with macromolecular crowders, Ficoll PM70, Ficoll PM400, and ascorbic acid, was used to support cell growth and increase ECM deposition for enhanced ring integrity.

C. Bead Formation

Alginate beads were selected to represent intramural fibroids. Alginic acid sodium salt was combined with a HEPES and NaCl buffer to reach a desired concentration, and gelatin was added at 0.5% w/v to aid cell adhesion. Alginate solution was extruded with a 27g needle into $CaCl_2$ for alginate crosslinking. Cells were encapsulated by suspending in an alginate solution, forming as described above, and incubating. Bead diameters were measured for average size at Day 0 and Day 2 and a degradation study was completed.

IV. RESULTS

A. Spheroid Formation

HD spheroids were larger than both sizes of AM spheroids. The HD spheroids had average diameters at D3 of 161.27 ± 69.9 μm, and the AM spheroids had D3 diameters of 118.97 ± 16.40 μm in the larger molds and 119.94 ± 12.32 μm in the smaller molds. AM spheroids had an aspect ratio of 0.94 at D3, while HD spheroids had a ratio of 0.87. The aspect ratio decreased as seeding density decreased. The sizes of the hanging drop spheroids were highly variable because larger (>150 μm) and smaller spheroids (< 100 μm) had formed within one hanging drop. There was some size variation for AM spheroids as well because spheroids towards the center of the mold were larger than at the edges, as expected. Though the AM spheroids were larger and had a higher variability, they were unexpectedly more viable than the AM spheroids. They had a D3 viability of $73.9 \pm 5.06\%$, which is not above the benchmark, but is significantly closer than the AM spheroids, which had a D3 viability of $45.62 \pm 12.03\%$ (large molds) and $39.32 \pm 12.80\%$ (small molds).

B. Ring Formation

RaSMC rings produced a thickness over the 10 days of culture of 344 ± 22.5 μm, and a successful removal percent yield of 75%. uSMC rings produced a thickness over the 10 days of culture of 959 ± 5 μm, and a successful removal percent yield of 0%. uSMC rings crowded with macromolecular crowders of Ficoll 70 and Ficoll 400 produced a thickness over the 10 days of culture of 843 ± 6.5 μm, and a successful removal percent yield of 79%. uSMC rings crowded with macromolecular crowders of Ficoll 70, Ficoll 400, and Ascorbic Acid produced a thickness over the 10 days of culture of 487 ± 5.5 μm, and a successful removal percent yield of 100%. Histology testing of Gomori Trichrome stain was conducted with both the uSMC rings crowded with Ficolls and the uSMC rings crowded with Ficolls and Ascorbic Acids, and resulted in successful stains that mimicked the collagen produced in the myometrial tissue.

C. Alginate Beads

The alginate beads formed were mostly spherically shaped and many beads could be formed during each trial. The alginate-gelatin beads both with and without cells were more transparent and teardrop shaped than those with only alginate. Cell distribution was inconsistent between beads. Average bead sizes used alginate concentrations of 2%, 1.2%, and 0.8% w/v and gelatin concentration of 0.5% w/v for all except the 0.8% alginate that failed to form beads. The largest bead size was 2% alginate-gelatin, and the smallest was 1.2% alginate. The average bead diameters from Day 2 produced the same results as above with reduced sizes. The 0.8% alginate beads were the most consistent in size and stability with the lowest standard deviation in diameter of 82.56 μm at Day 0 and the smallest change in size over 5 days.

V. DISCUSSION AND FUTURE DIRECTIONS

A. Discussion

Spheroids formed rapidly and consistently in agarose molds. The AM spheroids were consistently under the maximum benchmark size of 150μm, whereas HD spheroids were larger. HD spheroid shape was dependent on the shape of the initial seeding drop and became less circular as seeding density decreased. AM spheroids formed in a mold with set dimensions (400 μm diameter, 800 μm depth), and so were more consistent in size and shape. The spheroids formed by D1, however, did not hit all benchmark viabilities. HD was closer to hitting all benchmark viabilities than AM, though they were larger and more variable in size. Overall, spheroids are a quick way to form 3D cell cultures but may not be an effective model of fibroids due to issues with viability.

Because the uSMCs without any crowders were not successful in forming, it was hypothesized adding macromolecular crowders would increase the ECM deposition, resulting in more structurally compact rings. So, two more experiments were conducted using Ficoll 70, Ficoll 400, and Ascorbic Acid as crowders. The uSMC rings crowded with Ficolls-only were within the benchmark thickness after 10 days, 0.84-0.87 mm, and demonstrated that this ring is most structurally similar to the myometrial wall. However, the uSMC rings crowded with Ficolls and Ascorbic Acid produced the highest successful removal rate at 100%. This is due to the increased ECM deposition from all the macromolecular crowders. The Ficoll and Ascorbic Acid-crowded uSMC rings proved to have the most similar tissue composition to the myometrial wall. This stain showed collagen dispersed throughout the whole ring which is representative of human myometrial tissue. Overall, it was determined that uSMC rings are representative of myometrium tissue when combined with Ficoll and Ascorbic Acid crowders. It is recommended that more tests be conducted to accurately determine the best way to mimic the myometrium tissue.

The alginate beads were highly reproducible with minimal variability in size. The bead diameter decreased as expected when a smaller needle gauge was used for extrusion. Alginate-gelatin crosslinked beads with cells encapsulated had a higher degradation rate than alginate-only beads. Cell encapsulation in the beads resulted in an inconsistent distribution of cells across the beads with some beads having no cells. The alginate-gelatin beads had an unexpected result in morphology with many teardrop-shaped beads forming and transparent. The cause of the difference in shape between the alginate and alginate-gelatin beads is unknown. The 0.8% alginate beads were the most consistent in size and had the least degradation. In the degradation study the 2% alginate beads had the largest change in diameter with a difference of over 100 μm from 0 to 120 hours.

B. General Takeaways and Potential Future Applications

The use of rings and alginate beads in the predictive model seem most advantageous to the longevity and predictability of the model, however, more research is needed to confirm this. Future research and applications can include formulations of the three components working together in the same modeling system. Next steps to create this model would include attaching cells to alginate beads, attaching alginate beads to rings and spheroids, and adding fibroid cells and tissues into all models. These future steps would allow the team to achieve their main objective of replicating the fibroid/tissue interface and create a fully functioning model of a uterine fibroid.

Acknowledgments

The team would first and foremost like to thank Professor Catherine Whittington (PhD) for her dedication, encouragement, and advice throughout the creation and execution of this project. Her constant support helped bring the project to fruition and helped the team overcome obstacles encountered throughout the year, as well as significant contributions to the team's overall success.

The team would also like to thank Professor Marsha Rolle (PhD) for providing us with Rat Aortic Smooth Muscle Cells and guiding us through the initial steps of this project. The team would also like to express gratitude for providing staining materials.

The team also thanks Lisa Wall for her time and effort in ordering materials, locating resources and space, and maintaining the lab area for the team to complete their project. Without her resourcefulness and help, the team would not have been able to complete their project.

The team would like to thank PhD Candidate Andre Figueroa-Milla for his guidance with bioprinting research and taking the time to provide Rat Aortic Smooth Muscle Cells.

The team also shows appreciation to PhD Candidate Bryanna Samolyk for her guidance and help in providing the team with Uterine Smooth Muscle Cells and vascular basal media. The team also appreciates her patience and willingness to continue aiding the team in their research by providing them with protocols for cell culturing.

A special thanks to Jyostna Patel for providing her knowledge and support during the embedding, sectioning, and staining process of the uterine smooth muscle cell rings.

The team would also like to thank Professor Kristen Billian (PhD) and Grace Jolin for supplying spheroid molds and agarose, as well as for their help and instruction through the process.

1.0 Introduction

Uterine fibroids (UF) are benign tumor growths found in the uterus that range in size. The number of fibroids as well as symptoms vary based on the individual. Some symptoms of UF include pelvic pain, menstrual periods that last over a week, and heavy bleeding (Stewart et al., 2016). Fibroids can also cause complications with pregnancy and, in more serious cases, infertility. The true prevalence of UF is difficult to assess because symptoms are generally underreported, and many cases are asymptomatic. The main factors indicating development are ethnicity and age. Fibroids also disproportionately affect people of African ancestry, who experience an increased number of cases of uterine fibroids and more severe symptoms. They are also more likely to undergo major surgery than people of European ancestry. UF is often clinically diagnosed in more severe cases because many individuals do not recognize that they have fibroids unless symptoms appear (Stewart et al., 2016). The most common treatment for UF is a hysterectomy, which poses major risks and eliminates fertility (Stewart et al., 2016). A hysterectomy is a major procedure with a large recovery time and can induce menopause-like symptoms, however, it is the only treatment that is curative. There are various other treatments for UF including embolization, hormone therapy, and surgical excision (Stewart et al., 2016). Due to the asymptomatic nature of UF, severe cases are more likely to be diagnosed, so a hysterectomy is the most common course of treatment.

The field of uterine fibroids is generally under-researched, and much is still unknown about their cause and development. Increased understanding of UF and how they function will hopefully lead to improved treatment and earlier diagnosis to limit the effects on the body. There are currently limited preclinical models of UF that allow researchers to study its structures and functions. One common UF in-vivo model is the xenograft, which uses mice to grow fibroids, and poses both ethical and affordability concerns. Creating a three-dimensional (3D) in-vitro uterine fibroid model that replicates mechanical and physical properties will increase the understanding of UF, and their interface with uterine tissues, and create the potential for future treatment testing. Current methods often used for 3D in-vitro modeling are tissue rings, tumorspheres, and organ-on-a-chip models. Ring models are used in vascular and fibroid research, tumorspheres are used in cancer research, and organ-on-a-chip models are used in cancer and reproductive tissue research. These individual models are not representative of in-vivo fibroids and there is limited experience with using them to model uterine fibroids.

A successful model created from this project will replicate the structures and functions of UF. The goals for this project's uterine fibroid model are to replicate the fibroid and uterine tissue interface, replicate tissue composition to mimic in situ myometrium, create reproducibility in the model, ensure cell viability, and be affordable. In this project, the group used literature and advisor guidance to develop several components of a 3D in-vitro uterine fibroid model. Background research informed the selection of alternative designs that reflect elements of UF and the surrounding uterine muscle tissue.

2.0 Literature Review

2.1 Uterine Fibroids

Uterine fibroids, or leiomyomas, are one of the most common diseases found in people of reproductive age with a uterus. In the United States, current research indicates that uterine fibroids are present in most people with a uterus. Most cases of fibroids are asymptomatic, but approximately a quarter of people with fibroids will experience severe symptoms (McWilliams & Chennathukuzhi, 2017). Many cases go undiagnosed as many people have no symptoms or underreport them. Though there are several treatment options for this disease, there are no treatments that are curative and preserve fertility (McWilliams & Chennathukuzhi, 2017). UF is a type of benign tumor located in the uterus, and forms from a single-cell clonal expansion (Guilani et al., 2020). They are responsive to estrogen and progesterone, but little is known about their development.

2.1.1 Demographics

The risk of UF increases with age, with most women having fibroids by the age of 50 (Guilani et al., 2020). Most cases are mild, but about 25% of people with a uterus have severe symptoms. The risk of developing fibroids is highest in middle age, and it decreases significantly after menopause (Guilani et al., 2020).

Uterine fibroids are present differently in different ethnicities. People of African descent are affected at a higher rate and with more severe symptoms than people of European descent (Guilani et al., 2020). In the United States, African Americans have a higher risk of developing fibroids, with 80% of people of this demographic developing fibroids during their lives. Fibroids in people of African descent typically develop earlier in life and with more severe symptoms leading to the necessity of severe treatments like surgery. UFs in people of African descent are also typically larger and greater in number than in European Americans. An estimated 70% of people of European descent with a uterus will have fibroids (McWilliams & Chennathukuzhi, 2017). There is little data about the occurrence of uterine fibroids in other ethnicities in the United States compared to people of African and European descent, and little is known about why there is a difference between them (McWilliams & Chennathukuzhi, 2017). There is some research on fibroid demographics in other countries such as France, Saudi Arabia, and China, however, they are not prevalent articles, and most research seems to come from the United States. Furthermore, no review articles regarding world demographics could be found.

2.1.2 Location and Overall Structure

Uterine fibroids develop from uterine smooth muscle cells, also known as myometrium tissue. Normal myometrial cells grow uniformly, but uterine fibroids grow in a disorganized ball or nodule and can range in size from 1 mm to 20 cm (McWilliams & Chennathukuzhi, 2017) (Bulun, 2013). They can grow very rapidly and have some characteristics of malignant cells, but they are usually benign (Stewart et al., 2016). UFs can also be characterized by their extracellular

matrix (ECM), which is typically higher in volume and has a more disorganized structure compared to normal myometrium tissue, as shown in Figure 1 (McWilliams & Chennathukuzhi, 2017).
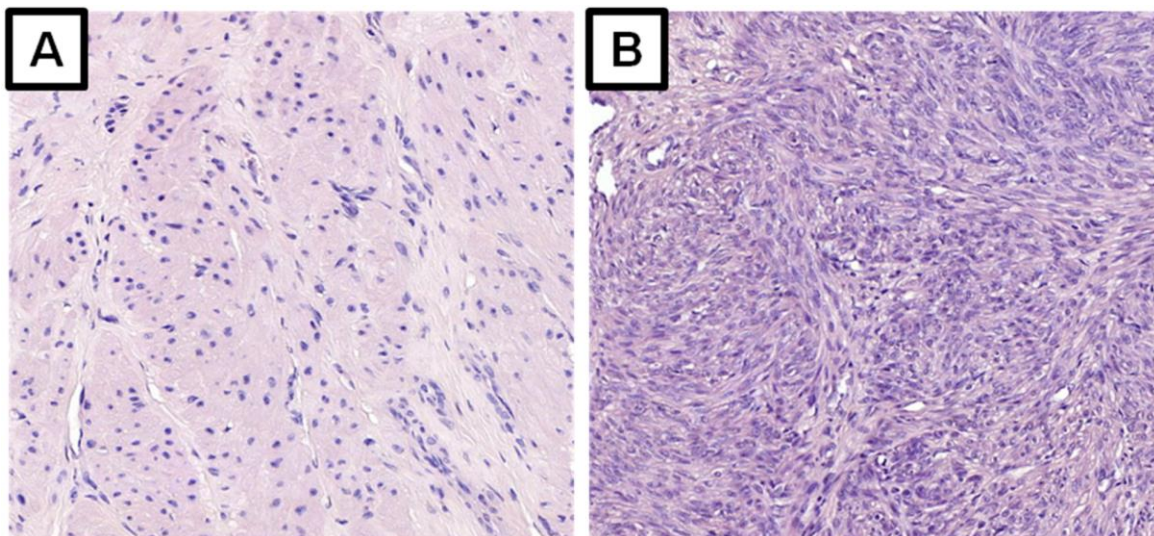
Figure 1. Image of normal myometrium tissue and structure (left) compared to uterine fibroid tissue structure and function (right) (Ciebiera et al., 2018).

The ECM in uterine fibroids is biochemically different from myometrium tissue and is secreted primarily by the fibroblasts derived from fibroid progenitor cells, which originate from mutated myometrium stem cells (Stewart et al., 2016). The ECM present in UF contains high amounts of glycosaminoglycans and crosslinked collagen, which increases the stiffness of the tissue (Yang et al., 2022). Collagens I, III, and IV are expressed heavily in uterine fibroids, differing from the expression of collagen in myometrial cells, which consists primarily of Collagens I, II, IV, V, and VI (Malik et al, 2010). However, despite this information, the development of the fibroid ECM and biochemical makeup is still not fully understood (Yang, et al., 2022). Research on the development and proliferation of uterine fibroids is still ongoing and not fully developed or widespread (Guilani et al., 2020).

UFs are classified by their location in the uterus. The main classifications are subserosal, intramural, and submucosal fibroids, as shown in Figure 2. Subserosal fibroids grow projected outside of the uterus; intramural fibroids grow within the myometrium tissue, and submucosal fibroids grow into the uterine cavity. The location of UF influences their symptoms and the available treatment options (McWilliams & Chennathukuzhi, 2017). Treatment options and symptoms are based on the location, size, and number of tumors (Cruz & Buchanan, 2017). For example, a myomectomy is a surgical removal procedure that can only be performed on submucosal fibroids (Guilani et al., 2020). There is also a difference in symptoms between different types of fibroids. Submucosal and intramural fibroids typically cause more abnormal urinary symptoms, whereas patients with subserosal or pedunculated subserosal fibroids may experience symptoms of pelvic pain and bowel or bladder dysfunction (Havryliuk, Y. et al., 2017).

The most common symptom of uterine fibroids is excessive menstrual bleeding, but symptoms can be more severe. More severe symptoms include pressure and pain on other organs, urinary symptoms, constipation, lower back pain, and lower pregnancy rates (McWilliams & Chennathukuzhi, 2017) (Cruz & Buchanan, 2017). They may also be associated with infertility, as well as a higher risk of developing emotional distress like depression and anxiety due to experienced symptoms (Guilani et al., 2020).
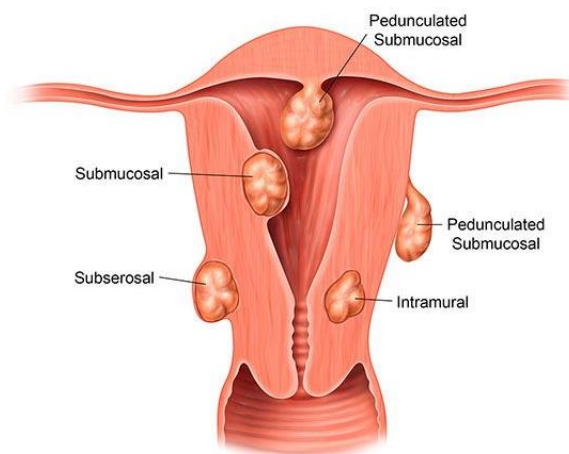
Figure 2. Image of the locations of different types of uterine fibroids, including subserosal, intramural, and submucosal fibroids. (Azura Vascular Care, 2017).

2.1.3 Growth and Development

Though UF is very prevalent in people with a uterus, there are several gaps in knowledge about how and why they grow (Guilani et al., 2020). Several studies have been performed both in-vivo and in-vitro to try to understand their development. So far, it is known that they are derived from a single cell, are responsive to gonadal steroids, and undergo chromosomal rearrangements (Stewart et al., 2016).

One characteristic feature of uterine fibroids is their dependency on gonadal steroids estrogen and progesterone (Bulun, 2013). Fibroids develop during reproductive years and then shrink after menopause (Bulun, 2013). When the uterus increases the production of these steroids, like in early pregnancy and postpartum, there is a significant effect on the growth of fibroids (Bulun, 2013). Gonadotropin-releasing hormone (GnRH) analogs can reduce fibroid size and the amount of associated bleeding (Bulun, 2013). GnRH suppresses ovarian activity and reduces the amount of estrogen and progesterone in circulation (Bulun, 2013).

UFs rapidly expand in size when they are forming, but have a relatively low mitotic index, meaning that the cells involved do not divide rapidly (Stewart et al., 2016). Most of the volume expansion is due to the presence of ECM, which binds growth factors and causes signaling that makes the fibroids stiff masses (Stewart et al., 2016). This ECM is produced primarily by the mutated fibroblasts and is important in the formation and physiology of UF. Little is known about the contributions that the ECM and the cells make individually to the formation of uterine fibroids.

However, research has indicated that fibroid development occurs with multiple steps, as shown in Figure 3.
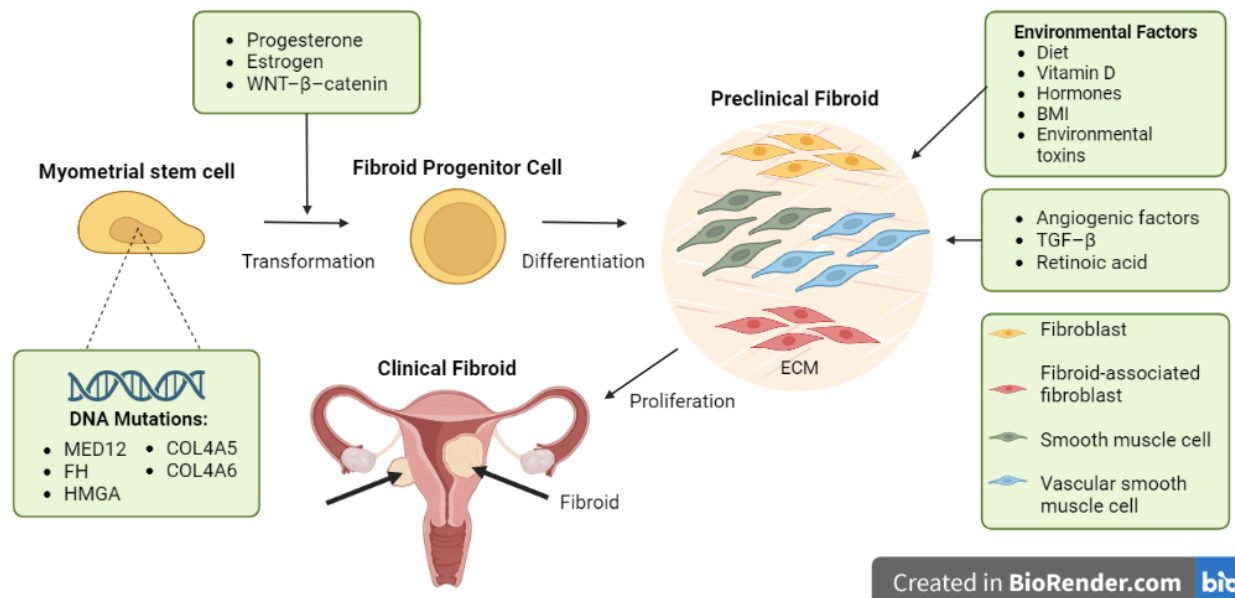
Figure 3. Image of current research on the development, growth, and proliferation of uterine fibroids (Created with BioRender.com)

Uterine fibroids are derived from smooth muscle stem cells (SMCs) that are present within myometrium tissue (Stewart et al., 2016). These SMCs can be converted into fibroid progenitor cells (Stewart et al., 2016). It is suggested that a paracrine mechanism enables the development of SMCs into fibroid cells since SMCs do not have gonadal steroid receptors, but fibroid cells do (Stewart et al., 2016). The SMCs transform into fibroid progenitors, then differentiate into preclinical fibroids and grow into clinical fibroids (Stewart et al., 2016). This paracrine pathway is mediated through driver mutations, WNT–β-catenin signaling, estrogen, and progesterone (Stewart et al., 2016). The paracrine pathway can activate the expression of TGF-β, which promotes fibronectin expression and cell proliferation in preclinical fibroid tissue over normal myometrium tissue (Stewart et al., 2016). Fibroids have four key cell types: smooth muscle cells, vascular smooth muscle cells, fibroblasts, and fibroid-associated fibroblasts, which all originate from the fibroid progenitors. The fibroid tissue itself also contains stem cells, but significantly less than normal myometrium (Bulun, 2013). Fibroid stem cells have mutations in the MED12 gene. The modification of this gene activates the expression of TGF-β, which can lead to drug resistance and cell proliferation (Bulun, 2013).

The cells derived from the clonal expansion of a single fibroid progenitor cell have a different genetic makeup than normal SMCs and myometrium tissue. They have a difference in the expression of the following genes: *CRABP2*, *PGR*, and *TGFβR2*. These genes are all fibroid-associated. *CRABP2* encodes cellular retinoic acid-binding protein 2, *PGR* forms progesterone receptor B, and *TGFBR2* helps to transcribe the receptor 2 of TGF-β (Stewart et al., 2016). The expression of these genes is different from myometrial tissue in fibroid tissue.

Fibroid cells also have mutations or alterations in the following genes: *MED12*, *HMGA2*, and the *FH* group. MED12 mutations are the most researched, because current research indicates that the mutations occurring in *MED12* seem to cause the formation of UF (Stewart et al., 2016). Most studied fibroids have contained *MED12* mutations, and they have been discovered in rare fibroid variants, but at a lower frequency (Stewart et al., 2016). The fibroids with *MED12* mutations tend to have higher amounts of WNT4–β-catenin than fibroids without the *MED12* mutations. Current research indicates that the *MED12* mutations affect the interaction between *MED12* and cyclin C, the regulator of β-catenin transcription (Stewart et al., 2016). *HMGA2* mutations are thought to affect fibroid growth and proliferation, and mutations in the *FH* group affect an enzyme essential to the Krebs cycle (Stewart et al., 2016). *HMGA2* is altered due to downregulation because of karyotypic rearrangements and mutations to the *FH* group can be missense, nonsense, frameshift, or the deletion of the whole gene (Stewart et al., 2016).

In addition, uterine fibroids are contained within a surrounding structure, the fibroid pseudocapsule (Tinelli, et al., 2012). This is seen in Figure 4. This capsule is constructed of ECM and clearly separates the fibroid tissue from the normal myometrium (Tinelli et al., 2012). It is characterized by a thick connective matrix surrounding the fibroid, consisting of a network of collagen fibers, neurofibers, and blood vessels (Ciarmela, et al., 2022). The fibroid pseudocapsule has a rich neurovascular network and surrounds the fibroid, which is attached to it through connective bridges (Malavasi, et al., 2011). This network compresses the fibroid. The fibroid itself does not have much vasculature running through it, so the pseudocapsule supplies blood to it (Malavasi, et al., 2011). A study conducted in 2012 indicated that the cells within the pseudocapsule are part of the myometrium and have similar features to it (Malavasi, et al., 2012). It seems to develop from myometrium tissue to protect the normal tissue from the fibroid. Not all fibroids form a capsule. There is little to no research on the pathophysiology of this pseudocapsule, as most research focuses on surgical approaches to reaching the fibroid without damaging the pseudocapsule. It is possible that the fibroid itself may promote the biochemical growth factors and intense angiogenesis found in the pseudocapsule, but more research is needed to fully understand the effect of the pseudocapsule on fibroid development and on the development of the pseudocapsule itself (Tinelli, 2019).
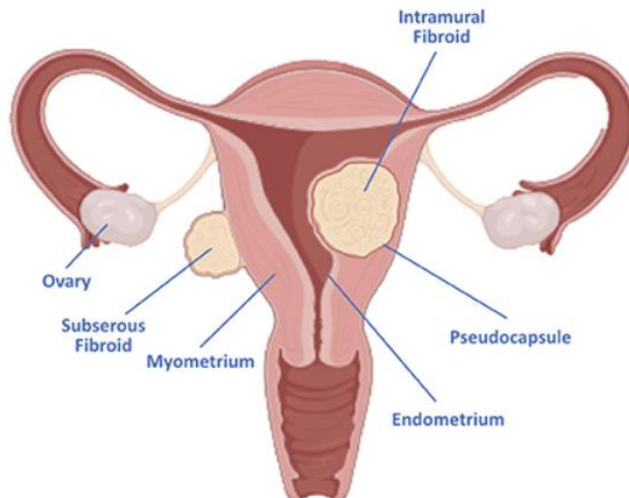
Figure 4. Image showing the location of the pseudocapsule in reference to a uterine fibroid and the uterus (Uimari et al., 2022).

2.1.4 Risk Factors

Risk factors associated with uterine fibroids are primarily diet and a high BMI, which are thought to influence their development. A BMI over 30 is thought to increase the risk of fibroids (Qin, H. et al., 2021). Several studies indicate that the occurrence of UF becomes more frequent as BMI increases (McWilliams & Chennathukuzhi, 2017). Studies have indicated that this is due to the metabolic functions of adipose tissue, or body fat, which produce cytokines and growth factors (Yang et al., 2022). Obesity may reduce the production of gonadal hormone-binding globulins, which can upset the balance of hormones in the body (Yang et al., 2022).

2.1.5 Treatment Options

Treatment options include several therapies and in extreme cases, surgeries. Current therapeutic treatments include hormonal contraceptives, non-steroidal anti-inflammatory drugs, and hormone therapies (McWilliams & Chennathukuzhi, 2017). Hormonal contraceptives, tranexamic acid, and non-steroidal anti-inflammatory drugs are used to reduce blood loss during menstruation, a symptom associated with fibroids. Hormonal contraceptives are often used as a method to relieve symptoms of UF before surgery (McWilliams & Chennathukuzhi, 2017). Tranexamic acid is a non-hormonal medication that promotes blood clot formation and can reduce excessive menstrual bleeding seen in people that are suffering from UF (Peitsidis & Koukoulomati, 2014). There are also several other medications that can be used to manage uterine fibroids, like progestins, selective progesterone receptor modulators (SPRMs) and anti-progestins, iron supplements, and more.

There are also several radiology procedures that can treat uterine fibroids like uterine artery embolization (UAE) (Guilani et al., 2020). UAE is a non-surgical treatment option that cuts off the blood supply to the fibroids and uterus and kills them. However, fibroids are likely to recur following this treatment and there are several complications that may arise following the procedure

(McWilliams & Chennathukuzhi, 2017). After five years, people who received UAE had 20% more recurrence of fibroids than those who had myomectomies (Guilani et al., 2020). There is also a lack of data on the effect of UAE on fertility.

Current surgery options include hysterectomy, myomectomy, UAE, and myolysis (McWilliams & Chennathukuzhi, 2017). Hysterectomies are the best treatment option because they cure fibroids and eliminate symptoms, but they cause infertility (McWilliams & Chennathukuzhi, 2017). A hysterectomy is a major surgical procedure where the uterus is removed from the body (Guilani et al., 2020). It causes infertility but reduces fibroid symptoms significantly. A myomectomy involves removing the fibroids from the uterus while still preserving the uterus. It can be performed on submucosal fibroids, which reduces fibroids and preserves fertility. However, the recurrence of fibroids after this treatment is likely, and the likelihood of recurrence increases significantly as the number of fibroids present in the uterus increases (Guilani et al., 2020). Myolysis uses heat to destroy fibroids but may cause several side effects following the procedure including pain and heavy bleeding (McWilliams & Chennathukuzhi, 2017). Many people will also need a second procedure following myolysis, and there is not much data on the effect of myolysis on fertility (McWilliams & Chennathukuzhi, 2017). Though there are several clinical treatment options, none of the available treatments work as long-term options that completely preserve fertility.

2.2 Tissue and Uterine Fibroid Modeling Systems

Current research on fibroids is achieved primarily through the study of animal models. Of these models, the Eker rat is very common due to a favorable mutation that enables the rats to spontaneously develop fibroids (McWilliams & Chennathukuzhi, 2017). Other common modeling systems include xenografts, where human fibroids are implanted in rats, mice, and rabbits (McWilliams & Chennathukuzhi, 2017). These methods of studying fibroids are not long-term and are lacking several characteristic components of the human fibroid system (McWilliams & Chennathukuzhi, 2017).

Three-dimensional (3D) tissue models are becoming increasingly prevalent in tumor modeling due to their advantages in mimicking the shape and physiological structure of tumors as compared to cells grown in two-dimensions (2D) (Carvalho et al., 2015). Several different models were researched and evaluated to determine which model to use. These include xenografts, tumorspheres, 3D rings, spheroids, microfluidic models, and the Eker rat model. Each model has unique advantages and drawbacks as well as various levels of research conducted with UF tissues specifically.

2.2.1 Xenografts

Xenografts are a modeling system where patient tissues are implanted into an animal as a living model system. Animal models are often used due to their applicability in treatment testing and observation of UF growth. In one xenograft model, human uterine fibroid tissue was harvested and transplanted into immunodeficient mice (Fritsch et al., 2015). The grafts were composed of

interwoven bundles of smooth muscle cells. This study assessed the growth of the fibroid and myometrial xenografts with estradiol and progesterone. The major outcome was determining the optimal dosage of hormones to successfully grow the grafts that can be used for treatment testing. This was measured by studying the weight of the xenografts after treatment of the various hormones, as shown in Figure 5, with the xenograft weight on the y-axis and the hormones present (if any) on the x-axis. There is also a homogeneous morphology shown between the grafts. Advantages of xenografts in UF modeling include mimicking UF tissues in-vivo, testing for treatment, and extensive research conducted. The main drawback of xenografts is budgetary and ethical concerns with using live mice in experimentation. This modeling system is also limited due to the physiology of mice varying from that of humans (Carvalho et al., 2015).
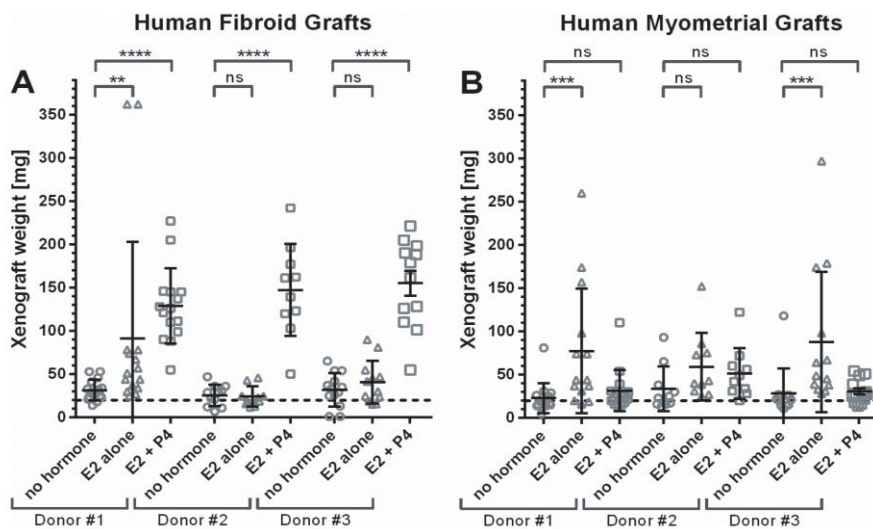
Figure 5. Human fibroid and myometrial xenograft growths in CB17-SCID mice with Estradiol (E2) and Progesterone (P4) addition (Fritsch et al., 2015).

2.2.2 Tumorspheres

Tumorspheres are spherical models synthesized from the proliferation of cancer cells (Weiswald et al., 2015). The model is maintained as free-floating cultures and is seeded at low cell densities to avoid aggregation. Tumorspheres proliferate and grow as floating clusters under culture, and they are used to investigate cancer stem cell properties (Weiswald et al., 2015). In tumorsphere models, cells can be embedded in 3D matrices, such as collagen, to simulate cell interactions and adhesion. The advantages of tumorspheres include easy replication and low cell density, and the major drawback is poor differentiation (Weiswald et al., 2015). Tumorspheres are primarily used in understanding cancer biology which is different from the structure of fibroids. Tumorspheres were explored along with other models used primarily in tumor research due to the lack of 3D in-vitro models for fibroids. These models have the potential to be customized to fit the specifications of a uterine fibroid.

2.2.3 Spheroids

Spheroids are self-assembling cell aggregates that reproduce tissue structure and material properties (Weiswald et al., 2015). Their shape and lack of vascularization mimic the glycolytic metabolic activity within tumors (Weiswald et al., 2015). Methods of fabrication include hanging drop, spinner flash, centrifugation, static liquid overlay, and cell growth on non-adherent micropatterned surfaces in microfabricated devices (Carvalho et al., 2015). Advantages of spheroids include the ability to study drug effects for extended periods of time and their similar behavior to tumors (Carvalho et al., 2015). Disadvantages of using spheroids include the challenges with the consistency of size in reproduction and the high cell count required (Ayvaz et al., 2021). Uterine fibroid spheroid models are useful for studying various aspects of uterine fibroid biology, such as cell proliferation, differentiation, and apoptosis. They can also be used to test the effectiveness of potential therapeutic agents and to identify new targets for drug development (Carvalho et al., 2015).

2.2.4 Microfluidic Models (Organs-On-Chips)

Microfluidic models, specifically organ-chips, are multi-channel microfluidic cell cultures to mimic the functions of an organ (Sontheimer-Phelps et al., 2019). They are composed of vascular microchannels, and, with ECM-coated membranes, they can provide tissue interfacing (Sontheimer-Phelps et al., 2019). To our knowledge, this modeling system has not been used with uterine fibroids, but background knowledge was provided with an IVF study using an organ-on-chip model of the placenta. This was achieved by replicating the placental barrier using trophoblast cells, endothelial cells, and blood flow within the system. Advantages of this modeling system include assessment of therapies/treatments, simulation of whole organs, and modification to mimic the structure and physiology of various organs. The main drawback of this model is the lack of application with UF tissues, specifically with the channels primarily being used for blood flow or another specific movement.

2.2.5 Tissue Rings

Engineered tissue rings have broad applications in modeling systems. They can be developed to model many tubular and enclosed structures present in the body, such as the trachea, vascular systems, and myometrium (Gao et al., 2022) (Strobel et al., 2017) (Souza et al., 2017). These ring structures are achieved in several ways. They can develop through the growth of cells onto a scaffold, which helps them assemble into a desired structure, or cells can assemble themselves into the desired structure (Strobel et al., 2017). Scaffolds can help cells grow into the desired structure and can be designed to replicate ECM and promote cell differentiation (Gao et al., 2022).

The use of self-assembling ring structures can be advantageous to the development of tissue rings that better model in-vivo tissue (Strobel et al., 2017). Tissue rings that are grown without the use of a scaffold tend to have structures and function more similar to that of naturally formed tissue. They also have better ECM production, increased cell density, better tissue strength, and

are less prone to injection and degradation (Strobel et al., 2017). Self-assembling tissue rings could be an effective way to model uterine smooth muscle tissues, or myometrium, and uterine fibroids. Tissue rings are shown to be easily reproducible (Strobel et al., 2017) (Souza et al., 2017).

There is a lack of in-vitro models of uterine fibroids that model the structures and functions of uterine tissues. Tissue rings have the potential to be an effective way to model both uterine cells and fibroid cells due to their inherent structure. Tissue rings also have the potential ability to replicate the interface between uterine fibroids and myometrium cells. With the use of self-assembling tissue rings and the attachment of uterine fibroids to the ring structures, a model with physical and mechanical properties similar to that in-vivo may be produced. This modeling system could then be used as a model for drug discovery and for the development of new treatments.

2.2.6 3D Bioprinting

3D bioprinting is a rapidly developing field to create three-dimensional structures by depositing layers of biomaterials in a specific pattern. Currently, applications of 3D bioprinting include artificial tissues such as skin grafts and artificial organs such as heart valves (Nawaz et al., 2022). These structures can be used to create models of different organs and tissues, including the uterus and fibroids. To create a 3D bioprinted model of uterine fibroids, a digital model of the fibroids is first created. This digital model is then used to guide the bioprinting process, which involves depositing layers of biomaterials to build up the structure of the fibroids and the surrounding uterine tissues. The biomaterials used in 3D bioprinting can be cells, proteins, or other biological materials. These biomaterials are typically mixed with a hydrogel or other support matrices to help them maintain their shape and structure during the bioprinting process, as shown in Figure 6.
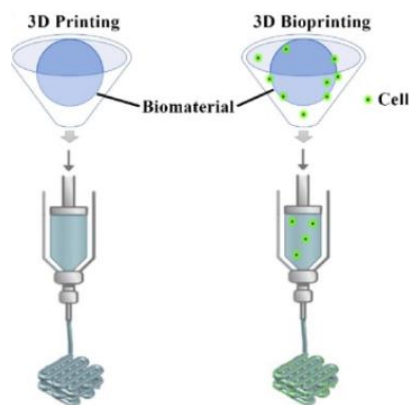
Figure 6. Diagram of 3D printed hydrogels (Li et al., 2020).

Uterine myometrium cells have been modeled effectively in the past using magnetic bioprinting, where the myometrium rings were assembled through the use of magnets to form the ring structure (Souza et al., 2017). In this study, cells were magnetized by incubation with a biocompatible nanoparticle assembly, then aggregated into rings using magnetic forces (Souza et

al., 2017). The cells were able to interact and build ECM after being aggregated which allowed them to be tested for contractility compared to an in situ uterus (Souza et al., 2017).

There are some limitations to the utilization of 3D bioprinting for uterine fibroid modeling due to the lack of research in this area. There is no published research on 3D bioprinting rings with both myometrial and uterine fibroid tissues. Another drawback of this technique for the scope of this project is the underdevelopment of the 3D bioprinting field. It is a relatively new technology, so it requires extensive practice to understand the techniques required for a successful print. There are also budgetary considerations that affect the decision not to use this modeling system. The 3D printers are very costly, as well as the bioinks required to create prints.

3.0 Project Strategy

3.1 Initial Client Statement

The focus of this project is to design and optimize the components of a scaffold-free tissue model to mimic structures that represent intramural uterine fibroids in the uterine muscular wall.

3.2 Technical Design Requirements

Initially, the goal was to create a 3D in-vitro model of uterine fibroid tissue. However, this initial goal was made without considering all aspects of the project and the design process. To be an effective modeling system, the model must be reproducible and ensure cell viability in order for the model to best mimic the fibroid in situ. The budgetary constraints given to the project by WPI should also be considered when designing and implementing an effective model. The following section contains the objectives, functions, and means that will be used to base any future models, designs, and tests.

3.2.1 Design Objectives

To accomplish the project goal, the following design objectives were determined:

Table 1. Design Objectives

Design Objectives
1. Replicate fibroid/tissue interface 2. Replicate tissue composition 3. Ensure reproducibility 4. Ensure cell viability 5. Be affordable

The first two objectives of the model make sure it is an effective modeling system of uterine and fibroid myometrium tissues. The design would replicate fibroid and uterine tissue interactions and compositions. The interface between the two tissues is an essential attachment point, and a model replicating this could be crucial to the development of new treatments. It is also very important that the model mimics the tissue composition of the myometrium tissue, so the ECM and collagen production can be representative of the in situ composition. The tissue interactions between the uterine fibroid tissue and the uterine smooth muscle cell were researched in depth and will be incorporated into the design.

To allow for the eventual use and distribution of the model in laboratory and clinical settings, the model must be reproducible. This ensures the consistency and effectiveness of each model and allows for the standardization of the models. Without reproducibility, different preparations of the modeling system could yield different results, which makes it difficult to accurately test therapies on the model.

The model must also ensure cell viability. To be an effective modeling system, the cells within the model need to be alive and proliferate without significant necrosis. This can be an issue with thicker, denser, and longer-lasting tissue models. The design should take this into consideration to ensure maximum viability for the longest period so that uterine fibroids can be studied and modeled effectively.

Finally, the model must also be affordable. This project has a set budget, and the project must adhere to that. This is also essential in laboratory and clinical applications of the model. The model is more likely to be used in research labs if it is affordable to produce.

3.2.2 Design Functions and Means

To meet the design objectives, the model, materials, and procedure must be considered. In the design, several behaviors from the myometrium tissue and the uterine fibroid tissue should model in-vivo events. To achieve this, culture characteristics, protocols, and budget need to be considered.

Table 2. Design Functions and Means

Objective	Functions of the Model	Means of the Model
Replicate Fibroid/Tissue Interface	● Reflect characteristics of previous in-vitro approaches ● Support the growth and proliferation of the cells	● Vary culture format: Spheroids, Tissue rings, and Embedding cells into alginate beads ● Vary cell density to increase ECM production
Replicate Tissue Composition	● Express extracellular matrix proteins ● Express collagen	● Use of macromolecular crowders to promote ECM decomposition ● Vary ring culture times
Ensure Reproducibility	● Culture characteristics within in-vitro testing ● Define size, structure, and shape of the designs	● Culture cells in the correct media and incubation conditions ● Vary cell density for each experiment ● Vary spheroid fabrication methods - agarose and hanging drop ● Use consistent needle gauge sizes ● Use commercial cell lines ● Use 2% w/v set-sized agarose molds
Ensure Cell Viability	● Provide Consistent culture conditions ● Sterile lab area, sterile cells	● Incubate at: 37°C, 20% O_2, and 5% CO_2 ● RaSMC media: Complete Media with 10% FBS

	● Cell viability assays to measure live and healthy cells	● Culture cells in recommended media (Rat Smooth Muscle Cell media: Compete Media with 10% FBS; uterine Smooth Muscle Cell media: supplemented Vascular Basal Medium) ● Sterilize equipment and materials according to lab protocols- Isopropyl 70%, autoclave ● Adjust spheroid and ring size and shape ● Vary culture time of the spheroids and rings in the molds
Be Affordable	● Complete all testing and experiments within given budget	● Optimize experiment and lab time

3.2.2.1 Functions to Accomplish Objective 1.

There are several components that must be taken into consideration when attempting to replicate the interface between myometrium tissue and uterine fibroid tissue. To do this, the uterine smooth muscle cells (uSMCs) must express the extracellular matrix (ECM) seen in in-vivo uterine fibroid tissue. The model must also be able to support the growth and proliferation of the cells, which should be accomplished using alginate beads.

One way to determine the interaction of uterine and fibroid tissues is to incorporate alginate beads into the culture of the cells. Alginate is biocompatible and very easy to fabricate (Lee & Mooney, 2012). It can be used as a form of protection and an environment for the cells to grow (Lee & Mooney, 2012). Creating the alginate beads and incorporating the SMCs into the beads will model the uterine and fibroid tissues very closely. The rings, spheroids, or cells will effectively model uterine tissues, as the uSMCs will be treated with supplemented Vascular Basal Media (VBM) which will help the cells express properties seen in-vivo, such as ECM and collagen levels (Koohestani et al., 2013). The alginate beads will model the fibroid tissue as it creates a similar ECM that is expressed in-vivo and will allow for protection for the cells to grow (Lee & Mooney, 2012). This will be determined by looking at the degradation of the beads and the viability of the cells.

SMCs express ECM which is part of tissue growth and development. The cell density should be increased in the model because the more cells that crowd each mold leads to more secretion of ECM proteins to maintain their three-dimensional architecture (Geiger, B. et al., 2019). Also, as the number of cells in the molds increases, the cells consume their nutrients and oxygen which leads to the synthesis and secretion of ECM proteins, including collagen I and fibronectin (Stolberg, T. et al., 2019). The increased level of ECM proteins allows for the testing of ECM through H&E staining to observe how well the ECM produced by the model mimics the ECM produced in situ.

3.2.2.2 Functions to Accomplish Objective 2.

To replicate the tissue composition of both the myometrial and fibroid tissue, the model needs to express both ECM proteins and collagen similar to in situ tissues. This can occur by adding macromolecular crowders to the media, or by varying the days of culture in the ring molds.

One very defining way in which uterine tissue and uterine fibroids interact is their expression of collagen. The stiffness of the ECM has a direct effect on fibroid formation and growth (Leppert et al., 2014). The stiffness of the ECM is due, in large part, to the large increase in collagen expression in the ECM. In fibroids, collagen fibrils are shorter and more disordered than normal myometrium, the ratio of Type I collagen to Type III collagen is altered, and there is much more Type V collagen in the ECM (Leppert et al., 2014). To determine the collagen ratio and amount expressed in the ECM, trichrome staining can be used. Trichrome staining visualizes connective tissues in the cells by staining the collagen blue, nuclei dark brown, muscle tissue red, and cytoplasm pink (Leonard et al., 2018).

Macromolecular crowders are used in cell culture to accelerate biochemical reactions and assembly, including ECM and collagen production (Zeiger et al., 2012). Ficoll and ascorbic acid should be added to supplemented VBM in the ring culture process. Ficoll is a hydrophilic polymer that is used to increase the density of cells within the media which creates a stable and supportive environment for cells (Zeiger et al., 2012). Ascorbic acid is a vitamin that aids in collagen synthesis when combined with media (Zeiger et al., 2012). This combination allows the rings to produce collagen and ECM that will mimic the tissue composition of myometrial tissue.

3.2.2.3 Functions to Accomplish Objective 3.

The model should be reproducible. For the model to successfully be replicated by any research company, it is important that the size, structure, and shape of the designs remain consistent when undergoing testing in the lab. To achieve reproducibility, each model should exhibit the same culture characteristics within in-vitro testing including media and incubation conditions. To culture the cells to ensure reproducibility, they should be cultured in Complete Media with 10% FBS for rat aortic smooth muscle cells (RaSMCs) or supplemented VBM for uSMCs, plated in tissue culture dishes or flasks, and incubated under normal SMC conditions at 37°C, 2% O_2, and 5% CO_2 (Prusinski Fernung et al., 2019). For best reproducibility, the cell density should also be well-defined throughout the project while varying for each experiment. As indicated in prior literature, cell densities for RaSMCs will be less, while uSMCs will be greater (Dikina et al., 2015). It is also very important that the needle gauges for the alginate beads and the 2% w/v agarose molds for the spheroids and rings remain the same throughout the experiments. The needle gauge sizes used include 22 g, 27 g, and 30.5 g. The dimensions of the spheroid agarose mold are 400 µL in diameter and 800 µL in depth. The dimensions of the ring agarose mold are 6 mm in depth, 3.75 mm in width, and 2 mm in the inner post (Gwyther et al., 2011).

For the design to be reproducible, the procedures must be followed closely for every test. This will allow for experiments with different types of cells, RaSMCs or uSMCs. RaSMCs are an

excellent modeling system to study all aspects of body function and disease as they proliferate quickly and are very forgiving cells (Dikina et al., 2015). It is important that the group understands how to undergo the protocols and designs with RaSMCs before working with uSMCs. The reproducibility of working with RaSMCs allows for simple and straightforward work with the uSMCs. The attention to detail in these procedures will also allow for different methods to be used. For example, two methods can be used to model spheroids, and these different procedures can be followed closely to repeat multiple times to determine which method is the best to create the spheroid model.

3.2.2.4 Functions to Accomplish Objective 4.

For the model to be effective, it needs to ensure cell viability. Cells, especially fast-growing cells, need to be properly distributed and maintained to stay viable. In models with thick layers of tissue, cells towards the middle of the model can be killed due to a lack of proper nutrient diffusion. The team will have to perform viability assays to ensure the model system is maintaining the viability of cells.

It is important that the model can react with nutrients and growth factors that will not harm it or the cells. It is important to ensure the culture conditions for each cell remain consistent and ensure viability throughout the whole project. As stated above, the cells should be incubated under normal SMC conditions at 37°C, 2% O_2, and 5% CO_2 to ensure viability (Prusinski Fernung et al., 2019). Throughout the experiment, different types of media are used to ensure the best viability for the cells. For RaSMCs, Complete Media with 10% FBS, glutamax, Pen-Strep, sodium pyruvate and non-essential amino acids are used for the media. This media allows the RaSMCs to proliferate and is carefully optimized for the characteristics for RaSMCs to be viable and have ideal cell health (Dikina et al., 2015). For uSMCs, supplemented VBM is used. Supplemented VBM is more specific to large human vessels, like the uterine cells (*Vascular Cell Basal Medium - PCS-100-030 | ATCC*, n.d.). It is also very important that the researcher follows the protocols very carefully and ensures sterility for the cells by cleaning everything with 70% isopropyl and making sure the hood stays sterile. Cell viability can also be measured through adjusting the size, shape, and culture time of the spheroid and ring. These parameters should be changed and tested to identify the viability of the cells.

Cell viability is very important when undergoing experiments that model an in-vivo problem. It measures the proportion of live and healthy cells within a population, and it is very important that as many cells are alive as possible to accurately mimic uterine fibroids in situ (*Overview of Cell Viability and Survival*, n.d.). To determine cell viability, cell viability assays will determine the health of the cells through the measurement of metabolic activity, ATP content, or cell proliferation (*Overview of Cell Viability and Survival*, n.d.). There are multiple different types of cell viability assays, including trypan blue, live/dead, and fluorometric assays. Trypan blue is a very cheap option but does not have enough direction to determine the color of the blue that indicates a live or dead cell (Piccinini et al., 2017). The live/dead cell imaging kit images cells under a microscope and shows whether the cells are alive (Sokolova et al., 2020). The fluorometric

assay works to determine cell viability through a resazurin-based solution and is the one the team will be using because it is within the budget and has multiple different tests in the product (*CellTiter 96® AQueous One Solution Cell Proliferation Assay | MTS Assay | MTT Assay*, n.d.).

3.2.2.5 Functions to Accomplish Objective 5.

The final design objective the model should achieve is that it is affordable and within budgetary constraints. The team is being given $750 to complete this project, so it is very important we do everything with the budget in mind. This includes having a low cell density and material usage and using multiple devices that are supplied by WPI. All assays and tests will be researched extensively before purchase. It also ensures that the team is optimizing materials, equipment, and time to get the most out of the budget.

3.3 Standard Design Requirements

For this project, a variety of standards will be needed for the approval and development of the model. One standard that is relevant to this project is "ASTM F2739-19: Standard Guide for Quantifying Cell Viability and Related Attributes within Biomaterial Scaffolds". This standard is considered relevant because it can be used for 3D scaffolds containing cells that have been cultured in-vitro, and the project is testing the viability of 3D scaffolds and cells in spheroids, rings, and alginate beads. Another standard that relates to the project is "ISO 10993-5 Third edition: Biological evaluation of medical devices - Part 5: Tests for in-vitro cytotoxicity" because it describes test methods that are designed to determine the biological response of mammalian cells in-vitro using appropriate biological parameters. Another standard that relates to the project is "ISO 11737-1 Third edition: Sterilization of health care products - microbiological methods - Part 1: Determination of a population of microorganisms on product" because it specifies the requirements and gives guidance on the enumeration and microbial characterization of the population of viable microorganisms on different products. This standard relates more to the sterilization and cleanliness of the lab area than the product.

It is also very important that ethical standards are incorporated into the design. These include multiple standards that reference risk assessments for safety and compliance with HIPAA laws. It is also important that the team follows aseptic techniques and good laboratory practices that are stated by the FDA guidelines throughout the whole project.

3.4 Revised Client Statement

As there are no effective in-vitro models used to mimic both uterine tissue and intramural fibroids, components of a 3D intramural uterine fibroid model will be developed. These components will have the potential to mimic the tissue composition of uterine fibroids and uterine tissue. The project will fulfill the objectives by replicating the fibroid/tissue interface, replicating tissue composition, allowing for reproducibility, ensuring cell viability, and being affordable. Successful cell viability is determined with 80% yield, affordability with the project cost remaining under $750, and reproducibility with consistency in the model fabrication and results. This will

allow for further research and increase understanding to develop treatment options for uterine fibroids.

3.5 Management Approach

Throughout this process, there have been major milestones that have been completed. The first milestone the team hit was finishing all testing on the RaSMCs. This was a large part of the process for the team to understand the protocols, perfect experiment technique, and gather equipment required for each test. The next milestone that the team achieved was attempting all experiments with uSMCs, excluding embedding the alginate beads. Once this milestone was completed, the team updated their paper and presentation with the results from the uSMC experiments. Figures 6, 7, and 8 show the Gantt Charts the team followed throughout B, C, and D terms, respectively.

The goals and experiments are technically connected because each experiment helped the team learn more about how the tissue composition and structural properties are expressed in each design. The largest goal was for the model to effectively mimic uterine and fibroid tissue, so each experiment provided more information about how the model can achieve that. Also, the goals and experiments are connected because there is an understanding of how the rings and spheroids grow, how the beads interact with the cells, and how the media and time help the cells, spheroids, and rings grow. These new discoveries fulfilled the client statement and developed components of a 3D intramural uterine fibroid.

Figure 7. Gantt chart for B term.

Stage	TASK TITLE	START DATE	DUE DATE	DURATION	TASK COMPLETION
1	Experimentation				
1.1	Order/arrange all necessary chemicals and equipment	12/16/22	1/10/23	24	0%
1.2	Revised Client Statement with specified goals	1/9/23	3/3/23	54	0%
1.3	Expand on desired functions for model and revise goals as needed	1/9/23	3/3/23	54	0%
1.4	Conduct experimentation with USMCs	1/11/23	3/3/23	52	0%
2	Methodology and Protocols				
2.1	Review existing methodology for experiments	1/9/23	3/3/23	54	0%
2.2	Refine methods for models	1/9/23	3/3/23	54	0%
2.3	Assess objective alignment with methodology	1/9/23	3/3/23	54	0%
2.4	Explore cell embedding in beads and refine protocol	1/9/23	1/20/23	11	0%
2.5	Refine protocols as needed	1/9/23	3/3/23	54	0%
2.6	Explore methods for alginate bead attachment	1/9/23	1/20/23	11	0%
3	Design Testing and Validation				
3.1	Write protocol for viability assay	1/9/23	3/3/23	54	0%
3.2	Assess objectives of viability and determine proper assay to use	12/16/22	1/9/23	23	0%
3.3	Refine test protocol	1/9/23	3/3/23	54	0%
3.4	Form concrete metrics for validation	1/9/23	1/20/23	11	0%
4	MQP Report				
4.1	Continue refining objectives, adjust as needed	1/9/23	3/3/23	54	0%
4.2	Review/refine client statement	1/9/23	3/3/23	54	0%
4.3	Review advisor comments and edit report	1/9/23	3/3/23	54	0%
4.4	Add results/conclusions as needed	1/15/23	3/3/23	48	0%
4.5	C-Term MQP Report submission	2/13/23	3/3/23	20	0%

Figure 8. Gantt chart for C term.

Stage	TASK TITLE	START DATE	DUE DATE	DURATION	TASK COMPLETION
1	Experimentation				
1.1	Viability testing	3/13/23	3/27/23	14	0%
1.2	Alginate bead degradation study	3/13/23	3/29/23	16	0%
1.3	Alginate gelatin copolymerized bead degradation study	3/19/23	3/29/23	10	0%
1.4	ECM testing of cells	3/13/23	3/15/23	2	0%
1.5	Ring experimentation and stains	3/16/23	4/9/23	23	0%
1.6	Spheroid Experimentation	3/13/23	3/27/23	14	0%
2	MQP Presentation				
2.1	Add new results as needed	3/15/23	4/12/23	27	0%
2.2	Review advisor comments and edit	3/15/23	5/3/23	48	0%
2.3	Add data and analysis of results	3/17/23	5/3/23	46	0%
2.4	Adjust experimentation as needed	3/18/23	5/3/23	45	0%
3	MQP Report				
3.1	Continue refining objectives, adjust as needed	3/13/23	5/3/23	50	0%
3.2	Add quantatative data and analysis from studies	3/13/23	5/3/23	50	0%
3.3	Review advisor comments and edit report	3/13/23	5/3/23	50	0%
3.4	Adjust discussion and conclusion as needed	3/13/23	5/3/23	50	0%
3.5	C-Term MQP Report submission	3/13/23	5/3/23	50	0%

Figure 9. Gantt chart for D term.

4.0 Design Process

4.1 Needs Analysis

To determine the best modeling approach to use for modeling uterine fibroids and the interactions between fibroids and the myometrium tissue, the team made a pairwise comparison chart. This decision-making matrix helped to condense all the information found in background research and apply it to the overall needs of the project.

These needs include replicating the fibroid/tissue interface, replicating tissue composition, making the model reproducible, ensuring cell viability, and an affordable model. The two most important aspects of making the model an effective modeling system are to replicate the fibroid/tissue interface and to ensure cell viability. It is essential that the model interfaces between the tissues as this could be used to develop new treatments for uterine fibroids and can accurately mimic in situ fibroids. Replicating tissue composition is important because collagen and ECM production should be comparable to myometrial tissue. Reproducibility is a very important need as this allows for the use and distribution of models, ensures consistent and effective testing during the project, and allows for standardization. The model should also ensure cell viability, and this is very important because the cells must be alive and proliferate for the model to function and form. Finally, it is important for the model to be affordable because it must adhere to the set budget and a lower overall budget makes it more likely to be used in research labs.

Table 3. Pairwise Comparison Chart

	Replicate fibroid/tissue interface	Replicate tissue composition	Be affordable within budget	Ensure reproducibility within model	Ensure cell viability	Total Score
Replicate fibroid/tissue interface		1	1	1	0.5	3.5
Replicate tissue composition	0		1	1	0.5	2.5
Be affordable within budget	0	0		0.5	0	0.5
Ensure reproducibility within model	0	0.5	1		0	1.5
Ensure cell viability	0.5	0.5	1	1		3.0

The pairwise comparison chart helped to orient the project around the objectives, and to prioritize some objectives over others. The team scored the replication of the fibroid/tissue

interface and cell viability as the most important objectives to keep in mind when moving forward with the project design. The entire goal of the project is to replicate the fibroid/tissue interface which must be a top priority when undergoing the experiments. It is also very important to ensure cell viability throughout the project because without viable cells, ECM and collagen will not be produced which will not correctly mimic the structure of the uterine tissue and composition of collagen and ECM.

4.2 Alternative Designs

After completing thorough research on modeling systems like 3D ring structures, 3D spheroids, 3D bioprinting, xenografts, and microfluidic models, the team generated different designs to figure out the best model for the project. These designs were created from the pairwise comparison chart shown above.

The first design that the team will use is a spheroid uterine SMC design, as seen in Figure 10. Spheroids are used in literature to study cancer and are used to test the effectiveness of potential therapeutic agents (Carvalho et al., 2015). In this design, the cells interact with each other to form a 3D spheroid and are representative of the cellular aggregate of fibroids. Spheroids are easy and fast to form, however, they are not a long-term method because internal necrosis happens very quickly. This design will be used to test the viability of cells in the spheroid, size, and yield.
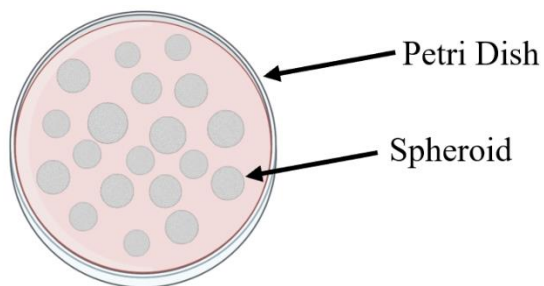
Figure 10. Model #1 - 3D spheroid design (created with BioRender.com).

The second design that the team will use is a 3D ring uSMC design, as seen in Figure 11. Rings have been used to represent muscular vascular tissue and uterine tissue in previous literature (Souza et al., 2017) (Strobel et al., 2017). This design requires cells to interact with each other to form a 3D ring and are representative of myometrial tissue. Rings are beneficial because they allow for easy testing of collagen deposition, however, they take more time and yield fewer runs per experiment than spheroids. This design will be used to test collagen deposition, ring thickness, and yield.

Figure 11. Model #2 - 3D ring design (created with BioRender.com).

The third design is embedded smooth muscle cells into the alginate bead, as seen in Figure 12. Alginate beads are used in a variety of biomedical areas primarily wound healing and drug delivery. They are advancing as a modeling system due to their biocompatibility and customizable properties (Ashimova et al., 2019). This design is very representative of fibroid cells interacting with fibroid ECM. The bead gives the cells a protected environment and can mimic the fibroid structure very well. This design allows for easy control of cell-ECM interactions. However, there is a difficult sterilization process to create the alginate beads to the viscosity of the solution. This design will be used to test the size, structure, shape, and reproducibility of the cells within the beads.
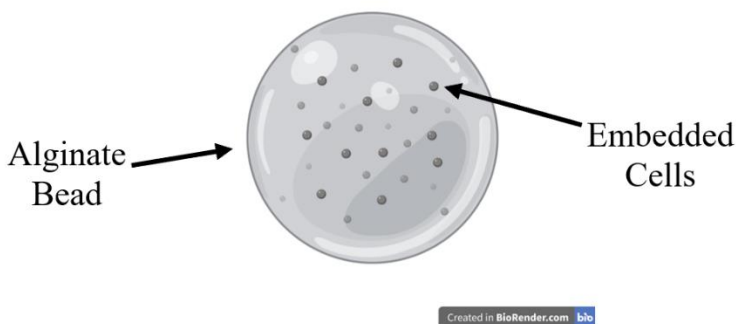
Figure 12. Model #3 - Alginate beads with embedded smooth muscle cells (created with BioRender.com).

The fourth design is combining rings with alginate beads, as seen in Figure 13. With the use of self-assembling tissue rings and the attachment of alginate beads to the ring structures, a model with physical properties and tissue composition similar to that in-vivo may be produced. This modeling system could then be used as a model for drug discovery and for the development of new treatments. This design is more representative of the interaction between the fibroid and myometrium tissue. This model will allow for the beads to be modeled inside and outside the ring, representing the different structures fibroids can take on around the myometrium. A limitation to this model is that surface modification is needed to allow the beads to interface with the rings. This design will be used to test ECM deposition and how fibroids/myometrium tissue could interface.
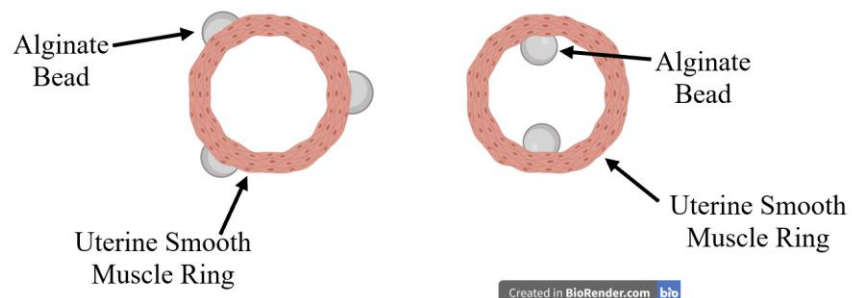
Figure 13. Model #4 - 3D ring design incorporated into alginate beads (created with BioRender.com).

4.3 Final Design Selection

Below is a selection matrix chart that compares each of the models shown above and relates them to the objectives and needs established. This chart weighs and ranks each model and helps the team determine the best model to use. The baseline used to gauge against alternative designs was the Xenograft model, the gold standard that was previously identified. The xenograft model that was researched for this baseline used human uterine fibroid tissue implanted into immunocompromised mice to assess the fibroid growth upon adding various hormones (Fritsch et al., 2015).

Table 4. Selection Matrix for Determining the Ideal Modeling System for Uterine Fibroids

Requirement	Weight	Baseline (Xenograft)	Model 1 – Spheroids	Model 2 – Rings	Model 3 – Alginate Beads with Cells	Model 4 – Rings with beads
Replicate fibroid/tissue interface	3.5	0	-1 (3.5)	-1 (3.5)	+1 (3.5)	+1 (3.5)
Replicate tissue composition	2.5	0	0 (2.5)	+1 (2.5)	+1 (2.5)	+1 (2.5)
Be affordable within budget	0.5	0	+1 (0.5)	+1 (0.5)	+1 (0.5)	+1 (0.5)
Ensure reproducibility within model	1.5	0	+1 (1.5)	+ 1 (1.5)	+1 (1.5)	+1 (1.5)
Ensure cell viability	3.0	0	0 (3.0)	0 (3.0)	+1 (3.0)	+1 (3.0)
Rank Score			-1.5	1.0	11.0	11.0

After going through the process of the pairwise comparison chart and the selection matrix, it was determined alginate beads with cells and rings with beads would make the best models because they have the highest rank score which means they hit all the objectives needed.

The selection matrix helped to prioritize the most important objectives outlined in the pairwise comparison chart and weighted how they were prioritized in different types of modeling systems. For example, the rings with beads replicate the fibroid/tissue interface and ensure cell viability throughout the growing process. Since these two objectives are high priorities, their influence over the overall score is higher.

5.0 Design Verification

5.1 Design of all Experiments and Tests

The alternative models mentioned in Section 4 were experimented with and tested on during the last seven weeks. After the alternative models were established, design processes were created for each model that elaborated on how the team would go about creating each model. These designs each include the goal, constant, independent, and dependent variables, and hypotheses.

5.1.1 Spheroids

The goal of developing 3D spheroids was to determine the most effective method of spheroid formation, to be used at first on the rat aortic smooth muscle cell line (WKY12-22, ATCC), then on primary human uterine SMC cell line (PCS-460-011, ATCC). The variables that were kept constant are the incubation and culture conditions. The spheroids were incubated at 37°C, 95% humidity, and 5% CO_2. The RaSMC spheroids were cultured in Complete Media. This media consisted of Dulbecco's Modified Eagle Medium (DMEM), FBS, Nonessential Amino Acids (NEAA), Glutamax, Pen-Strep, 10% FBS, and sodium pyruvate. The uSMCs were cultured in supplemented Vascular Basal Media (PCS-100-030, ATCC), supplemented with the Vascular Smooth Muscle Cell Growth Kit (PCS-100-042, ATCC). The independent variables for this experiment were the method of creating the spheroids and the incubation time. The two different methods of spheroid formation: the agarose mold method and the hanging drop method, were chosen because most prior research in forming spheroids used one of these two methods. In the agarose mold method, an agarose mold is filled with a cell suspension, which settles into rounded wells. The cell suspension then self-aggregates into spheroids. In the hanging drop protocol, a cell suspension is pipetted onto the lid of a petri dish, then inverted. Spheroids form within the drops. A detailed protocol for these two methods can be seen in Appendix E and F. They are highly documented methods and were accessible to the team.

The spheroids were incubated for 1, 3, and 5 days. These times were chosen because all protocols state the spheroids need 24 hours to form, and the extra hours were to allow for the further growth of the spheroids. The dependent variables were the size consistency, the number of spheroids produced, and the viability of the cells. The hypothesis stated that the agarose method would produce more spheroids, would have better size consistency between spheroids, and would contain more live and healthy cells than the hanging drop method. The agarose mold method has the potential to produce a maximum of 256 spheroids per large mold and 96 spheroids per small mold, whereas the hanging drop method produces 20-25 spheroids per run. It was also hypothesized that 48 hours of incubation time would grow the cells to the size that the team needed for them to interact with the alginate bead.

Determination of the ideal spheroid formation protocol was achieved using three benchmarks: spheroid viability, number, and size. Many larger spheroids (>150μm) exhibit hypoxia-induced necrosis at their core due to a lack of gas and nutrient exchange (Anada et al, 2012). Due to the potential necrosis in the interior, a benchmark viability of 80% after 3 days and

50% after 5 days were established, as discussed in prior literature (Ningsih et al, 2021). The spheroid number was also taken into consideration and was quantified simply by counting the number of spheroids that were able to be extracted from the molds. The percent yield of the total amount of spheroids produced per run was also considered in deciding the best spheroid formation protocol. The benchmark yield of 70% was established, to consider the high likelihood of spheroids remaining stuck inside the mold. Current research indicates that the maximum spheroid diameter before necrosis is approximately between 100–150μm (Anada et al, 2012). However, this varies between cell types and is an approximation. To account for this, the benchmark for spheroid size was established at no greater than 200μm. Viability testing was performed to determine the viability at this diameter using the CellTiter 96® AQueous One Solution Cell Proliferation Assay, a colorimetric assay that measures viability through the measurement of metabolic activity. A larger diameter decreases the viability at the core of the spheroid. Consistency in spheroid diameter was also determined, by determining the standard error of the average measurements of the spheroids.

5.1.2 Rings

The goal of developing 3D rings was to determine the most time and cell-efficient ring formation, to be used at first on rat smooth muscle cells (RaSMCs), then human uterine smooth muscle cells (uSMCs). The variables that were kept constant were the incubation, culture, and ring conditions. The rings were incubated at 37°C, 95% humidity, and 5% CO_2. The RaSMC rings were cultured in Complete Media with 10% FBS. The uSMCs were cultured in supplemented Vascular Basal Media. Constant experiment conditions were that the ring would be incubated initially for 24 hours unbothered, and the media would be changed every two days after that initial period. The independent variable was the growth time of the rings. The rings were removed from their mold and tested for the dependent variables on days 8, 10, and 14. The dependent variables were ring size, structure, and collagen production. It was hypothesized the rings grown at 10 days will grow into the most consistently shaped and sturdy rings that produce collagen most similar to in situ myometrial tissue production.

For the rings to reach this goal, three benchmarks were created including thickness, collagen expression, and intactness. This thickness will range anywhere between 0.84 to 0.87 mm diameter after 14 days in ring culture with a 2 mm inner diameter (Dash et al., 2016). This benchmark has been tested previously in Dash et al., 2016 and proves this ring size allows for the rings to withstand stretching and compacting. A plentiful and strong collagen expression on the edges of the ring proves a strong ring structure, helpful when removing the rings from the mold and during possible contraction. This collagen will be abundant and isolated to the inside and outside of the ring as well as the fibrils should be long and uniform in these locations (Dash et al., 2016). The collagen was tested using Gomori's Trichrome staining and stained the collagen blue and the muscle fibers pink (Aleksandrovych, 2018). Intactness relates to both the ring and the agarose well. The intactness of the ring shows the self-aggregation of the cells while the intactness of the agarose well makes sure the posts and wells stay in shape so the rings can grow uniformly.

The rings break during the removal process, and this differs according to each experiment (Dash et al., 2016). During the RaSMC experiments, one ring was allowed to break because they are stronger and adhere better than the uSMCs. During the uSMC experiments, three rings were allowed to break because they are more sensitive and fragile than the RaSMCs.

5.1.3 Alginate Beads

The goal of creating alginate beads was to determine the most effective method of creating alginate beads while maintaining structural integrity and consistent reproduction. The initial constant variables for this design were a 15-minute wait time for crosslinking, Complete Media with 10% FBS rinse, stir speed, and temperature. The independent variables were the speed of the solution during extrusion and needle size. The dependent variables were consistency in the size and shape of the beads. It was hypothesized that the beads would be more reproducible, structurally solid, and the smallest in diameter with ionic crosslinking using calcium chloride and using the homogenizer during the formation. The goal changed upon consideration of how the alginate beads would be used as an independent modeling system and after issues in fabrication. The smaller bead size was no longer the goal of this model due to cell encapsulation. The needle size and speed of extrusion was consistent, and a homogenizer was no longer used. All aspects of bead formation, aside from alginate concentration and the presence of cells or gelatin, remained consistent. Alginate concentrations of 2%, 1.2%, and 0.8% were used.

To achieve the goal of using alginate beads as an independent modeling system the benchmarks of bead size, number of beads, and reproducibility were created. The bead size ensured that there was enough room within the beads for cells to proliferate. The number of beads selected provided a sufficient amount to be observed over time. Reproducibility ensured that the bead fabrication was consistent throughout experiments. When exploring the interface of beads with cell adhesion or rings various techniques of surface modification were researched. Gelatin was selected due to easy access and ease of inclusion in the fabrication process. Crosslinking gelatin with the alginate in beads was meant to aid in the cell adhesion process, and it was added at 0.5% (w/v).

5.2 Experimental Methods to Test Designs

To test the designs stated above, different experimental methods were followed, keeping the design in mind. The team followed the step-by-step protocols that are written out in the Appendices D, E, F, G, H, I, J, K, and L very closely.

5.2.1 Spheroids

Two methods of spheroid formation were tested to determine the most effective method. This was determined using the benchmarks of viability, spheroid size, and spheroid number.

5.2.1.1 Hanging Drop Method.

To create spheroids using the hanging drop method, cells were first cultured to 80% confluency to ensure that there were enough cells to form the spheroids. The following steps were performed to prepare the cells for seeding and to ensure the molds were seeded at the right density: trypsinization, neutralization of trypsin, cell counting, and cell suspension. A detailed explanation of the specific culturing processes for each cell type can be seen in Appendix B and Appendix L. The final cell suspension concentration used to seed the hanging drop spheroids was 2.5×10^6 cells/mL. This cell suspension was dropped onto the lid of a 60 mm tissue culture dish at 25 drops per dish. The formed spheroids are visible to the naked eye, so it is apparent when they are formed. They will be floating in the middle of the drop on the lid. This process can be seen in Figure 14. To harvest the spheroids, media should be added to the lid, pipetted up with the spheroids, and transferred to another dish with media. The protocols for each spheroid formation method can be seen in Appendix E and F.
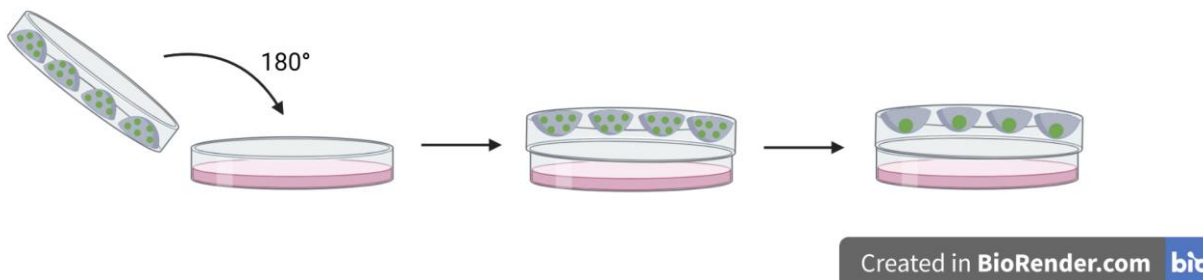
Figure 14. Image of the steps to the hanging drop method (Created with BioRender.com).

5.2.1.2 Agarose Method.

To create spheroids using the agarose method, cells were cultured for approximately 3 days from passage to reach a confluency of about 80%. Like the hanging drop method, cells underwent trypsinization, neutralization of trypsin, cell counting, and cell suspension before they were seeded into the molds. The spheroid molds, shown in Figure 15, were made beforehand with 3% (w/v) agarose. The cells were seeded into the molds at a cell density of 0.5 million per 100 µL. The smaller molds held 75 µL of cell suspension and the larger molds held 190 µL These molds have the same spheroid well dimensions (400µL diameter, 800µL depth), but the larger mold has 256 spheroid wells, and the smaller mold only has 96 wells. The molds sat in the hood to settle, then were incubated overnight to allow the spheroids to form in the wells. Spheroids were cultured for a maximum of 5 days and were imaged and tested for viability at days 1, 3, and 5. The spheroids were considered formed when the spheroids were visible in the middle of the well and took up more than ¾ of the well diameter. To harvest the spheroids, the molds were flipped upside down and carefully dropped with the plate to force the spheroids down into the media.
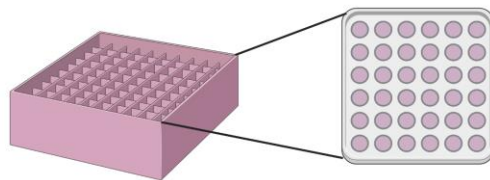
Figure 15. Image of the agarose mold (Created with BioRender.com).

5.2.2 Rings

Just like the spheroids, before the rings can be created, the cells were cultured and grown, as well as trypsinized, counted, and cell suspension was made. The 2% (w/v) agarose ring molds, as seen in Figure 16, were made, and set to rest for a day in the media beforehand.
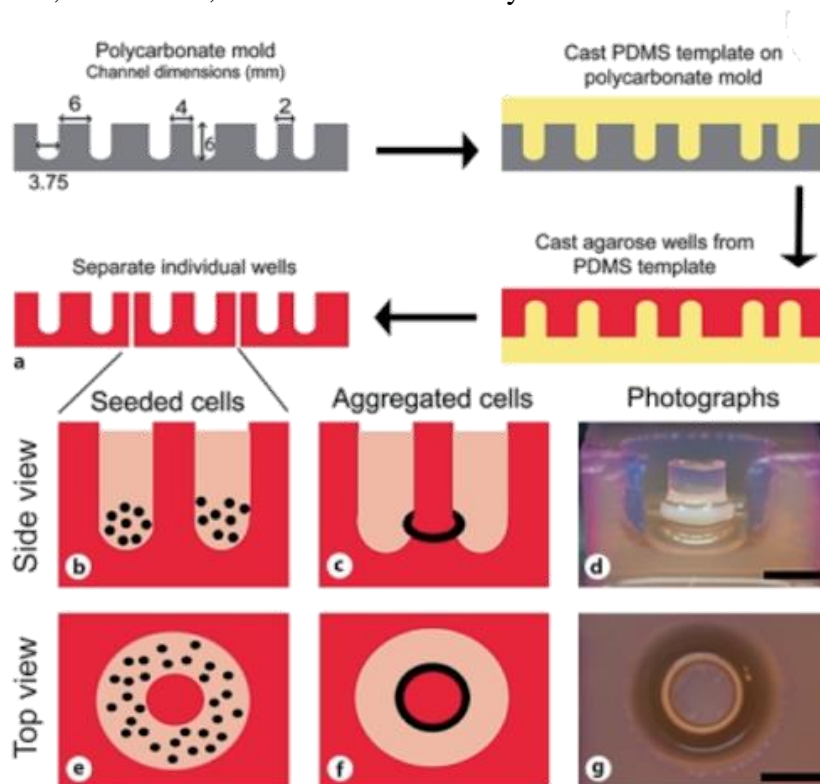
Figure 16. A. How the agarose wells are made from the PDMS template. B and E. View of the seeded cells on day 0. C and F. View of the aggregated cells after formation. D and G. Real visuals of a formed ring in the mold (Dash et al., 2016).

The cell concentration for RaSMCs was 1×10^9 cells/mL and for uSMCs was 1.2×10^9 cells/mL. The cell concentration differs for the different cell types because human smooth muscle cells produce less ECM than rat smooth muscle cells, which prohibits their growth (Dash et al., 2016). The cells were seeded at 5×10^5 cells per well for RaSMCs and 6.5×10^5 for uSMCs. 50

µL of cell suspension was added into each well of the molds along with fresh media. The rings were then cultured for the desired amount of time of 8, 10, or 14 days. The rings were formed when visible to the naked eye and 8, 10, or 14 days passed. To harvest the rings, tweezers were used to carefully remove the ring from the post and placed in a different dish with PBS-. Images of the rings were taken every day with a Zeiss microscope and the thickness was measured with ImageJ software.

The rings were then fixed in 10% Formalin for one hour and processed overnight. The processed rings were then embedded in paraffin and sectioned into 5 mm sections. These sections were dried and prepared to be stained. The stain used was Gomori's trichrome stain to evaluate the collagen production of the rings and compare it to the collagen produced by myometrium tissue, as seen in Figure 17 below, produced by Aleksandrovvch, 2018.
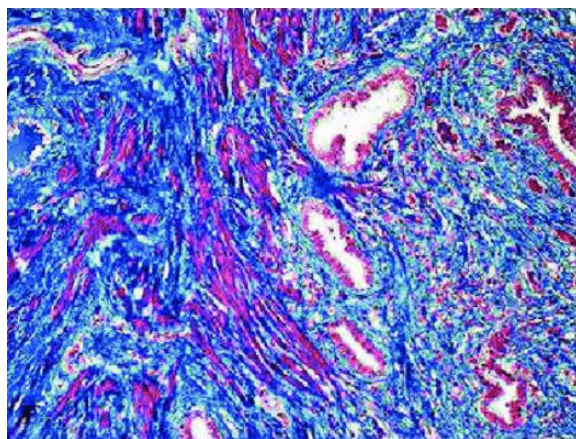
Figure 17. Trichrome stain of human myometrium tissue. The blue represents collagen while the pink represents muscle fibers (Aleksandrovych, 2018).

5.2.3 Alginate Beads

A buffer solution of HEPES and NaCl as well as a calcium chloride solution was first prepared before forming the beads, as well as the alginate solution using these buffers. The alginate solution was fabricated using a 2% alginate solution composed of alginic acid sodium salt along with a HEPES and NaCl buffer. The solution was heated and stirred for 30 minutes to dissolve the alginate. The bead extrusion used a 0.1 M calcium chloride solution and syringe. The solution was slowly extruded into the calcium chloride and left for 15 minutes to crosslink into beads. This process can be seen below in Figure 18. After stabilization, they were rinsed in a conical tube with Complete Media with 10% FBS. These steps formed the beads quickly, and they were tested using 22g, 27g, and 30.5g needles to form different bead sizes. Ultimately a 27g needle was used in the majority of these studies including the degradation study for consistency in size.

Figure 18. Image of the alginate bead fabrication method.

Gelatin was selected for surface modification to aid in the cell adhesion process due to its easy accessibility and inclusion in the fabrication process. Gelatin was combined with sodium alginate solution at 0.5% w/v as described in Appendix D. All other fabrication procedures remained the same as stated previously when creating alginate-gelatin crosslinked beads. RaSMCs were encapsulated in the beads during the first degradation study. The cells were seeded at 600 cells/mL to achieve approximately 20 cells per be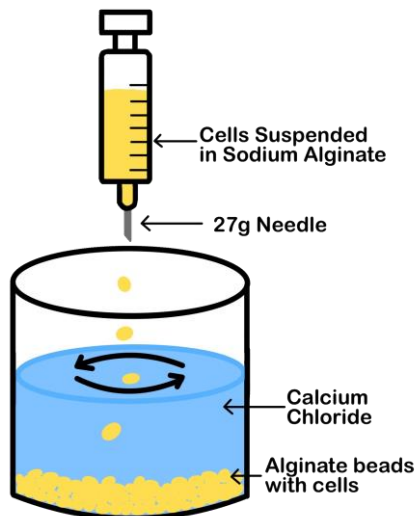ad with 30 beads being fabricated from 1 mL. Detailed cell encapsulation procedure for alginate beads can be found on Appendix H. Cells were encapsulated by suspending the cell pellet in the alginate solution and completing the fabrication process as normal, and the media was changed every 2 days.

A degradation study was completed to determine the ideal concentration for forming alginate and alginate-gelatin crosslinked beads. The bead fabrication protocol was consistent for this experiment, the variables were alginate concentration and the presence of gelatin. The first study was conducted without cells using alginate concentrations of 0.8%, 1.2%, and 2% w/v all with and without 0.5% w/v gelatin. The degradation was studied by recording the bead diameter for 10 days without cells and 5 days with cells. The beads were placed in a 24 well plate and their diameters were recorded every 2 days prior to media changes for beads with cells embedded. For the second trial of this experiment, it was determined that more frequent measurements could provide detailed data in studying the degradation. This experiment was completed without cells at alginate concentrations of 2%, 1.2%, and 0.8% w/v and gelatin at 0.5% w/v combined with the 2% and 1.2% w/v alginate. Measurements were taken every 12 hours for five days in the second degradation study in beads without cells encapsulated. Detailed procedure for the degradation study of alginate beads can be found in Appendix I.

5.3 Experimental Results

All the experiments stated above resulted in preliminary data for the initial tests. Experiments with RaSMCS and uSMCs were performed throughout the year. RaSMC testing

occurred as a preliminary step to ensure that protocols were understood and that the cells were handled correctly before testing occurred with more fragile uSMCs.

5.3.1 Spheroids

5.3.1.1 Hanging Drop Method.
Spheroids were created using the Hanging Drop Method described in Appendix E. After the incubation period (two days), 80% of the spheroids in 20 drops were able to be removed from the lid. This was because the size of the pipet tip was not small enough to accurately pick up the size of the spheroids. It was also possible that not enough media was used to cover the entire lid and immerse the spheroids into the new media. The average size of the spheroids was 236 ± 9.67 µm. This size was the largest of both the spheroid iterations, and well above the benchmark value of 150 µm diameter. All 16 spheroids that were removed from the lid were consistent in size and shape, with only one spheroid having an elongated-oval shape. The images below show three different spheroids from this experiment and their diameters. These spheroids were not self-aggregated well, and most of them fell apart when removed from the plate. Viability for these spheroids was measured through the trypan blue viability assay described below, but the results were inconclusive.
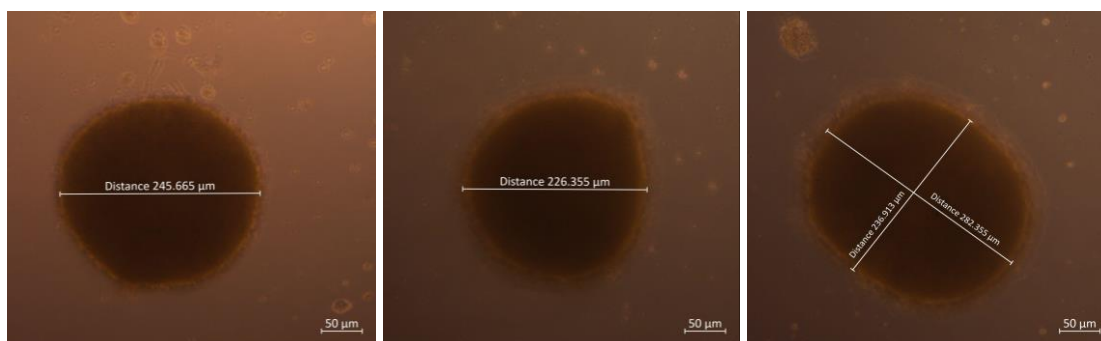
Figure 19. Three different spheroids collected from the first hanging drop experiment. Images taken at 10x objective (scale bar = 50µm).

To definitively measure the viability of the spheroids and to experiment with different seeding densities, another hanging drop experiment was performed. The drops were seeded at 2.5 x 10^6 cells/mL, as stated in the protocol, 1.25 x 10^6 cells/mL, or 0.75 x 10^6 cells/mL. These drops were imaged and tested for viability at D1, D3, and D5 of the experiment. To test viability, the CellTiter 96® AQ$_{ueous}$ One Solution Cell Proliferation Assay was used to test viability instead, because the results were more quantitative. It is a colorimetric assay that measures viability through absorbance when compared to a standard curve.
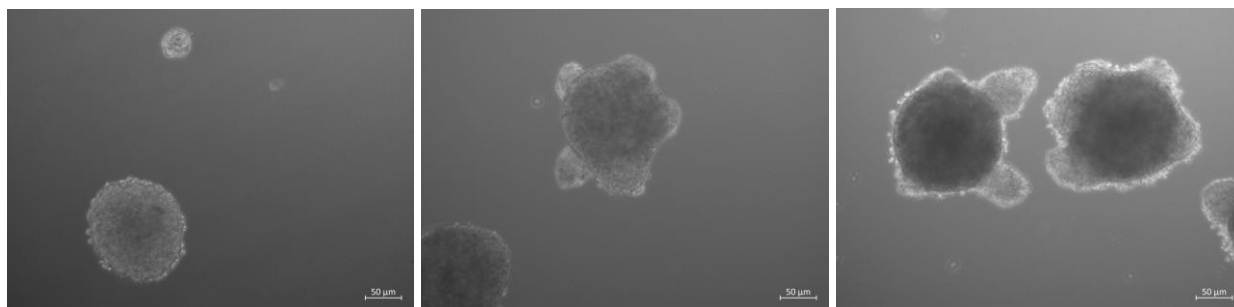
Figure 20. D1 (left), D3 (center), and D5 (right) images of the spheroids of a suspension density of 0.75 x 10⁶ cells/mL. Images taken at 10x objective (scale bar = 50μm).
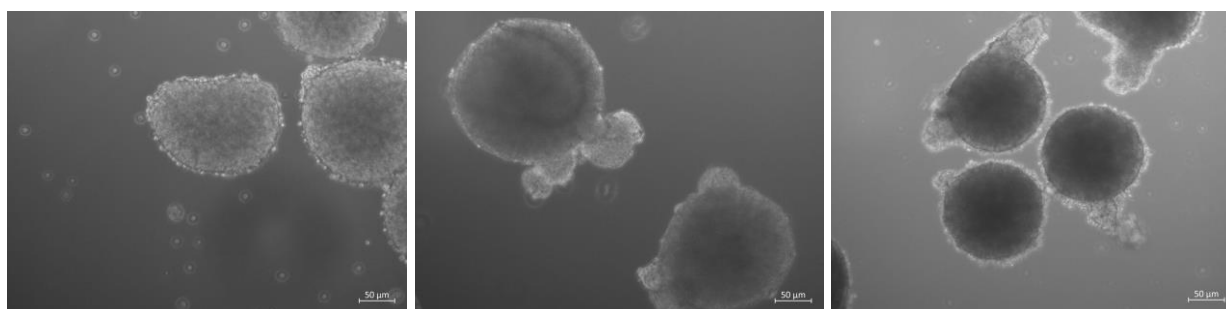
Figure 21. D1 (left), D3 (center), and D5 (right) images of the spheroids of a suspension density of 1.25 x 10⁶ cells/mL. Images taken at 10x objective (scale bar = 50μm).
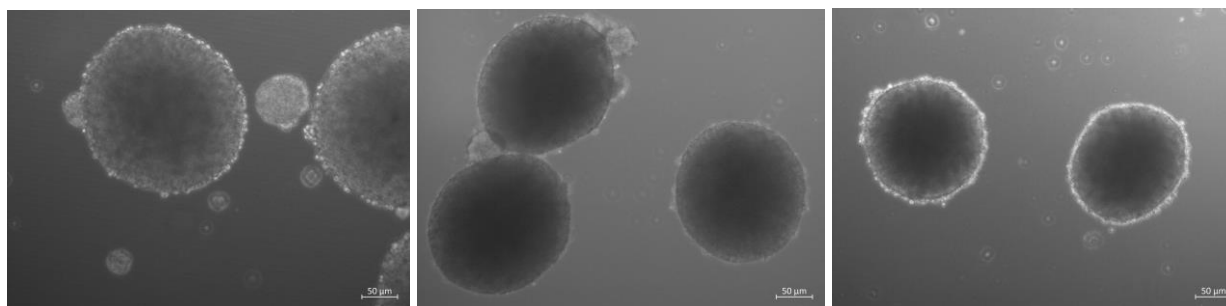
Figure 22. D1 (left), D3 (center), and D5 (right) images of the spheroids of a suspension density of 2.5 x 10⁶ cells/mL. Images taken at 10x objective (scale bar = 50μm).

Interestingly, the spheroids seeded at a lower cell density had significantly more shape abnormalities, which became more pronounced over time. The spheroids seeded at 2.5×10^6 cells/mL did not have the same degree of protrusions as the 1.25×10^6 and 0.75×10^6 spheroids.

The 2.5×10^6 spheroids had an average diameter of 212.02 ± 65.63 μm at D1, 161.27 ± 69.99 μm at D3, and 123.50 ± 54.51 μm at D5. The average aspect ratio for each of these days was 0.86 ± 0.11, 0.87 ± 0.07, and 0.81 ± 0.16, respectively.

The 1.25×10^6 spheroids had an average diameter of 155.79 ± 34.83 μm at D1, 129.46 ± 64.47 μm at D3, and 135.87 ± 43.99 μm on D5. These spheroids had an average aspect ratio on each day of 0.83 ± 0.11, 0.88 ± 0.10, and 0.81 ± 0.11 respectively.

The 0.75 x 10^6 spheroids had an average diameter of 133.77 ± 16.93 μm at D1, 158.97 ± 55.40 μm at D3, and 150.16 ± 21.62 μm at D5. They also had aspect ratios of 0.88 ± 0.06, 0.75 ± 0.16, and 0.74 ± 0.12, respectively. The wide range in diameter between days and spheroids is due to the formation of smaller spheroids (<50 μm diameter) alongside the larger spheroids, as seen in the left image of Figure 22. In addition, multiple spheroids appear to form in Histograms of spheroid size distribution are shown for each cell seeding density and day below. A higher number of smaller spheroids formed in the hanging drop experiments seeded at lower cell densities.

Table 5. Average Size of Hanging Drop Spheroids at Different Seeding Densities Over Time

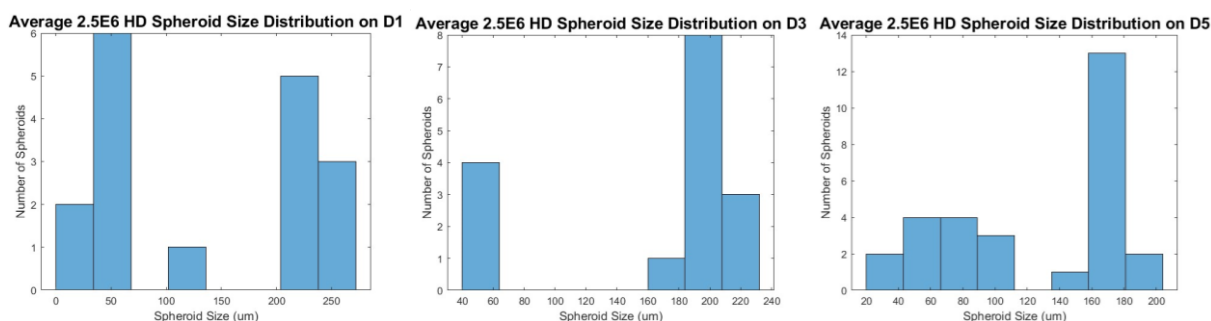| Seeding Density (cells/mL)	Size on D1 (μm)	Size on D3 (μm)	Size on D5 (μm)
2.5 x 10^6	212.02 ± 65.63	161.27 ± 69.9	123.50 ± 54.51
1.25 x 10^6	155.79 ± 34.83	129.46 ± 64.47	135.87 ± 43.99
0.75 x 10^6	133.77 ± 16.93	158.97 ± 55.40	150.16 ± 21.62

Figure 23. Histograms of the average spheroid size distribution of the spheroids seeded at 2.5 x 10^6 cells/mL for D1 (left) (N=1, n=17), D3 (center) (N=1, n=16), and D5 (right) (N=1, n=29).
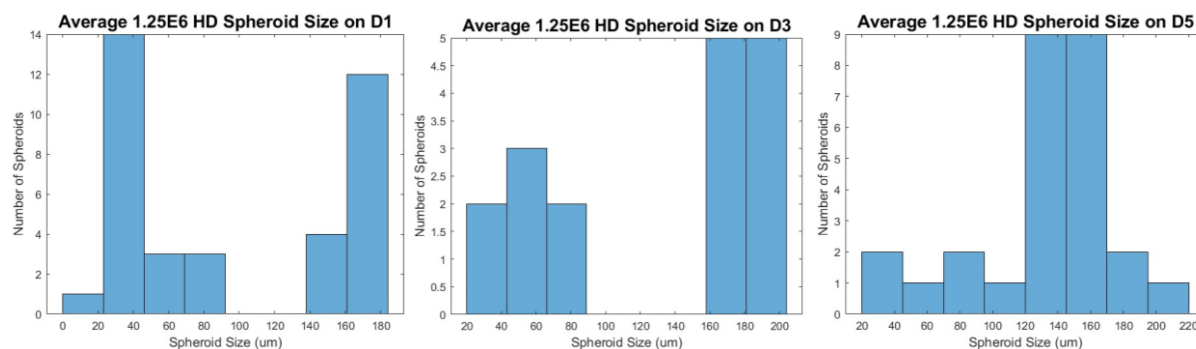
Figure 24. Histograms of the average spheroid size distribution of the spheroids seeded at 1.25 x 10^6 cells/mL for D1 (left) (N=1, n=37), D3 (center) (N=1, n=17), and D5 (right) (N=1, n=27).
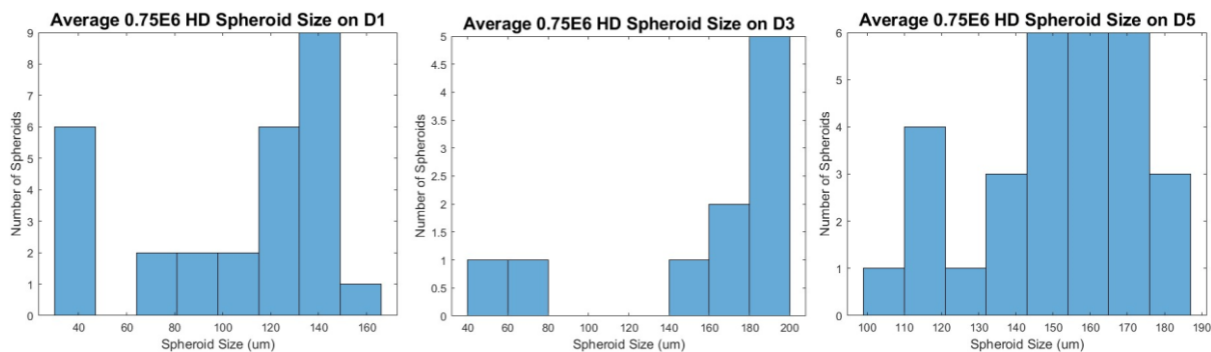
Figure 25. Histograms of the average spheroid size distribution of the spheroids seeded at 0.75 x 10⁶ cells/mL for D1 (left) (N=1, n=28), D3 (center) (N=1, n=10), and D5 (right) (N=1, n=30).

The percent yield for each day and each cell density were also calculated for this experiment, as shown in the table below. This was relatively consistent across all days and all densities. The yield staying relatively consistent means that it is likely that there were few issues with cells sticking to the petri dish and that the methods of spheroid retrieval work well for this application. Though there are high percent yields, this is not indicative of the actual numbers collected. The hanging drop method can only yield 20-25 spheroids per run, which is expensive in time and cost.

Table 6. Percent Yield of Hanging Drop Spheroids at Different Seeding Densities Over Time (N = 1; n =1)

Seeding Density (cells/mL)	Yield on D1	Yield on D3	Yield on D5
2.5 x 10⁶	88%	80%	92%
1.25 x 10⁶	100%	80%	92%
0.75 x 10⁶	92%	80%	88%

The viability of the spheroids was taken at D1, D3, and D5 using the CellTiter 96® AQ$_{ueous}$ One Solution Cell Proliferation Assay (G3582, Promega), a colorimetric assay that measures viability through absorbance when compared to a standard curve. The protocol can be found in Appendix K. The results of these viability tests are shown in Figures 26-29. The 1.25 x 10⁶ spheroids appear to have the highest consistent viability, as they had the highest viability on D1 and D5. None of the spheroid formulations hit the benchmark viability of 80% on D3, but the 1.25 x 10⁶ and 2.5 x 10⁶ spheroids hit the 50% viability benchmark on D3.

Figure 26. Graph of the average percent viability and standard deviation of the hanging drop spheroids for each spheroid cell density on D1 (N = 1; n = 3).

Figure 27. Graph of the average percent viability and standard deviation of the hanging drop spheroids for each spheroid cell density on D3 (N = 1; n = 3).
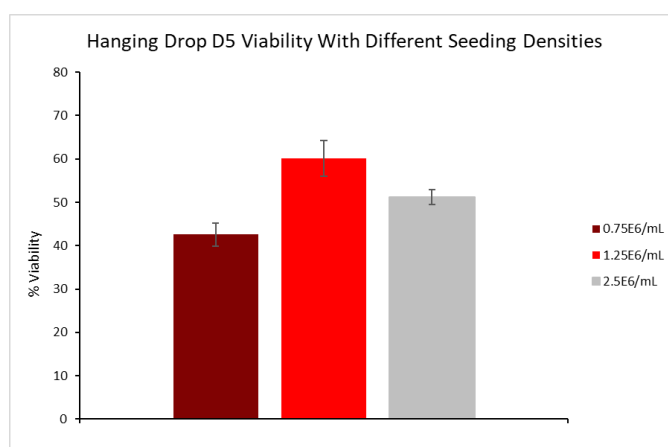
Figure 28. Graph of the average percent viability and standard deviation of the hanging drop spheroids for each spheroid cell density on D5 (N = 1; n = 3).
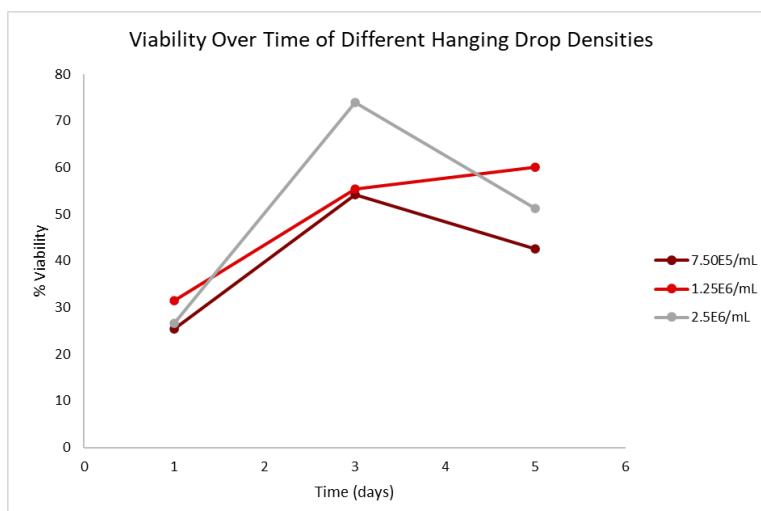
Figure 29. Graph of the change in viability for each spheroid cell density over time.
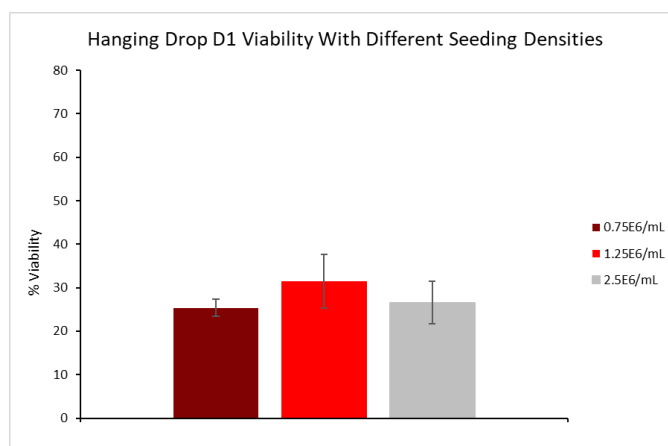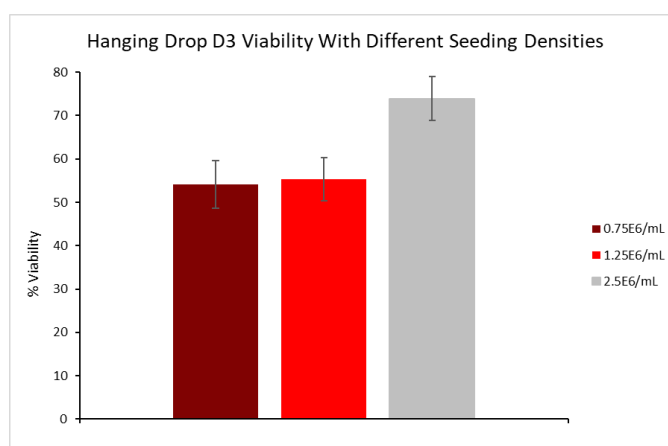
The jump in every viability on D3 across the spheroids indicates that the absorbance read much higher that day. This could be due to several reasons. The highest viability was the viability of the 2.5 x 10^6 spheroids, at 73.9%. This could be due to a higher number of cells on the surface, or at a distance into the spheroid that allowed for O_2 and nutrient exchange. More testing is needed to definitively determine if spheroid viability is higher on D3 because this experiment was only run once.

An important objective the team wanted to ensure throughout the experiments was cell viability. There are many ways to determine cell viability, however, the one type that was available to the team was the trypan blue assay. A protocol was found in the literature, stated in Appendix C, and followed closely by the team (Piccinini, F. et al., 2017). However, the team did not get adequate results due to a lack of set definitions of "live" and "dead" and varying counts between researchers, it was determined the Trypan Blue assay is not an effective assay for this application. Instead, the CellTiter 96® AQ_{ueous} One Solution Cell Proliferation Assay was purchased and used to ensure much better results during viability testing.

5.3.1.2 Agarose Mold Method.

The method for forming spheroids using agarose molds is stated in Appendix F. The agarose mold experiment was attempted three separate times to ensure reproducibility and to confirm results. All experiments used three small agarose molds and three large agarose molds. The small molds fit 75 µL of cell suspension per well and the large molds fit 190 µL of cell suspension per well. Before any experimentation to produce meaningful data, spheroids were formed via the agarose method and cultured for 3 days, to ensure correct cell handling and procedure implementation. In this initial run, spheroids were seeded at 5 x 10^6 cells per mL and then incubated for three days before being imaged or removed from the mold. Upon return, the spheroids were no longer only in their individual wells, they were all merged in both the large and small molds. This was likely due to an error in cell density calculations.

Another initial experiment was performed with the same procedure as described above to ensure that the agarose method protocol was perfected. The spheroids were seeded at 5 x 10^6 cells per mL and then incubated for three days before being imaged and/or removed from the mold. This incubation period and seeding density created very consistently sized and shaped spheroids that did not overflow from their wells. An image of the spheroids from this run in their molds is shown below.
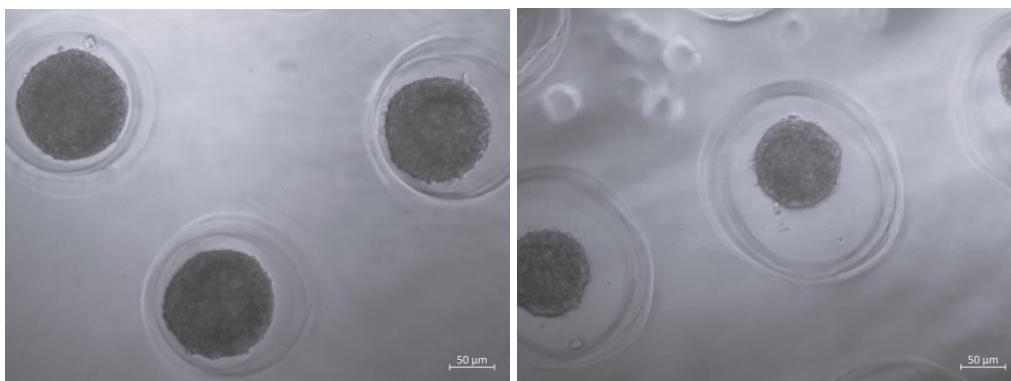
Figure 30. Large (right) and small (left) molds imaged on D3 of the second experiment. Images taken at 10x objective (scale bar = 50μm).

This experiment was then run three times with RaSMCs to ensure consistent side distribution and viability. No testing with uSMCs was performed due to several bouts of contamination and human error in handling the cells. The spheroids were seeded at 5 x 10^6 cells per mL and cultured for five days, with imaging and viability testing at D1, D3, and D5. Viability testing was performed for these spheroids using the CellTiter 96® AQ$_{ueous}$ One Solution Cell Proliferation Assay. The first run was not tested for viability, as the viability test reagent was not available at the time. These spheroids were significantly smaller than the HD spheroids and their size was more consistent. The average diameters of the larger (190 µL) mold spheroids were 111.83 ± 9.40 µm at D1, 118.97 ± 16.40 µm at D3, and 100.50 ± 12.95 µm at D5. The aspect ratios of these spheroids were 0.94 ± 0.3, 0.94 ± 0.3, and 0.90 ± 0.09, respectively. The average diameters of the smaller (75 µL) mold spheroids were 108.95 ± 8.09 µm on D1, 119.94 ± 12.32 µm on D3, and 126.22 ± 14.02 µm on D5. The average aspect ratios of these spheroids were 0.95 ± 0.04, 0.95 ± 0.03, and 0.93 ± 0.05, respectively. Images of the agarose mold spheroids taken on D1, D3, and D5 are shown below. The spheroids get smaller over time, presumably because the spheroid was getting more constrained, and the cells were packing more tightly together over time.
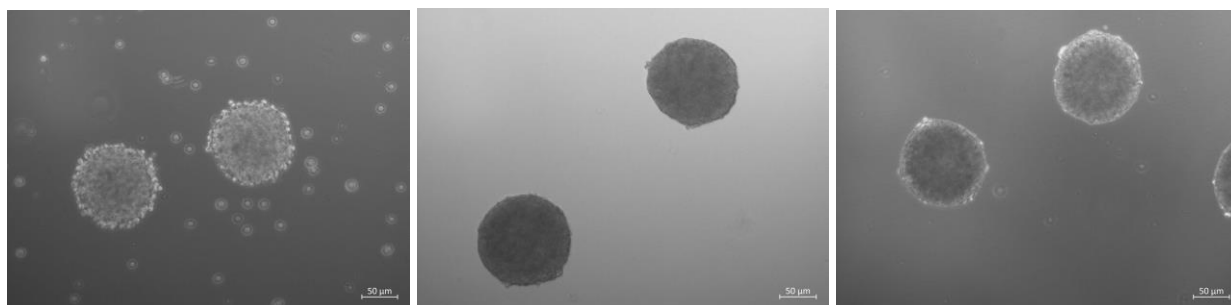
Figure 31. D1 (left), D3 (center), and D5 (right) images of the spheroids from the 75 µL molds. Images taken at 10x objective (scale bar = 50µm).
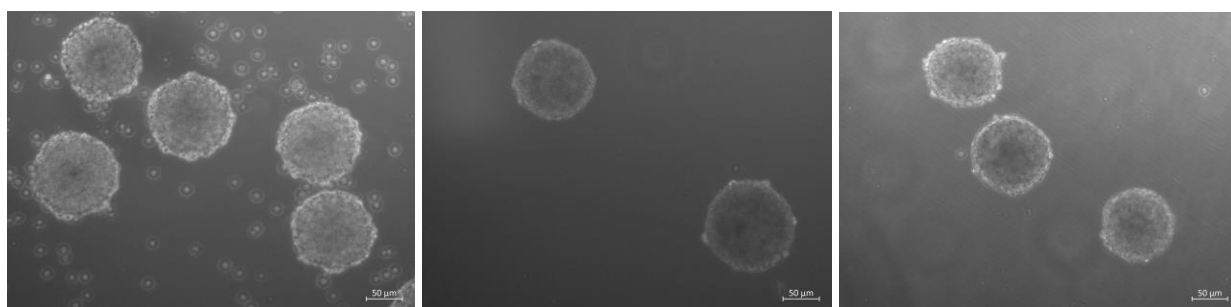
Figure 32. D1 (left), D3 (center), and D5 (right) images of the spheroids from the 190 µL molds. Images taken at 10x objective (scale bar = 50µm).

There were significantly fewer tiny (<50 µm) spheroids produced, as one mold well typically produced one spheroid. This is different from the results seen in the HD method, where there were incredibly large spheroids (>150 µm) and very small spheroids (< 50 µm) produced in the same run. There were multiple spheroids produced in the same drop. The agarose spheroids were also more spherical than the HD spheroids, and less globular. There were little to no protrusions from the agarose mold spheroids. The distribution of size for each mold type on D1, D3, and D5 can be seen below. The distribution is more normal than the hanging drop spheroids.

Table 7. Average Size of AM Spheroids Over Time

Mold Type	Size on D1 (µm)	Size on D3 (µm)	Size on D5 (µm)
190	111.83 ± 9.40	118.97 ± 16.40	100.50 ± 12.95
75	108.95 ± 8.09	119.94 ± 12.32	126.22 ± 14.02
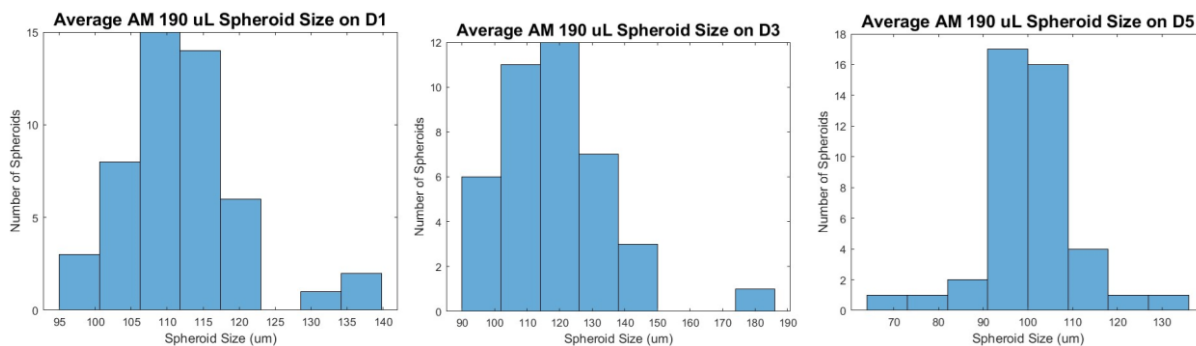
Figure 33. Histograms of the average spheroid size distribution of the spheroids formed in the 190 μm agarose molds for D1 (left) (N=3, n=49), D3 (center) (N=3, n=40), and D5 (right) (N=3, n=43).
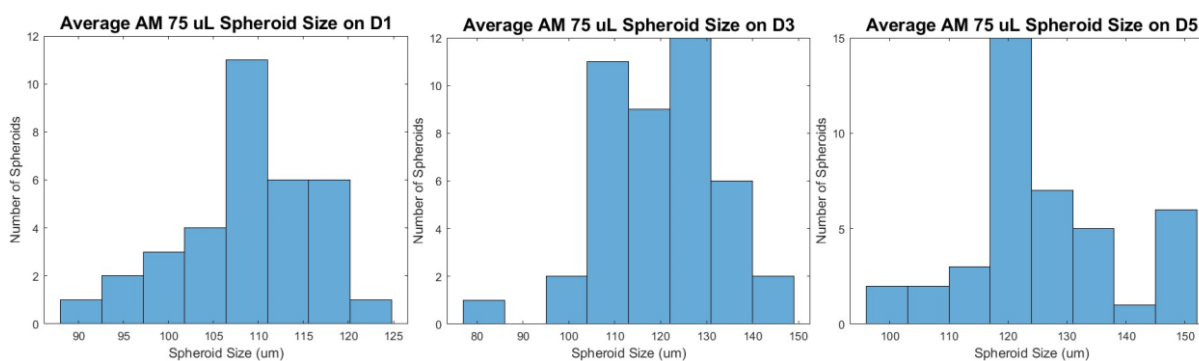
Figure 34. Histograms of the average spheroid size distribution of the spheroids formed in the 75 μm agarose molds for D1 (left) (N=3; n = 34), D3 (center) (N=3; n = 43), and D5 (right) (N=3, n=41).

The percent yield for each day and each cell density were also calculated for this experiment, as shown in the table below. The percent yield was not consistent, nor did it decrease over time. This could mean that size and time in the molds do not have an impact on percent yield, however, more testing is required to come to this conclusion since yield was only measured once with the agarose mold spheroids. The percent yields here are lower than those of the hanging drop spheroids, however, a much higher number of spheroids was produced per run and day due to the maximum number of spheroids that the molds produce.

Table 8. Percent Yield of AM Spheroids Over Time (N = 1; n = 1)

Mold Type	Yield on D1	Yield on D3	Yield on D5
190	70%	59%	74%
75	57%	92%	80%

5.3.1.3 Spheroid Viability Testing.

Viability testing occurred using the CellTiter 96® AQ$_{ueous}$ One Solution Cell Proliferation Assay. The protocol for this assay is found in Appendix K. The graphs below show the day-by-day viability for the different methods of spheroid formation. The data for the original hanging drop protocol cell density of 2.5 x 10^6 cells/mL is used for the hanging drop data in the following graphs.
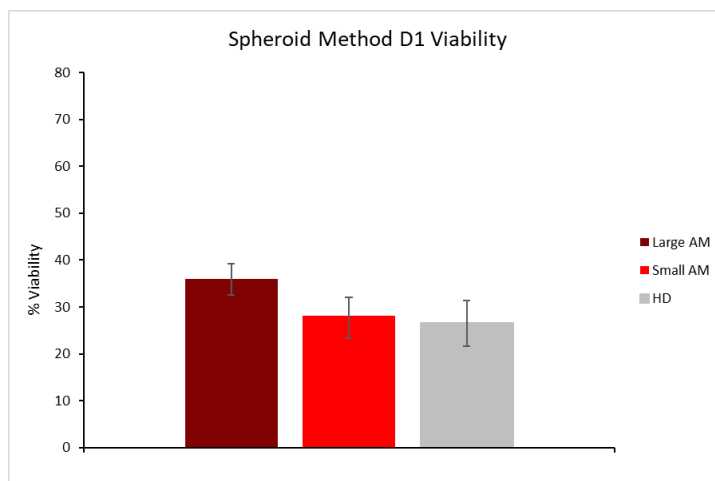
Figure 35. Graph of the average percent viability and standard deviation of the agarose mold and hanging drop spheroids for each spheroid formulation type on D1 (agarose mold: N = 3; n = 9; hanging drop: N = 1; n = 3).
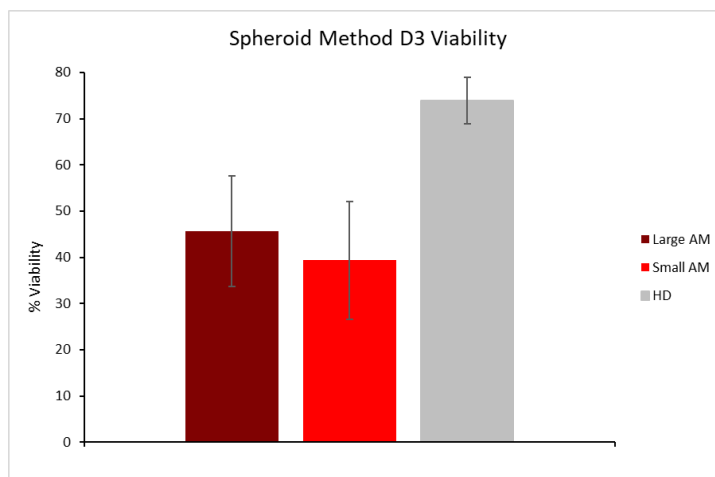
Figure 36. Graph of the average percent viability and standard deviation of the agarose mold and hanging drop spheroids for each spheroid formulation type on D3 (agarose mold: N = 3; n = 9; hanging drop: N = 1; n = 3).
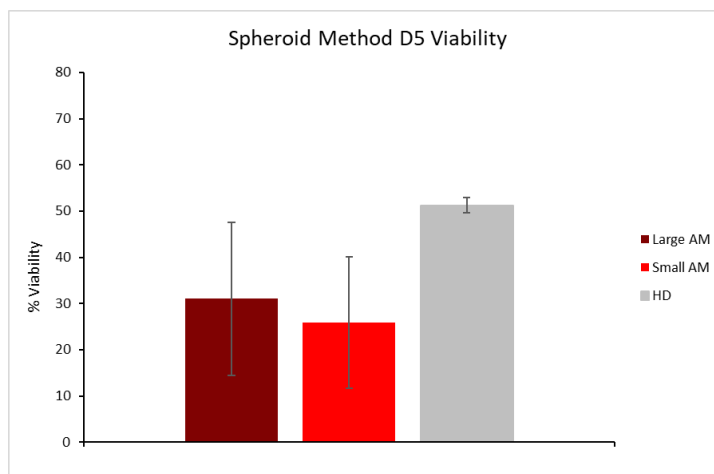
Figure 37. Graph of the average percent viability and standard deviation of the agarose mold and hanging drop spheroids for each spheroid formulation type on D5 (agarose mold: N = 3; n = 9; hanging drop: N = 1; n = 3).
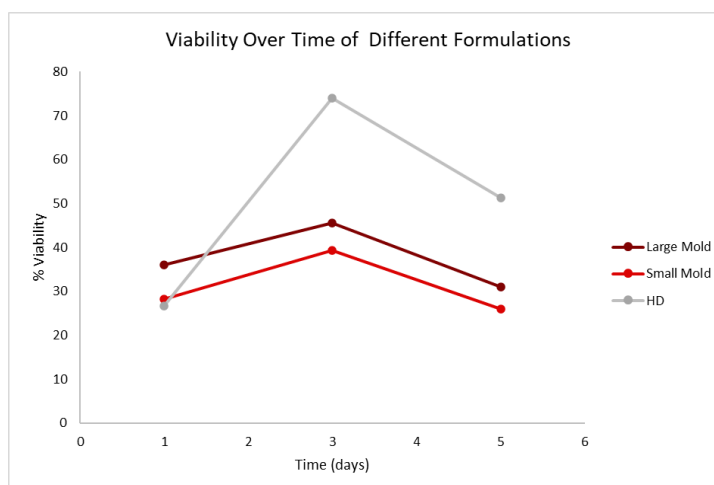
Figure 38. Graph of the change in viability for each spheroid formation over time.

Unexpectedly, the hanging drop spheroids had the highest viability. More testing is needed to confirm this, as the hanging drop experiment with viability testing was only run once due to time constraints. The agarose mold spheroids did not hit either viability benchmark, of 80% viability at D3 or 50% at D5. The hanging drop method was able to hit the benchmark of 50% viability at D5 and just missed the 80% at D3 benchmark. Viability increased in all formations at D3. More testing is needed to confirm this because viability tests were performed in triplicate, but not performed in three isolated instances.

5.3.2 Rings

To form rings, the procedure stated in Appendix G was followed. Figure 16 shows how the agarose molds are made and how the cells are seeded and self-adhere. For this experiment, the 2 mm inner post diameter will be used.

5.3.2.1 Rat Aortic Smooth Muscle Cells Rings.

The Rat Aortic Smooth Muscle Cells (RaSMCs) rings were seeded at 5×10^5 cells per well in a 6-well plate then incubated for 10 and 14 days. The rings were not touched for the initial 24 hours, then the media in each well was changed every two days. The media used throughout the culture and ring period was Complete Media with 10% FBS. The rings were imaged every day, with days 0, 8, and 10 shown Figure 39 below, demonstrating the changes in shape and thickness of the rings throughout the incubation period. The thickness of the ring is deciphered as the red line on Figure 39B, and the rings compacted over time.

A.   B.   C.

Figure 39. The same RaSMC ring in the 6-well plate agarose mold. A. Image taken on day 0. B. Image taken on day 8. C. Image taken on day 10. Images taken at 4x objective (scale bar = 100 µm).

Table 9. Thickness of RaSMC Rings Over Time (N = 1; n = 18)

Day 0 (µm)	Day 8 (µm)	Day 10 (µm)
663 ± 8	425 ± 32	344 ± 22.5

On day 8 of ring culture, four of the ten rings were removed from the mold, but one broke during the removal process. The three rings that did stay intact were very easy to remove from the post and could withstand the pressure of the tweezer when being removed. Figure 40 shows the four rings removed from the molds.
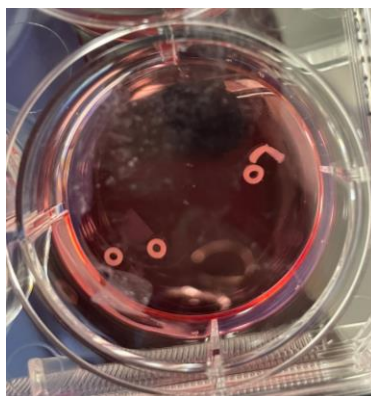
Figure 40. Four rings removed from the 6-well plate mold on day 8 in ring culture. Imaged with an iPhone camera.

On day 10 of ring culture, the remaining six rings were removed, and one broke during the removal process. Same as in day 8, the five other rings were simple to remove, but the broken ring broke in more places than one. The percent yield of the RaSMC removal process was 75% and was calculated using the equation below.

$$Percent\ Yield\ =\ \frac{Actual\ Yield\ (Rings\ that\ make\ it\ out)}{Theoretical\ Yield\ (Rings\ that\ are\ set\ up)}\ *\ 100$$

5.3.2.2 Uterine Smooth Muscle Cells (uSMCs) Rings.

The Uterine Smooth Muscle Cells (uSMCs) rings were seeded at 6.5×10^5 cells per well in a 6-well plate then incubated for 8 and 10 days. Similar to the RaSMCs, the rings were not touched for the initial 24 hours, then the media in each well was changed every two days. Supplemented Vascular Basal Media was used throughout the culture and ring period. The rings were imaged every day, with days 0, 8, and 10 shown in Figure 41 below, expressing the changing of the shape and thickness of the rings throughout the incubation period. The thickness of the ring is deciphered as the red line on Figure 41B. Just like the RaSMCs, these rings compacted over time.
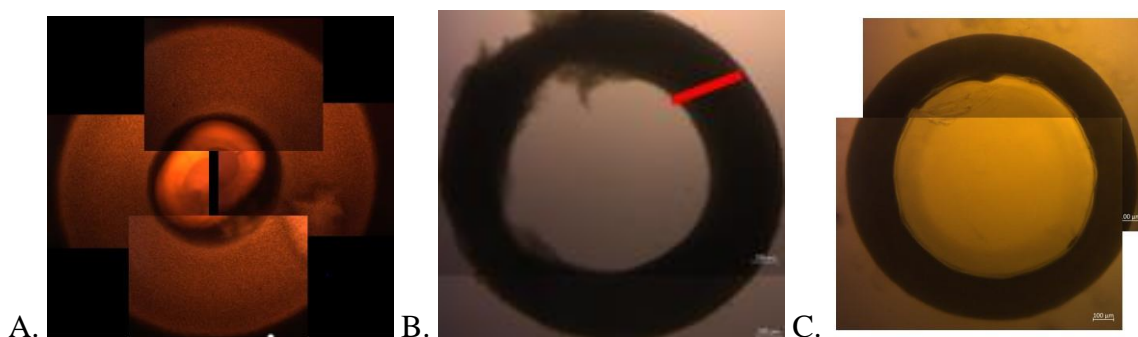

A.   B.   C.
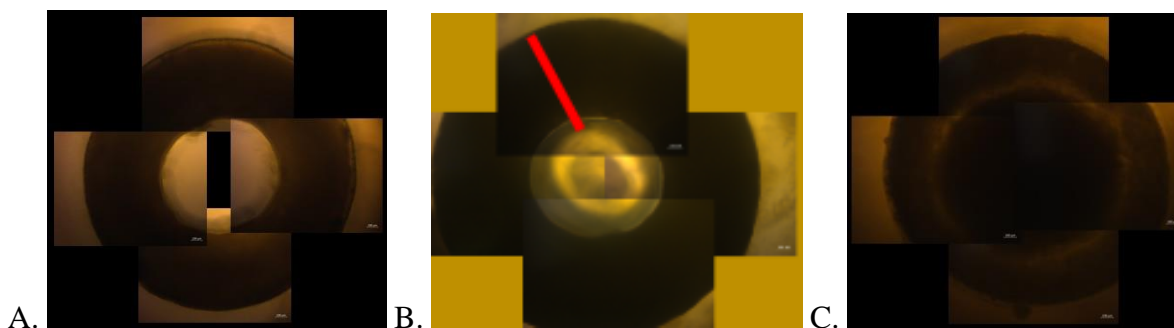
Figure 41. The same uSMC ring in the 6-well plate agarose mold. A. Image taken on day 0. B. Image taken on day 8. C. Image taken on day 10. Images taken at 4x objective (scale bar = 100 μm).

Table 10. Thickness of uSMC Rings Over Time (N = 1; n = 18)

Day 0 (µm)	Day 8 (µm)	Day 10 (µm)
1265 ± 17.5	972 ± 1	959 ± 5

On day 8 of ring culture, four of the twelve rings were removed. However, the rings did not stay in shape when they were removed from the wells like the RaSMCs did. Once the middle post was removed from the well to start the removal process, the uSMCs did not stay in their ring shape. Instead, they formed back into a mass of cells in the middle of the well. This was very unpredictable for this experiment, as the RaSMC rings stayed in shape when the middle post was removed from the well.

On day 10 of ring culture, four of the remaining eight rings were removed. The same thing happened on this day as it did on day 8, however the rings stayed intact for longer than the day 8 rings did. But, when attempting to remove the rings with the tweezers, the cells morphed into a mass and did not retain their shape. So, no uSMCs rings were successfully removed throughout this period. Using the same percent yield calculation as above, the percent yield for the uSMCs was 0%.

5.3.2.3 Uterine Smooth Muscle Cells (uSMCs) Rings with Ficoll and Ascorbic Acid Crowders.

Because the initial cultures of uSMC rings formed with only supplemented Vascular Basal Media did not remain in their shape during the removal process, crowders of Ficoll 70, Ficoll 400, and Ascorbic Acid were added to the media. The same cell culture conditions, cell density, and ring culture conditions were followed as previously described, except for adding the macromolecular crowders to the media. The crowders were calculated and prepared as stated in Appendix M, for 20 mL of media.

The rings were imaged every day, with days 8 and 10 shown in the images below, expressing the changing of the shape and thickness of the rings throughout the incubation period. The thickness of the ring is deciphered as the red line on Figure 43D. These rings also compacted over time, with the Ficolls only crowded ring meeting the benchmark thickness of 840-870 µm.

A.   B.   C.   D.
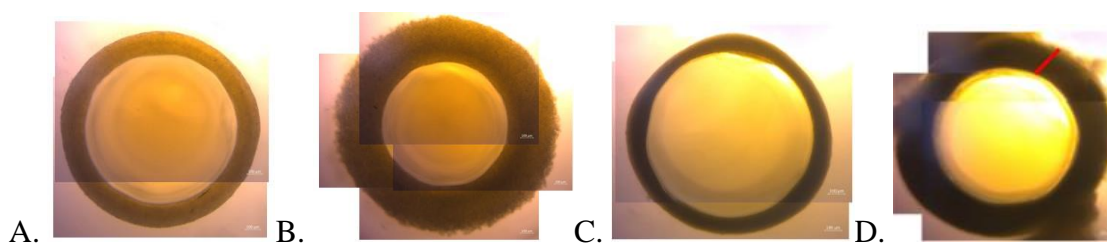
Figure 42. uSMC rings in the 6-well plate agarose mold. A. uSMC ring with Ficolls and Ascorbic Acid crowders on day 8. B. uSMC ring with Ficolls crowders on day 8. C. uSMC ring

with Ficolls and Ascorbic Acid crowders on day 10. D. uSMC ring with Ficolls crowders on day 10. Images taken at 4x objective (scale bar = 100 μm).

Table 11. Thickness of uSMC Rings with Crowders Over Time (N = 1; n = 18)

Crowder Type	Day 0 (μm)	Day 8 (μm)	Day 10 (μm)
uSMC w/ Ficolls	922 ± 4	869 ± 8	843 ± 6.5
uSMC w/ Ficolls + Ascorbic Acid	697 ± 7	519 ± 5	487 ± 5.5

On day 10 of ring culture, all eighteen rings were removed (nine of each type). Of the nine rings that were crowded with just the Ficolls, seven of the rings remained intact. Using the percent yield calculation, the uSMC rings with Ficoll had a 79% yield. Of the nine rings that were crowded with both Ficoll and Ascorbic Acid, all nine remained intact, making the percent yield 100%.

The graph below shows the ring thickness over time for each cell type and media configuration. Ring thickness was collected with ImageJ throughout the whole culture period, 0 to 10 days.
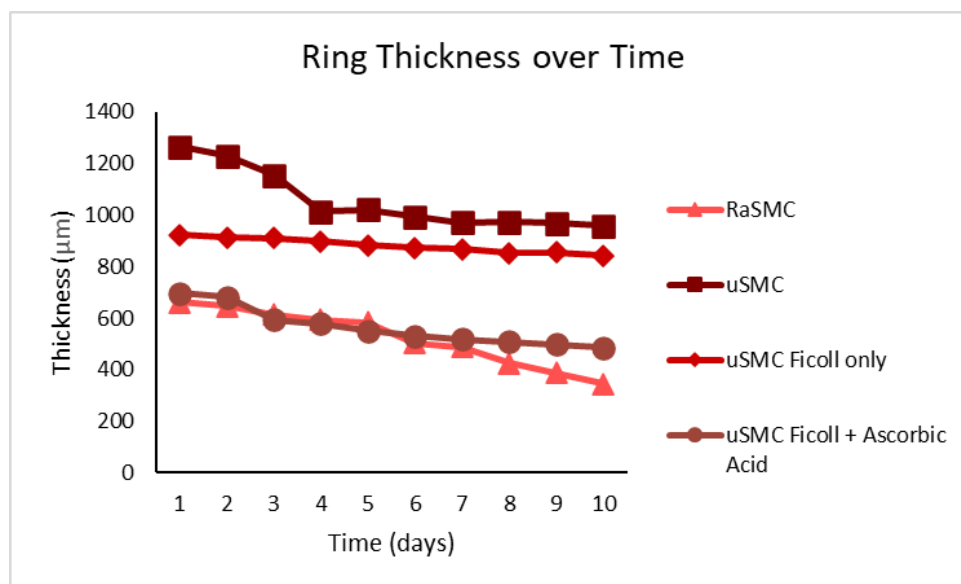
Figure 43. Graph of ring thicknesses (μm) over time (days). The pink triangle line is Rat aortic Smooth Muscle Cell rings, the maroon square line is uterine Smooth Muscle Cell rings, the red diamond line is uterine Smooth Muscle Cell rings crowded with Ficoll 70 and Ficoll 400, and the brown circle line is uterine Smooth Muscle Cell rings crowded with Ficoll 70, Ficoll 400, and Ascorbic Acid.

5.3.2.4 Collagen Production Testing.

After the uSMC rings with macromolecular crowding were removed from the molds, they were fixed in 10% Formalin, processed, embedded in paraffin, sectioned at 5 mm, and stained for collagen using Gomori's Trichrome Stain. RaSMC and uSMC rings were not used because there was no testing of the production of collagen in RaSMCs as they would not compare to human myometrial tissue, and the first trial of uSMC rings did not remain intact to embed. The staining procedure for the Gomori Trichrome Stain is outlined in Appendix L and resulted in the stains imaged by the Nikon Eclipse microscope shown in Figure 45. The images below show the collagen production of the uSMC rings crowded with either the Ficolls, or Ficolls and Ascorbic Acid. The rings were imaged on day 10, the final day of uSMC ring culture.

A.   B.
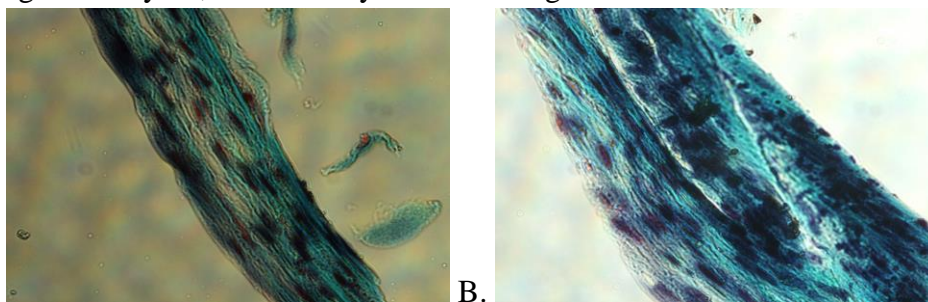
Figure 44. uSMC rings with Gomori's Trichrome Stain imaged at 20x objective (scale bar = 20 µm). The nuclei are black, cytoplasm/muscle fiber are red, and the collagen is green/blue. A. uSMC ring with Ficolls crowders. B. uSMC ring with Ficolls and Ascorbic Acid crowders.

5.3.3 Alginate Beads

The protocol used for fabrication of the alginate beads is listed in Appendix D. Two trials were conducted to create the beads. For both trials an alginate solution was used, created with 2% alginic acid sodium salt. The solution was then cooled and extruded into a calcium chloride solution on a stir plate using a syringe. Over 50 beads were formed with each 1 mL extrusion of the alginate solution. The first trial was conducted with a 22g needle, then the second trial used a 27g needle to achieve a smaller diameter.

The average diameter for the beads formed with a 22g needle was roughly 1300 µm, but many beads could not be measured under a microscope because they were too large to be imaged. The beads were structurally sound and had a consistent spherical shape as shown in Figures 45 and 46. The second trial of beads using a 27g needle had an average diameter of 800 µm. Many of these beads had a teardrop shaped appearance.

Gelatin was used to aid in the cell adhesion process with the protocol described in Appendix D. The beads were formed using the same procedure as described above all with a 27g needle. The alginate-gelatin crosslinked beads had a more transparent appearance as compared to solely alginate and more teardrop shapes. The alginate-gelatin beads formed structurally intact beads with relatively consistent shape.
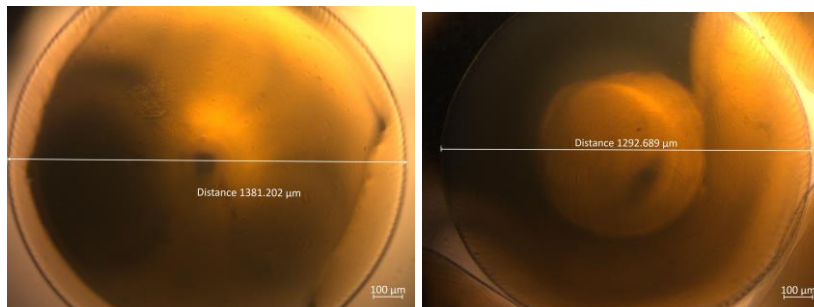
Figure 45. Two 2% alginate beads synthesized with a 22 g needle in the first trial. Images taken at a 4X objective (scale bar = 100 µm).
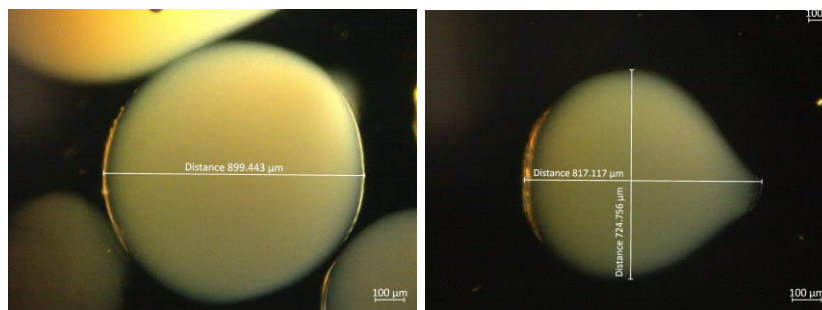
Figure 46. Two 2% alginate beads synthesized with a 27 g needle in the second trial showing teardrop shape on the right. Images taken at a 4X objective (scale bar = 100 µm).

5.3.3.1 Alginate Bead Cell Encapsulation and Degradation Study.

The protocol used for cell encapsulation in alginate beads is described in Appendix I. Two experiments were conducted with alginate beads encapsulated in cells, one of which used alginate-gelatin crosslinked beads as described in Appendix D. These beads were fabricated with 2% w/v alginate and 0.5% w/v gelatin. There were at least 30 beads of each type formed using a 27g needle. Both types of beads had an uneven distribution of cells with many beads appearing to have a high number of embedded cells on Day 2 as shown in Figures 48 and 49. The alginate beads remained in a uniform spherical shape while the alginate-gelatin crosslinked beads were often elongated and teardrop shaped.
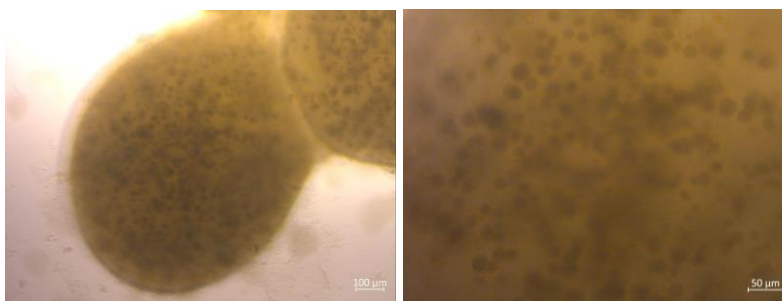
Figure 47. Degradation Study: Two 2% alginate beads synthesized with a 27g needle with rat smooth muscle cells encapsulated imaged on day 3. Left images taken at 4X objective, right image taken at 10X objective (left: scale bar = 100 µm, right: scale bar = 50 µm).

Figure 48. Degradation Study: Two 2% alginate 0.5% gelatin crosslinked beads synthesized with a 27g needle with rat smooth muscle cells encapsulated imaged on day 3. Left images taken at 4X objective, right image taken at 10X objective (left: scale bar = 100 μm, right: scale bar = 50 μm).

During this experiment the beads were exposed to contamination as shown below in Figures 50 and 51 resulting in cell death and unidentified debris in the images. While both types of beads had substantial degradation, it was more visible within the alginate-gelatin crosslinked beads. This degradation can be seen with deterioration in the edges of the beads and a more transparent appearance as compared to those with just alginate as shown in Figures 55 and 56. The 0.8% alginate-gelatin in this study was unable to form beads, and its appearance was inconsistent without any clear spherical structures as shown in Figure 54. There were similar inconsistencies in structure with other bead concentration, but they were not as frequent as with the 0.8% alginate-gelatin.
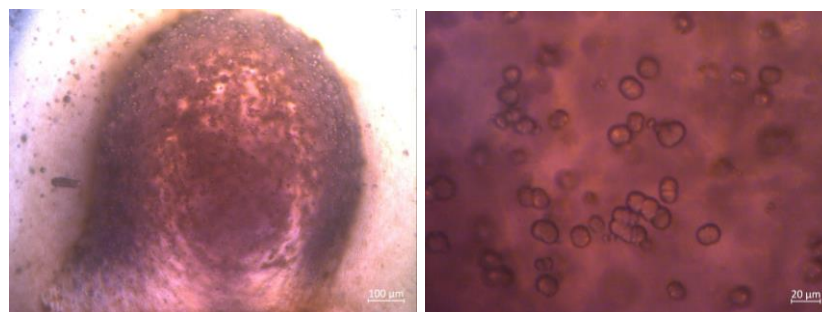
Figure 49. Degradation Study: Two 2% alginate beads synthesized with a 27g needle with rat smooth muscle cells encapsulated imaged on day 10 after contamination occurred. Left images taken at 4X objective, right image taken at 20X objective (left: scale bar = 100 μm, right: scale bar = 20 μm).

Figure 50. Degradation Study: Two 2% alginate and 0.5% gelatin crosslinked beads synthesized with a 27g needle with rat smooth muscle cells imaged on day 10 after contamination occurred. Left images taken at 4X objective, right image taken at 40X objective (left: scale bar = 100 µm, right: scale bar = 10 µm).

A second degradation study was conducted using the same fabrication parameters as stated above, but without cells and without the 0.8% alginate and gelatin crosslinked beads. These beads were imaged every 12 hours to measure the average diameter of the 30 beads of each concentration type. Figure 51 shows two stable beads formed with 0.8% alginate; this concentration formed the most consistent bead shape. The beads had a circular shape, clear edges, and intact structure. The 1.2% alginate beads had difficulty in formation shown in figure 52 with inconsistent composition. The image on the right illustrates extruded alginate that was unable to crosslink into a bead shape. The 2% alginate beads had similar issues as described with the 1.2% alginate but resulted in a larger average diameter.
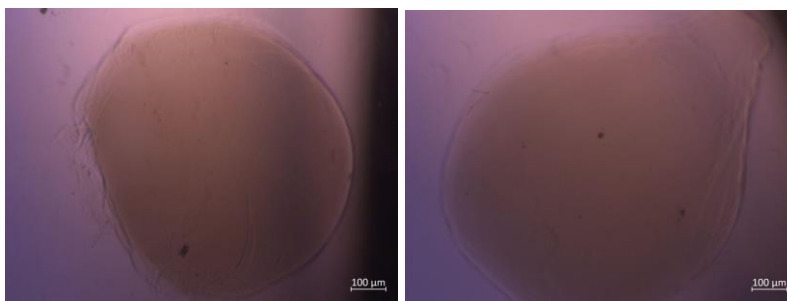
Figure 51. Degradation Study 2: Two 0.8% alginate beads synthesized with a 27g needle without cells imaged on day 2. Images taken at 4X objective (scale bar = 100 µm).
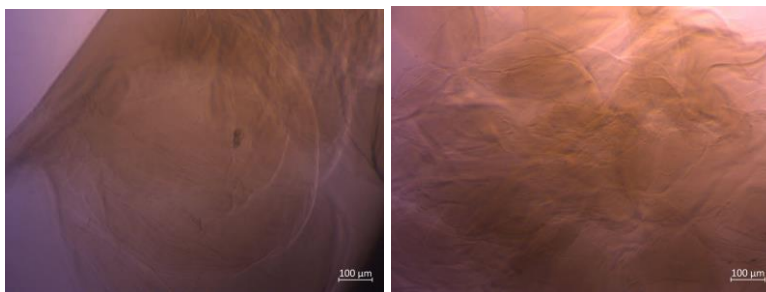
Figure 52. Degradation Study 2: Two 1.2% alginate beads synthesized with a 27g needle without cells imaged on day 2. Images taken at 4X objective (scale bar = 100 µm).
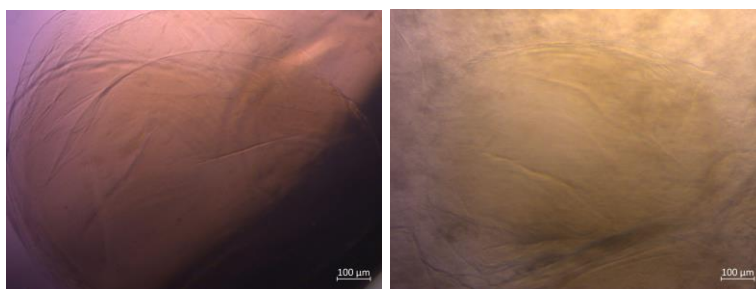
Figure 53. Degradation Study 2: Two 2% alginate beads synthesized with a 27g needle without cells imaged on day 2. Images taken at 4X objective (scale bar = 100 µm).

The alginate-gelatin beads had a more transparent appearance and lack of visible structure with translucent edges. Alginate-gelatin crosslinking resulted in generally more consistent bead fabrication as opposed to alginate only beads. This was accurate for all concentrations except the 0.8% alginate and 0.5% gelatin crosslinked beads that were unsuccessful in forming any stable beads as seen in figure 54. Figures 55 and 56 show the 1.2% and 2% alginate-gelatin crosslinked beads that had similar results with primarily successful bead formation. The 2% alginate-gelatin beads had a larger appearance than the 1.2% alginate beads.
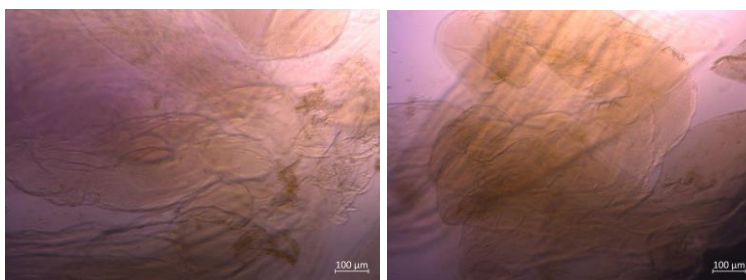
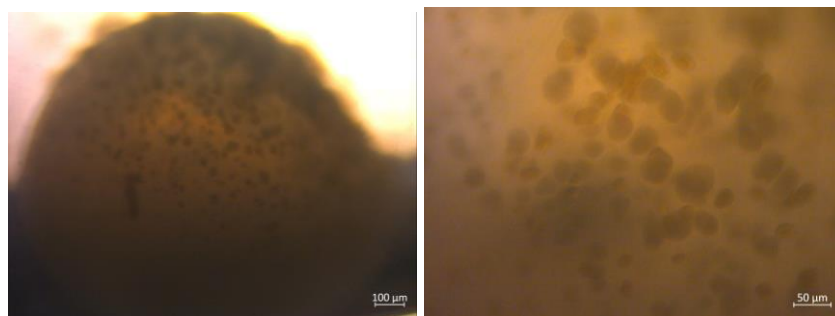*Figure 54. Degradation Study 2: Two 0.8% alginate and 0.5% gelatin crosslinked beads synthesized with a 27g needle without cells imaged on day 2. Images taken at 4X objective (scale bar = 100 µm).*
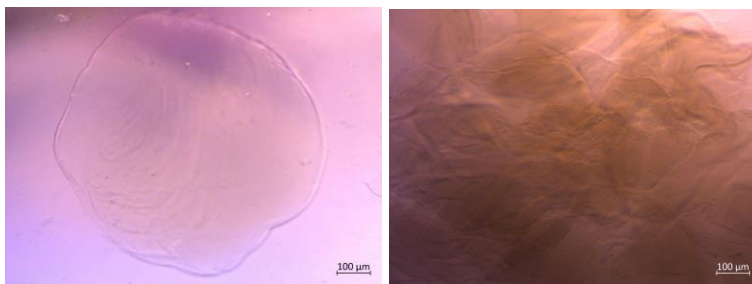
Figure 55. Degradation Study 2: Two 1.2% alginate and 0.5% gelatin crosslinked beads synthesized with a 27g needle without cells imaged on day 2. Images taken at 4X objective (scale bar = 100 μm).

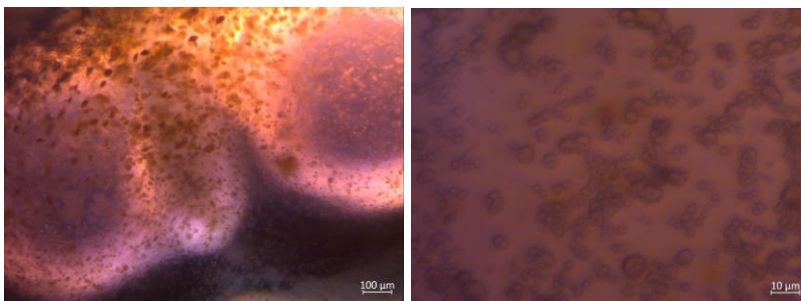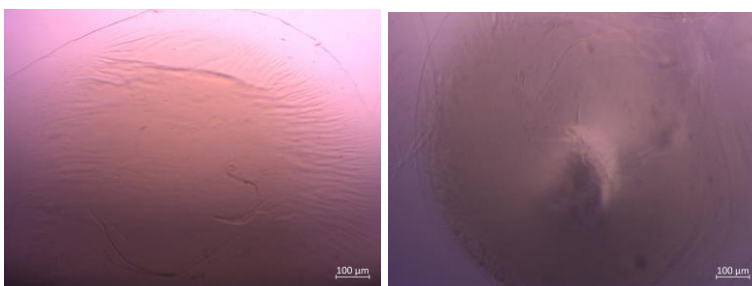*Figure 56. Degradation Study 2: Two 2% alginate and 0.5% gelatin crosslinked beads synthesized with a 27g needle without cells imaged on day 2. Images taken at 4X objective (scale bar = 100 μm).*

The beads had a wide range of diameters upon fabrication as shown in Figure 57 with the standard deviations for each concentration. The 1.2% alginate had the largest range in bead sizes and the smallest average diameter at 722.45 μm ± 175.47 μm at Day 0. The 0.8% alginate beads were the most consistent in size with an average diameter of 855.81 μm and a standard deviation of 82.56 μm at Day 0. Figure 58 shows the average bead size at day 0. The decrease in bead size can be observed for all bead concentrations when comparing the diameters in figures 57 and 58. The 2% alginate-gelatin had the highest average diameter at 1023.85 μm ± 126.68 μm at Day 0. Figure 59 shows the average bead diameter that was measured every 12 hours over a period of 5 days. The 2% alginate-gelatin beads had the largest change in size within this period having a difference of over 100 μm from initial diameter to diameter at 120 hours. The 0.8% alginate beads had the lowest degradation rate with the most consistent bead size over this time.
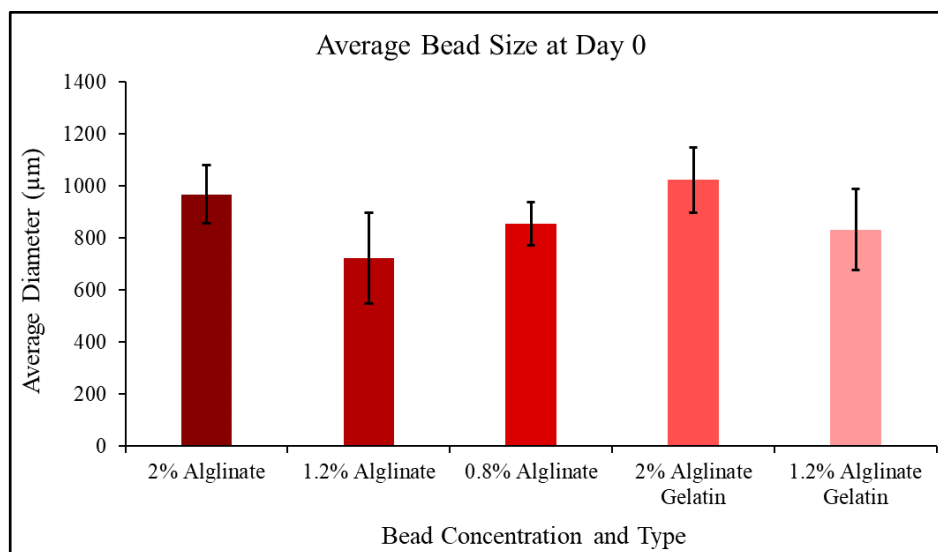
Figure 57. Graph of average bead size showing average bead diameter (µm) over bead formulation. Beads were fabricated without cells and measured at day 0 (N=1; n=30).
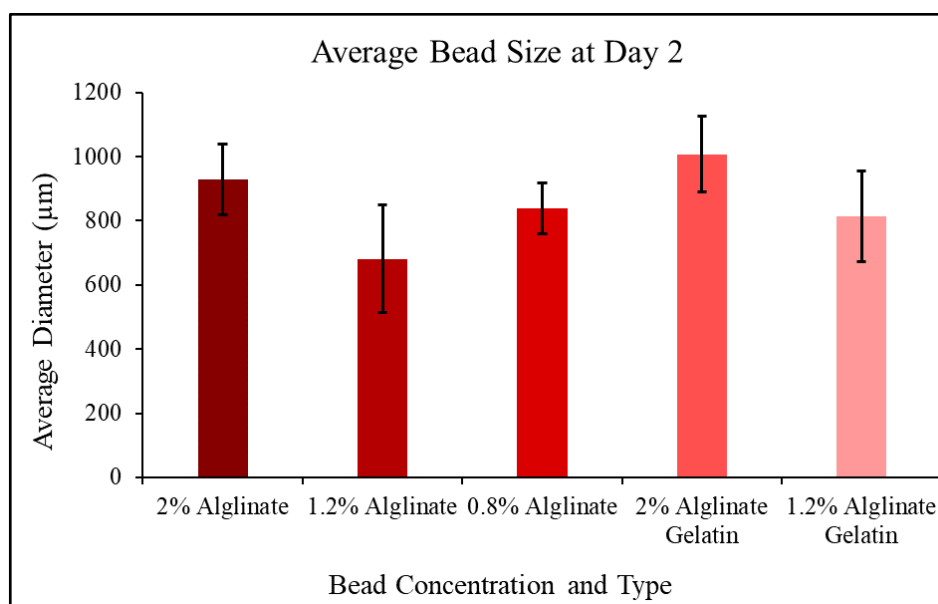
Figure 58. Graph of average bead size showing average bead diameter (µm) over bead formulation. Beads were fabricated without cells and measured at day 2 (N=1; n=30).
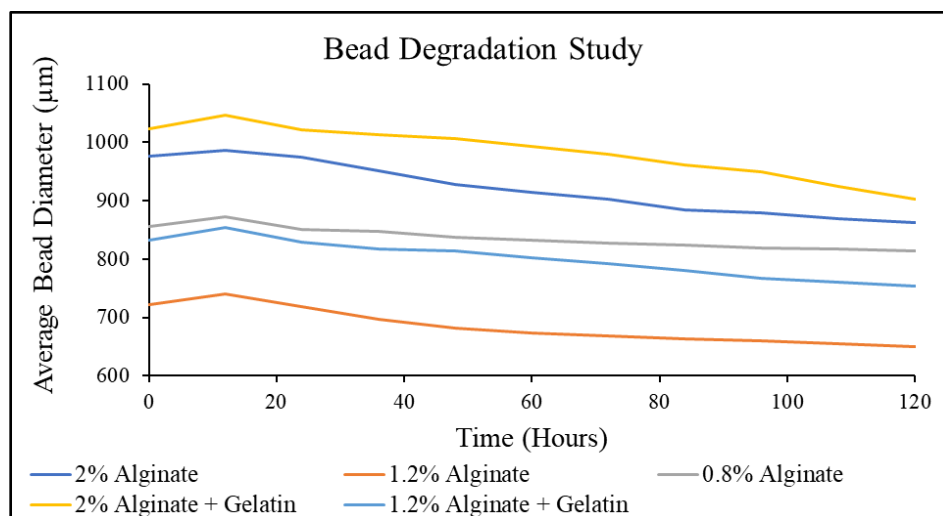
Figure 59. Graph of bead degradation study showing average bead diameter (μm) over time (hours). Beads were fabricated without cells and measured every 12 hours over 5 days (N=1; n=30).

6.0 Final Design and Validation

Throughout this project, it was imperative that the team focused on the objectives to create the final design.

The most important objectives, forming an effective model that mimics the interface of uterine fibroids and tissues and producing similar tissue composition as in situ myometrium tissue, was the key point to many experiments. The ring and spheroid formation experiments as well as encapsulating cells into alginate beads were all geared towards forming an effective model. The rings underwent histology tests to show the extracellular matrix and collagen production and the similarity of the tissue composition of the in-vitro models to the in situ tissues. Although the team was successful in being able to model the components of an effective in-vitro uterine fibroid model, they were not able to complete their objective of mimicking the interface of uterine fibroids and myometrium tissues. No components that represent the fibroid and the myometrium were combined to create a concise model, so there was no testing or evaluation done to understand the interface of the two tissues. In addition, the pseudocapsule, which can separate fibroid tissue from the myometrium, was not considered when developing the modeling systems. Because of this, the objective was not met. However, the objective of producing similar tissue composition as myometrium tissue was partially completed because the rings were able to demonstrate ECM and collagen production that mimics myometrium tissue. The other components of the model (spheroids and cells in alginate beads) did not undergo histology testing to understand the ECM and collagen deposition.

The second most important objective, ensuring cell viability, was partially achieved by conducting cell viability assays on the spheroids, though the other modeling systems were not tested. Two viability testing methods were experimented with, and the CellTiter 96® AQ$_{ueous}$ One Solution Cell Proliferation Assay was determined to be the most effective of the two methods, as it gave definite quantifiable viability data through absorbance readings. Upon application to experimentation with hanging drop and agarose mold spheroids, only one benchmark viability was reached, 50% viability on Day five by the hanging drop spheroids. This was unexpected because the agarose mold spheroids were hypothesized to be more viable. More testing is needed to clarify these results and to determine the next steps.

The objective of having the project be reproducible was also achieved. Each methodology followed a step-by-step protocol and contained benchmarks that defined the experiments. Spheroid size and shape benchmarks as well as spheroid viability benchmarks were consistently met. Ring size, structure, and ECM production benchmarks were met using the uSMC rings with macromolecular crowders. Bead size and number benchmarks were also met. There was variance between different samples and different cell types. It was also made sure that the cell culture conditions, media and supplements, and lab equipment remained the same throughout the entire project to ensure the highest chance of reproducibility for the team and future experiments. Because all benchmarks were met, and there was little variance within the experiments, reagents, and equipment used, the model is reproducible and met the objective.

The final objective, affordability, was partially achieved. The group was given $750 for

the entirety of the project and the team stayed in the budget, ensuring the affordability of the project. The team spent a total of $621 throughout the MQP. However, cells and some media were taken from advisors and their labs, and if this cost was accounted for, the team would not have remained in their budget. Because of this, the team partially met their objective because the team remained within the budget without the cost of the cells graciously provided by the advisors' labs. This model creation would likely be affordable within other wet labs deciding to take on this project, knowing the cost of cells and media is a large sum.

The standards stated above in section 3.3 are applicable to the project. All of these standards were incorporated into the three terms of work, especially standard ISO 11737-1 Third edition: Sterilization of health care products - microbiological methods because it was very important that the biomedical equipment used in the lab was sterilized before coming into contact with any cells. Also, aseptic techniques and good laboratory practices were followed during the project for general safety.

As the project progressed, the team needed to evaluate how the project would impact different areas such as economics, environment, society, politics, ethics, health and safety, manufacturing, and sustainability.

6.1 Ethics Statement

With the development of a 3D in-vitro model of uterine fibroids, models that are less reflective of human biology, like rat models, can be slowly phased out of laboratories. Rat models are not as reflective of human biology as they were thought to be at the time they were developed. The use of rat models to test developing treatments is ethically contested, but with the development of in-vitro models, the need for rat models becomes obsolete. For future iterations of this project, there are possible concerns if human fibroid cells are used. These cells are harvested from individuals with fibroids during surgery and utilizing human tissue raises issues with patient consent, confidentiality, and the potential for exploitation of vulnerable populations. If treatments are developed with the future of this model there is potential for commercialization which may prioritize profits over access to the treatment, specifically in countries with private healthcare. This section reviews different areas that have ethical implications including environmental, social, global, and economic impacts.

6.1.1 Environmental Impact

The environmental impact of this project is complex, as with most research conducted in laboratories, due to the variety of equipment used and the energy required. In sterile lab procedures, a large amount of plastic is used when new equipment is required for each experiment including well plates, gloves, petri dishes, and pipette tips. To keep this equipment protected it is often packaged individually in plastic, thus resulting in more waste. These procedures involved autoclaving some equipment prior to usage which requires energy, as does the fume hood, incubator, and various electronics used. A large portion of the equipment had to be discarded after usage due to contact with cells or other chemicals, so there were many single-use plastics and a

large amount of biohazard waste. Biohazard waste requires additional effort to dispose of the equipment by transporting it to a specific facility for removal. One consideration of the impact is the xenograft model for uterine fibroids which often uses mice. This uses a substantial amount of energy as well as food and water. Using animals in the lab also requires additional protective equipment which can include disposable gowns, masks, and shoe covers. A large portion of the equipment was used in experimentation with new techniques to determine protocols and understand the modeling systems which will be established by this project and will not need to be repeated.

6.1.2 Societal Influence

Research and development regarding uterine fibroid treatment is still ongoing. New models and new medications are currently being worked on and published. There is currently no market for 3D models of uterine fibroids because there are none, and the only modeling systems that exist are 2D culture and rat models. There are also no treatments for uterine fibroids available that are effective at removing fibroids permanently while also preserving fertility. The creation of a robust in-vitro 3D modeling system of the physical and chemical properties of uterine fibroids will help further the development of new treatments and hopefully get them to market. Though the impact will not be felt immediately by ordinary people, the research developed in this paper will help to develop an in-vitro 3D model of uterine fibroids, which can be used to develop new therapeutics for the treatment of uterine fibroids. This will impact ordinary people, as they will be involved in the process of development of fibroids treatment and will be using it if it is approved by the FDA. The development of this model can also help to increase awareness of uterine fibroids as an issue with its increased development. New medications or other treatments will give patients more options and more flexibility with how they are treated, which ultimately improves the experience for patients.

6.1.3 Global Influence

At its current state, this project will have minimal influence on the global market. Some global factors involve facility requirements and disparities in healthcare access globally. There are certain requirements for the usage of this model including a biosafety level 2 laboratory. Equipment requirements include an incubator, autoclave, and fume hood. There is potential for future influence depending on the continuation of the modeling systems. For future iterations of this project, creating an in-vitro uterine fibroid model could have extensive political ramifications in women's health and reproductive rights. A reliable model could result in improved treatments of uterine fibroids and reduce invasive surgeries as the most common treatment for severe fibroids. These potential treatments could increase funding in the field of reproductive health. It could also result in debates as to who can access the new treatments due to private healthcare and socioeconomic barriers if they are costly. There are other global factors including differences within groups of people relating to fibroid development with environmental factors. To improve

understanding there needs to be research conducted into genetic ancestry and impacts on what causes development in fibroids.

6.1.4 Economic

One of the objectives to consider for the project was the total cost. The team was given a total of $750. $300 was used to pay lab fees, leaving the team with $450. The final design used the entire budget as getting different media formulations, viability assays, and media supplements cost the team the full budget. All smooth muscle cells were gifted to the team by Dr. Rolle and Dr. Whittington's labs. The results of this project would not influence the economy of everyday living as this model will not be produced or available worldwide. However, this project will influence the biology economy because many cells and media components will have to be bought to continue making the model. This in turn will allow for the completion and widespread use of the model which will reduce the need for other uterine fibroid treatments that could cost the patient money and time. The future implications of this product could ease the economic burden caused by fibroids with potential direct treatment resulting in less surgery and avoiding expensive drugs and treatments. The ethical impact in economics includes accessibility with the potential for future treatments and what the cost of those could be. This could result in issues specifically with privatized healthcare and the high cost of newer treatments making them difficult to access.

7.0 Discussion

The work accomplished during this project expanded upon previous knowledge of the three modeling systems used. This project expanded upon previous work by creating a new way to accomplish building different components of a 3D in-vitro model of uterine fibroids. To create this method, a significant amount of literature had to be combined to create feasible design elements. It explores the possibility of using older technologies in combination with each other in new applications. Much of the design was proven in prior literature before being applied to this project, such as specific benchmarks describing how each component should turn out, detailed protocol specifying particle and model fabrication with uSMCs, viability studies, and histology studies.

As stated above, the uniqueness of this project arises from the potential combination of the three modeling systems into a cohesive model. The use of alginate beads and spheroids in this context is also new, as is the multicomponent 3D model. Furthermore, research on forming uSMCs rings with a mold and not a bioprinter was not found during any literature reviews, and according to those reviews, forming uSMCs into spheroids at all is also novel. Finally, uSMCs have not yet been embedded into alginate beads. This model is original, and unlike any 3D model of uterine fibroids made prior.

7.1 Spheroids

Overall, neither formation technique appears to have met all of the benchmarks set for their formulation. The spheroids produced during experimentation only partially fulfill the objectives described earlier. As research stands right now, spheroids do not appear to be a feasible method for modeling fibroid tissue in-vitro. Further research is required to confirm this. uSMC spheroids were not produced during experimentation due to several limitations, but testing with uSMCs in both spheroid formations could occur in the future.

It was hypothesized that the agarose molds would produce more consistent, spherical, and viable cells. However, this was not the case. The agarose mold spheroids were consistent in size and under the benchmark diameter (150 µm) throughout the course of the experiment, however, did not hit the benchmark viabilities at Day three and Day five. The hanging drop spheroids had a wide distribution of size and a lower aspect ratio but were able to hit the Day five benchmark viability of 50% viability and almost hit the Day three benchmark viability of 80% viability. The spheroids appeared to decrease in size over time, presumably due to increased compaction and more ECM production, however, this is not confirmed in spheroid experimentation.

The higher viability in the hanging drop spheroids may be due to the compaction of the spheroids. The agarose mold spheroids were incredibly constrained, and it was significantly more difficult to break up the spheroids when attempting viability tests. In the hanging drop spheroids, the cells were loosely attached to each other and were easily reduced to independent cells when performing viability tests. This decreased spheroid density may allow for more oxygen and nutrient diffusion. The higher viability may also have to do with surface area and volume. The larger spheroids have more cells, a higher surface area, and a higher volume. There are more cells dying due to necrosis in the larger spheroids, however, there are also more cells that receive oxygen

and nutrients through diffusion due to the overall size of the spheroid. The ratio of live to dead cells may be skewed by the overall increase in the volume of the larger spheroids. More work is needed to confirm this. These viability results are not statistically significant due to a lack of reproduction, so more testing is required to definitively draw any conclusions.

The agarose method spheroids were within the benchmark sizes of 150 µm, which was set in accordance with prior literature to reduce internal necrosis. They were more consistent in size and were more spherical than the hanging drop. This is due to the molds that they were formed in. In the hanging drop method, the shape of the spheroid is dependent on the circularity of the drop, as the spheroids form at the lowest points from the petri dish lid. In the agarose molds, each mold was the same size and shape, which allowed for more consistent spheroid formation. The hanging drop spheroids were inconsistent in their sizing. There were two main populations of spheroid size, large (>150 µm) and small (<100 µm). This divide in populations was made more apparent with a decrease in cell seeding density. More testing is needed to confirm these results; however, this may be due to gravity which aids in the formation of the spheroids. In spheroids with a higher seeding density, there are more cells per drop, meaning more weight and more volume is taken up. At a higher seeding density, this may work towards the overall unity and symmetry of the spheroids. In spheroids of lower density, there is less weight and less volume taken up by cells, which may cause multiple smaller spheroids to form. More testing is required to confirm these theories.

7.2 Rings

The formation of rings is a large part of this project and achieves every objective. The most important objective the ring experiment was trying to achieve was mimicking the tissue composition of myometrial tissue. The first experiments conducted with RaSMCs formed structurally intact rings. This was expected as the results of these experiments matched the results of work done in previous literature (Dash et al., 2016).

The formation of uSMC rings followed the same protocol that was used for RaSMC rings, except with supplemented VBM instead of Complete Media with 10% FBS. There is no literature on creating uSMC rings using self-adhering methods, however, there is literature on a magnetically bioprinted ring with uSMCs incorporated into the structure (Souza et al., 2017). The uSMCs in the bioprinted rings nicely formed into the ring shape, interacted, and built ECM that mimicked in situ environments as well as the contractility expressed by the uterus (Souza et al., 2017). Based on this information and using the protocol defined by the RaSMC rings used to form vascular tissue rings, the formation of uSMC rings was attempted. From Dash et al., 2016, it was expected the cells would self-adhere and create a structurally sound ring. From Sozua et al., 2017, it was expected this ring would express ECM, collagen, and contractility similar to in situ uterine cells and tissues. However, this was not the case under standard media conditions. The uSMC rings created did not hold any ring structure when attempts were made to remove them from the agarose mold. There are two reasons that the rings did not hold their shape, one being the low ECM deposition and the other being the length of time given for the rings to form. In Dash et al., 2016, the time of formation for the RaSMC rings was 12 days, however, the uSMC rings did not follow

this timeline standard, as they fell apart when attempted to be removed from the mold at day 12. So, it was hypothesized that if the uSMC rings were in the agarose mold for a longer period, they would form a more structured ring. This proved to be correct as the uSMC rings removed on day 14 held their structure slightly longer, but still were not able to be removed from the agarose mold and hold their shape. Another possible reason the rings did not hold their shape could be the ECM deposition.

Macromolecular crowders of Ficoll 70, Ficoll 400, and Ascorbic Acid were then used to make the second round of uSMC rings. These macromolecular crowders are used in cell culture to promote ECM through a more stable and supportive environment for the cells to grow and function (Zeiger et al., 2012). These properties exhibited by Ficoll 70, Ficoll 400, and Ascorbic Acid play specific roles in the structural properties and ECM deposition in uterine fibroids. Fibroids are monoclonal, but present a universal fibrotic phenotype, so targeting ECM deposition can prove applicable in yielding treatments (Winter et al., 2020). Macromolecular crowders in in-vitro uterine cell culture are one way to adjust the cell-matrix interactions and potentiate signaling between the ECM and the cell, which can model the ECM deposition in-vivo (Winter et al., 2020). The presence of Ficoll and Ascorbic Acid macromolecules in the cultures of uterine smooth muscle cells limited the extracellular fluid available which, in turn, promoted collagen fibril deposition (Winter et al., 2020).

The uSMC rings that contained the macromolecular crowders worked as described in Souza et al., 2017, stable and able to be removed and handled with tweezers. These rings were able to be removed with very little breakage. Because these rings remained 80-100% more intact than the uSMC rings with no crowders, it is evident that the increased production of ECM aided the ring structure.

The Ficoll-only crowded uSMC rings proved to be the most structurally similar to the myometrial wall because they were at 0.843 mm when removed and structurally intact. The thickness benchmark of the rings was 0.84-0.87 mm because this is the ring thickness that can withstand the stretching and contraction of the uterus (Dash et al., 2016). The other rings, RaSMCs, uSMCs, and uSMC with Ficoll and Ascorbic Acid were over 0.2 mm away from the benchmark while being less structurally sound than the uSMCs with Ficoll-only.

The Ficoll and Ascorbic Acid-crowded uSMC rings proved to have the most similar tissue composition to the myometrial wall. This was determined by running the uSMC ring with Ficoll-only crowders and uSMC ring with Ficoll and Ascorbic Acid-crowders through a Gomori Trichrome stain for collagen production. The ring crowded with Ficoll and Ascorbic Acid has collagen dispersed throughout the whole ring compared to the uSMC with Ficoll-crowded ring that has collagen isolated more at the outside of the ring. This wide-spread dispersion with many nuclei is very representative of human myometrial tissue as seen in Figure 44.

Overall, it was determined that uSMC rings are representative of myometrium tissue when combined with Ficoll and Ascorbic Acid crowders. Although the rings with crowders showed positive results, only one test was able to be run due to time constraints and contamination issues in the lab. It is recommended that more tests be conducted to accurately determine the best way to

mimic the myometrium tissue.

7.3 Alginate Beads

The alginate bead model functions independently with cells encapsulated and fulfills some of the objectives described above. The initial experiments using alginate beads remained structurally intact for at least 15 days when stored in 4℃. The diameter of the beads decreased as expected when a smaller needle gauge was used. The alginate beads with rat smooth muscle cells had a more uneven distribution of cells between beads than expected. They had minimal degradation after 3 days but became contaminated during the first study. Alginate-gelatin crosslinked beads with cells embedded had a similar cell distribution as the alginate beads. They also had an unexpected result in morphology with many teardrop-shaped beads forming and the cause of that was unknown. The alginate-gelatin beads had a faster degradation as compared to the alginate alone which is consistent with literature. The overall degradation requires more experimentation to gather data over an extended period without contamination impacting the results. Overall, the general structure and size of the beads formed as expected based on literature.

During the second degradation study, average bead sizes were collected at day 0 for the various concentrations and overall, the 0.8% alginate beads formed the most consistent and stable bead sizes. As expected, the beads' structure deteriorated much more quickly when stored in the incubator rather than the refrigerator. This can be observed in the bead degradation study with most beads having a considerable change in average diameter between hours 0 and 120. The 2% alginate and 2% alginate-gelatin beads had the largest change in diameter with both having a difference of over 100 µm. More research is required to observe the degradation using uSMCs to determine what impact cell embedding would have on the change in bead size. This study should also be conducted for a longer period and would ideally include measurements of cell viability after the study is concluded.

7.4 Limitations

There are various limitations that should be considered in this project including contamination, time, and resources. There were multiple experiments affected by contamination and it also prevented multiple studies from being conducted. This contamination could be due to many factors, but one important component was the use of a shared lab space including the fume hood, refrigerator, and incubator. The lab also had many different groups using the space and was often not kept clean. There was an issue of mold in the ceilings and leaking from that area which further impacted the cleanliness of the lab. Due to the nature of this project, time was a constraining factor. The cells had to be cultured and the modeling systems also had to be observed over time to gather results. The shared space also created issues with time as there was not always a fume hood available, so experiments were sometimes delayed. Equipment was one of the most impactful resource issues for this project. The lab space did not contain much of the equipment that was necessary, like an absorbance reader, a working microscope, cell plates, media, media supplements, sterile filters, and more, so this required many requests to be made as experiments

progressed. Budgetary constraints prevented the modeling systems from being tested with human fibroid cells. There was also only one type of cell used, uterine smooth muscle cells, whereas there are many different cell types within the uterine myometrium tissue that should be considered for this project. The chemicals and media available were limited to what was in the lab and within the budget provided. The final limitation to be discussed for this project is the background information available. This resulted in a substantial amount of background research and testing prior to considering the experimental procedures and model types. There was limited knowledge of cell behavior with 3D culture in-vivo. There were many unknown aspects of this project that had to be addressed on a case-by-case basis.

8.0 Conclusions and Recommendations

All three proposed modeling systems were initially fabricated successfully with either RaSMCs or uSMCs. Extensive background research was conducted to select these three models. Literature review was conducted on uterine fibroids to understand the cell types and interactions with surrounding tissues. Many tissue modeling systems were explored to determine the models that would be explored in this project. A selection matrix and pairwise comparison chart were used to select rings, alginate beads, and spheroids. Design functions and means as well as the client statement and objectives were used to create the protocols for experimentation. Future work is necessary to determine the conclusion of this project with the efficacy of modeling systems.

There were three main modeling systems explored throughout this project: rings, spheroids, and alginate beads. The rings were formed successfully with rat smooth muscle cells and had minimal breakage upon removal. The uSMC rings had unexpected results, but when the macromolecular crowders were combined with supplemented Vascular Basal Media, the uSMC rings better represented myometrial tissue composition and structure. Neither spheroid formation method hit all benchmarks, and in some circumstances, not enough replicates of experiments were performed to draw conclusions. As it stands, the hanging drop method hits the Day five viability benchmark, but the agarose molds are more consistent in size, are more reproducible, and produce more spheroids. More data is needed to verify these results, as the hanging drop viability was only run once due to time constraints. Though more data is needed to make this conclusion with any significance, current results indicate that spheroids should be phased out of the model due to failures to meet all benchmarks in full. These methods should be experimented with more to verify results and to determine if experimental conditions can be adjusted to meet the benchmarks. In addition, uSMCs should be phased in as the primary cell type in spheroid formation. The beads formed successfully with concentrations of 2%, 1.2% and 0.8% alginate and 0.5% gelatin (with all alginate concentrations except 0.8%). The beads had unexpected results with inconsistencies in structure that occurred after the filtration process that should be explored further. Overall, the 0.8% alginate beads were the most consistent with structure and size, and the 2% alginate and 2% alginate-gelatin beads were the most inconsistent with the largest degradation.

Recommendations for further work include formulations of the three components working together in the same modeling system. This project determined the feasibility of these three separate 3D modeling systems to be applied to the formation of a 3D model of uterine fibroids, and their efficiency at working together. Next steps to create this model would include attaching cells to alginate beads, attaching alginate beads to rings and spheroids, and adding fibroid cells and tissues into all models. These future steps would allow the team to achieve their main objective of replicating the fibroid/tissue interface and create a fully functioning model of a uterine fibroid.

References

Anada, T., Fukada, J., Sai, Y., &Suzuki, O. (2012). An oxygen-permeable spheroid culture system for the prevention of central hypoxia and necrosis of spheroids. *Biomaterials 33*(33), 8430-8441. https://doi.org/10.1016/j.biomaterials.2012.08.040

Ashimova, A., Yegorov, S., Negmetzhanov, B., & Hortelano, G. (2019). Cell Encapsulation Within Alginate Microcapsules: Immunological Challenges and Outlook. *Frontiers in Bioengineering and Biotechnology*, *7*. https://www.frontiersin.org/articles/10.3389/fbioe.2019.00380

Ayvaz, I., Sunay, D., Sariyar, E., Erdal, E., & Karagonlar, Z. F. (2021). Three-Dimensional Cell Culture Models of Hepatocellular Carcinoma — a Review. *Journal of Gastrointestinal Cancer*, *52*(4), 1294–1308. https://doi.org/10.1007/s12029-021-00772-1

Azura Vascular Care. (2017). A Glossary Guide to Uterine Fibroids. *Azura Vascular Care.* https://www.azuravascularcare.com/infoufe/glossary-to-uterine-fibroids/

Bulun, S.E. (2013). Uterine Fibroids. *The New England Journal of Medicine, 369*, 1344-55. https://doi.org/10.1056/NEJMra1209993

Carvalho, M. R., Lima, D., Reis, R. L., Correlo, V. M., & Oliveira, J. M. (2015). Evaluating Biomaterial- and Microfluidic-Based 3D Tumor Models. *Trends in Biotechnology*, *33*(11), 667–678. https://doi.org/10.1016/j.tibtech.2015.09.009

Ciarmela, P., Delli Carpini, G., Greco, S., Zannotti, A., Montik, N., Giannella, L., Giuliani, L., Grelloni, C., Panfoli, F., Paolucci, M., Pierucci, G., Ragno, F., Pellegrino, P., Petraglia, F., & Ciavattini, A. (2022). Uterine fibroid vascularization: from morphological evidence to clinical implications. *Reproductive BioMedicine Online, 44*(2), 281–294. https://doi.org/10.1016/j.rbmo.2021.09.005

Ciavattini, A., Di Giuseppe, J., Stortoni, P., Montik, N., Giannubilo, S. R., Litta, P., Islam, Md. S., Tranquilli, A. L., Reis, F. M., & Ciarmela, P. (2013). Uterine Fibroids: Pathogenesis and Interactions with Endometrium and Endomyometrial Junction. *Obstetrics and Gynecology International*, *2013*, 173184. https://doi.org/10.1155/2013/173184

Ciebiera, M., Włodarczyk, M., Zgliczyńska, M., Łukaszuk, K., Męczekalski, B., Kobierzycki, C., Łoziński, T., & Jakiel, G. (2018). The Role of Tumor Necrosis Factor α in the Biology of Uterine Fibroids and the Related Symptoms. *International Journal of Molecular Sciences, 19*(12), 3869. https://doi.org/10.3390/ijms19123869

Cruz, M. S. D. D. L., & Buchanan, E. M. (2017). Uterine Fibroids: Diagnosis and Treatment. *American Family Physician*, *95*(2), 100–107. https://www.aafp.org/pubs/afp/issues/2017/0115/p100.html

Dash, B. C., Levi, K., Schwan, J., Luo, J., Bartulos, O., Wu, H., Qiu, C., Yi, T., Ren, Y., Campbell, S., Rolle, M. W., & Qyang, Y. (2016). Tissue-Engineered Vascular Rings from Human iPSC-Derived Smooth Muscle Cells. Stem Cell Reports, 7(1), 19–28. https://doi.org/10.1016/j.stemcr.2016.05.004

Fritsch, M., Schmidt, N., Gröticke, I., Frisk, A.-L., Keator, C. S., Koch, M., & Slayden, O. D. (2015). Application of a Patient Derived Xenograft Model for Predictive Study of Uterine Fibroid Disease. *PLoS ONE*, *10*(11), e0142429. https://doi.org/10.1371/journal.pone.0142429

Foty, R. (2011). A Simple Hanging Drop Cell Culture Protocol for Generation of 3D Spheroids. *J Vis Exp.* (51), 2720. https://doi.org/10.3791/2720

Gao, E., Li, G., Cao, R., Xia, H., Xu, Y., Jiang, G., Xiao, K., Chen, J., Chen, R., & Duan, L. (2022). Bionic tracheal tissue regeneration using a ring-shaped scaffold comprised of decellularized cartilaginous matrix and silk fibroin. Composites Part B: Engineering, 229, 109470. https://doi.org/10.1016/j.compositesb.2021.109470

Giuliani, E., As-Sanie, S., & Marsh, E. E. (2020). Epidemiology and management of uterine fibroids. I*nternational Journal of Gynecology & Obstetrics, 149*(1), 3–9. https://doi.org/10.1002/ijgo.13102

Havryliuk, Y., Setton, R., Carlow, J.J., & Shaktman, B.D., Symptomatic Fibroid Management: Systematic Review of the Literature. *JSLS, 21*(3). https://doi.org/10.4293/JSLS.2017.00041

Li, J., Wu, C., Chu, P. K., & Gelinsky, M. (2020). 3D printing of hydrogels: Rational design strategies and emerging biomedical applications. *Materials Science and Engineering: R: Reports*, *140*, 100543. https://doi.org/10.1016/j.mser.2020.100543

Malvasi, A., Cavallotti, C., Morroni, M., Lorenzi, T., Dell'Edera, D., Nicolardi, G., & Tinelli, A. (2012). Uterine fibroid pseudocapsule studied by transmission electron microscopy. European Journal of Obstetrics and Gynecology and Reproductive Biology, 162(2), 187–191. https://doi.org/10.1016/j.ejogrb.2012.02.017

Malvasi, A., Tinelli, A., Cavallotti, C., Morroni, M., Tsin, D. A., Nezhat, C., Stark, M., & Mettler, L. (2011). Distribution of Substance P (SP) and Vasoactive Intestinal Peptide (VIP) in pseudocapsules of uterine fibroids. Peptides, 32(2), 327–332. https://doi.org/10.1016/j.peptides.2010.10.034

Malik, M., Norian, J., McCarthy-Keith, D., Britten, J., Catherino W.H., Why leiomyomas are called fibroids: the central role of extracellular matrix in symptomatic women *Semin Reprod Med, 28* (2010), 169-179. https://doi.org/10.1055/s-0030-1251475

McWilliams, M. M., & Chennathukuzhi, V. M. (2017). Recent Advances in Uterine Fibroid Etiology. *Seminars in Reproductive Medicine*, *35*(2), 181–189. https://doi.org/10.1055/s-0037-1599090

Nawaz, I., Nawaz, Y., & Nawaz, E. (2022). An Avant-garde Approach to Life: Reviewing the Current Applications of 3D Bioprinting. *McGill Journal of Medicine*, *20*(2). https://doi.org/10.26443/mjm.v20i2.919

Ningshi, S.S., Avissa, R., Stujanna, E.N., et al. (2021). Evaluation of morphology and viability of spheroid derived from Insulin-GLase cell line: A model system to understand Type 2 Diabetes Mellitus. *J Exp Clin Med 38*(3), 211-215. https://doi.org/10.52142/omujecm.38.3.1

Omari, E. A., Varghese, T., Kliewer, M. A., Harter, J., & Hartenbach, E. M. (2015). Dynamic and Quasi-Static mechanical testing for characterization of the viscoelastic properties of human uterine tissue. *Journal of Biomechanics*, *48*(10), 1730–1736. https://doi.org/10.1016/j.jbiomech.2015.05.013

Peitsidis, P., Koukoulomati, A., (2014). Tranexamic acid for the management of uterine fibroid tumors: A systematic review of the current evidence *World J Clin Cases, 2*(12), 893-898. https://doi.org/10.12998/wjcc.v2.i12.893

Piccinini, F., Tesei, A., Arienti, C., Bebilacqua, A. (2017) Cell Counting and Viability Assessment of 2D and 3D Cell Cultures: Expected Reliability of the Trypan Blue Assay. *Biological Procedures Online, 19*(1). https://doi.org/10.1186/s12575-017-0056-3

Prusinski Fernung, L. E., Al-Hendy, A., & Yang, Q. (2019). A Preliminary Study: Human Fibroid Stro-1+/CD44+ Stem Cells Isolated From Uterine Fibroids Demonstrate Decreased DNA Repair and Genomic Integrity Compared to Adjacent Myometrial Stro-1+/CD44+ Cells. *Reproductive Sciences*, *26*(5), 619–638. https://doi.org/10.1177/1933719118783252

Qin, H., Lin, Z., Vásquez, E., Luan, X., Guo, F., Xu, L. (2021). Association between obesity and the risk of uterine fibroids: a systematic review and meta-analysis. *Epidemiology & Community Health 75*(2). http://dx.doi.org/10.1136/jech-2019-213364

Sontheimer-Phelps, A., Hassell, B., & Ingber, D. (2019). Modelling cancer in microfluidic human organs-on-chip. *ProQuest*, *19*(2), 65-81. https://doi.org/10.1038/s41568-018-0104-6

Souza, G. R., Tseng, H., Gage, J. A., Mani, A., Desai, P., Leonard, F., Liao, A., Longo, M., Refuerzo, J. S., & Godin, B. (2017). Magnetically Bioprinted Human Myometrial 3D Cell Rings as A Model for Uterine Contractility. International Journal of Molecular Sciences, 18(4), 683. https://doi.org/10.3390/ijms18040683

Stewart, E. A., Laughlin-Tommaso, S. K., Catherino, W. H., Lalitkumar, S., Gupta, D., & Vollenhoven, B. (2016). Uterine fibroids. *Nature Reviews Disease Primers*, *2*(1), 1–18. https://doi.org/10.1038/nrdp.2016.43

Strobel, H. A., Dikina, A. D., Levi, K., Solorio, L. D., Alsberg, E., & Rolle, M. W. (2017). Cellular Self-Assembly with Microsphere Incorporation for Growth Factor Delivery Within Engineered Vascular Tissue Rings. Tissue Engineering. Part A, 23(3–4), 143–155. https://doi.org/10.1089/ten.tea.2016.0260

Suo, G., Sadarangani, A., LaMarca, B., Cowan, B., & Wang, J. Y. J. (2009). Murine Xenograft Model for Human Uterine Fibroids: An In Vivo Imaging Approach. *Reproductive Sciences*, *16*(9), 827–842. https://doi.org/10.1177/1933719109336615

Tinelli, A., Favilli, A., Lasmar, R. B., Mazzon, I., Gerli, S., Xue, X., & Malvasi, A. (2019). The importance of pseudocapsule preservation during hysteroscopic myomectomy. *European Journal of Obstetrics & Gynecology and Reproductive Biology, 243*, 179–184. https://doi.org/10.1016/j.ejogrb.2019.09.008

Tinelli, A., Malvasi, A., Hurst, B. S., Tsin, D. A., Davila, F., Dominguez, G., Dell'edera, D., Cavallotti, C., Negro, R., Gustapane, S., Teigland, C. M., & Mettler, L. (2012). Surgical Management of Neurovascular Bundle in Uterine Fibroid Pseudocapsule. *JSLS : Journal of the Society of Laparoendoscopic Surgeons, 16*(1), 119–129. https://doi.org/10.4293/108680812X13291597716302

Uimari, O., Subramaniam, K. S., Vollenhoven, B., & Tapmeier, T. T. (2022). Uterine Fibroids (Leiomyomata) and Heavy Menstrual Bleeding. *Frontiers in Reproductive Health, 4*. https://www.frontiersin.org/articles/10.3389/frph.2022.818243

Uterine Fibroids: Symptoms, Causes, Risk Factors & Treatment. (n.d.). Cleveland Clinic. Retrieved December 15, 2022, from https://my.clevelandclinic.org/health/diseases/9130-uterine-fibroids

Winter, A., Salamonsen, L. A., & Evans, J. (2020). Modelling fibroid pathology: development and manipulation of a myometrial smooth muscle cell macromolecular crowding model to alter extracellular matrix deposition. Molecular Human Reproduction, 26(7), 498–509. https://doi.org/10.1093/molehr/gaaa036

Yang, Q., Ciebiera, M., Bariani, M. V., Ali, M., Elkafas, H., Boyer, T. G., & Al-Hendy, A. (2022). Comprehensive Review of Uterine Fibroids: Developmental Origin, Pathogenesis, and Treatment. *Endocrine Reviews*, *43*(4), 678–719. https://doi.org/10.1210/endrev/bnab039

Zeiger, A. S., Loe, F. C., Li, R., Raghunath, M., & Van Vliet, K. J. (2012). Macromolecular Crowding Directs Extracellular Matrix Organization and Mesenchymal Stem Cell Behavior. PLoS ONE, 7(5), e37904. https://doi.org/10.1371/journal.pone.0037904

Appendix A

Materials and Protocol for Making New Rat Smooth Muscle Media

Materials:

- 500 mL bottle of Dulbecco's Modified Media (DMEM)
- 50 mL 10% Fetal Bovine Serum (FBS)
- 5 mL 1% NEAA

- 5 mL Glutamax
- 5 mL Pen-Strep
- 5 mL sodium pyruvate
- 2 50 mL conical tubes
- Pipettes

Protocol:

1. Thaw all materials if needed.
2. Pipette out 70 mL of DMEM from the bottle and place it into two 50 mL conical tubes.
3. Add supplements to the media, beginning with Pen-Strep.
   a. Add the 50mL of 10% FBS last. The order of the other supplements does not matter.
4. Screw on the cap of the bottle and mix the media by rocking the bottle back and forth. It is ready for use after this step. Be sure to label the bottle with the contents and the date of formulation.

Appendix B
Materials and Protocol for Passaging Rat Smooth Muscle Cells

Materials:

- 10% FBS Complete Media
- Dulbecco's Phosphate Buffered Saline without calcium and magnesium (DPBS-)
- 0.25% Trypsin-EDTA

- Trypan Blue and hemocytometer
- 15 mL conical tube
- (micro)Pipettes and their tips
- 100 mm tissue culture dish(es)

Protocol:

Preparation and Counting of the Cells:

1. Aspirate the old media from the cell culture plate.
2. Wash the cell culture plate with 5 mL DPBS, rock the plate back and forth several times, then aspirate off the DPBS.
3. Add 4 mL of 0.25% Trypsin-EDTA to the cell culture plate, then place it in the incubator for 3-5 min until the cells become rounded and lifted off of the plate. This can be seen under a microscope.
4. Add 4 mL of 10% FBS Complete Media to the plate, rock back and forth several times, then slowly pipette up the cell suspension liquid. Carefully pipette the suspension up and down several times to break up any clumps. Transfer the suspension into a 15 mL centrifuge tube.
5. Spin the tube at 200g for 7 minutes. Make sure to add a counterweight.
6. Remove the centrifuge tube from the centrifuge and aspirate off the supernatant.
7. Add 1 mL media to the cells to the conical tube, then pipette the liquid up and down to mix the cell suspension.
8. Count the cells.
    a. Add 10 μL cells to the 50 μL of trypan blue. This has a dilution factor of 6.
    b. Mix the cells in the trypan blue by pipetting up and down, then add 7 μL of the mixture into a hemocytometer.
    c. Count the cells using a microscope, then determine cell concentration.
    d. Dilute the cell suspension to a concentration of 1 million cell/mL.

Cell Seeding:

1. Add 17 mL of 10% FBS Complete Media into a new plate.
2. Add 1 mL of the cell suspension to the plate (the cell suspension should be 1 million cells/mL).
3. Swirl the plate to distribute the cells and check the plate under the microscope.
4. Incubate them for 48 hours.

Appendix C
Materials and Protocol for a Viability Study Using Trypan Blue

Materials:

- Cultured Spheroids in the 60 mm tissue dish
- New 60 mm dish
- 0.25% Trypsin-EDTA
- 10% FBS Complete Media

- 15 mL conical tube
- 0.4% Trypan Blue
- Hemocytometer
- (micro)Pipettes and their tips

Protocol:

1. Remove the desired number of spheroids from the plate and transfer them to a different plate.
2. Digest spheroids into single cells using 0.25% Trypsin-EDTA.
3. Place into a 15 mL conical tube.
4. Centrifuge the cell suspension for 5 min at 1200 rpm.
5. Resuspend the pellet in 200 μl of culture media using a pipette to obtain a single-cell suspension.
6. Remove an aliquot of 100 μl.
7. Add 100 μl of Trypan Blue (TB) solution 0.4% to obtain a final 1:2 dilution.
8. Wait for 5 min to allow the TB to stain the dead cells.
9. Count the cells using a haemocytometer and microscope.
10. Calculate the percentage of viability and number of cells in the culture by considering the final dilution factor.

Things to consider:

Subjective definition of a "cell": There are guidelines but no well-defined rules to help an operator define a cell. From a practical point of view, distinguishing a cell from cell debris or other particles is often challenging, even for an expert biologist.

Subjective perception of a "dead cell": With TB there is no official color threshold for discriminating between a dead cell and a living one. Individual operators performing the manual count have a certain specific set of criteria to define the threshold of brightness of the stain to count a cell as being viable or not. Such interpersonal differences in the manual identification of dead cells are crucial for defining the percentage of viability of the cell culture.

Appendix D

Materials and Protocol for the Formation of Alginate Beads and Alginate-Gelatin Crosslinking

Materials:
- Alginic acid sodium salt
- 0.1 M $CaCl_2$ Solution
- 0.025M HEPES buffer
- Complete Media with 10% FBS
- 0.15 M NaCl

- Heat plate and stir plate with stir bar
- Syringe and needle gauges
- Tweezers
- Measuring Spatula
- 100 mm tissue culture dish

Protocol:

Solution Prep:
1. Pour buffer with 0.025M HEPES and 0.15M NaCl into a beaker, amounts varying depending on the volume of solution desired.
2. Add alginic acid slowly into the beaker to achieve desired concentration.
3. Heat and stir solution at 65°C and 500 rpm for 30 minutes and breakup clumps.
4. Cool for 5-10 minutes and pour alginate solution into a tube.
5. Sterile filter solution.
6. Store in 4°C for a maximum of 3-5 days.

Forming Beads:
1. Add 10 mL of 0.1 M CaCl2 in beaker per 1mL of alginate solution (alginate solution in separate container).
2. Place the beaker on a stir plate, add stir bar, and turn on ensuring no funnel is formed.
3. Use a 5 mL syringe to collect alginate slowly (no air bubbles).
    a. Needle gauge will determine bead size.
4. Begin to release the alginate in the CaCl2 solution slowly with a syringe.
5. Wait 15 minutes for bead stabilization.
6. Remove stir bars with tweezers and remove beads from solution with measuring spatula.
7. Move beads into a 100 mm tissue culture dish and rinse with Complete Media with 10% FBS.
8. Repeat as needed using fresh CaCl2 solution each time.

Alginate-Gelatin Crosslinking Protocol:
1. Complete solution preparation as outlined above in steps 1-2.
2. After step 2 add the gelatin solution at the desired amount to achieve 0.5% w/v based on the total volume.
3. Complete all other steps as normal.

Appendix E

Materials and Protocol for Formation of Spheroids via the Hanging Drop Method

Materials:

- 10% FBS Complete Media
- Dulbecco's Phosphate Buffered Saline without calcium and magnesium (DPBS-)
- 0.25% Trypsin-EDTA

- Trypan Blue and hemocytometer
- 15 mL conical tube
- 60 mm tissue culture dish
- (micro)Pipettes and their tips

Protocol:

1. Take a plate with cells at 90% confluence and rinse them twice with PBS.
2. Trypsinize the cells by adding 2 mL of 0.25% trypsin-EDTA.
3. Incubate for 5-10 minutes.
4. Add 2 mLs Complete Media (CM).
5. Use a 5 mL pipette to mix and transfer cells to a 15 mL conical tube.
6. Incubate for 5 minutes.
7. Centrifuge at 200 XG for 5 minutes.
8. Discard supernatant and wash the pellet with 1 mL CM twice.
9. Resuspend cells in 2 mL of CM.
10. Count the cells with a hemocytometer.
    a. Final concentration should be 2.5×10^6 cells/mL.
11. Remove the lid from the 60 mm tissue culture dish.
12. Place 5 mL PBS in the bottom of the dish.
13. Invert the lid and deposit 10 μL drops of cells with a 20 μL pipette to the bottom of the lid.
    a. Drops should be placed apart so they do not touch.
    b. Can put 20 drops per dish.
14. Invert the lid onto PBS-filled bottom and incubate at 37°C, 5% CO_2 and 95% humidity.
15. Monitor the drops daily.
    a. Incubate until cell sheets or aggregates have formed.
16. Remove the spheroids from the lid by washing the lid with CM and picking the spheroids up into a pipette.
17. Transfer the spheroids into a new dish with CM to observe with a microscope.

Appendix F

Materials and Protocol for Formation of Spheroids via Agarose Molds

Materials:

- Media
    - 10% FBS Complete Media
    - Supplemented Vascular Basal Media
- Dulbecco's Phosphate Buffered Saline without calcium and magnesium (DPBS-)
- 0.25% Trypsin-EDTA
- Trypan Blue

- Spheroid Agarose Molds
    - 12 series molds
    - 24 series molds
- Trypan Blue and hemocytometer
- 2 15 mL conical tubes
- (micro)Pipettes and their tips
- 60 mm tissue culture dish(es)
- Tweezers

Protocol:

Preparing the Cells and Loading the Agarose Molds:

1. If using RaSMCs, follow the protocol seen in Appendix B up to step 4. If using uSMCs, follow the protocol seen in Appendix B through step 9.
2. Count the cells.
    a. Add 10 μL cells to the 50 μL of trypan blue. This has a dilution factor of 6.
    b. Mix the cells in the trypan blue by pipetting up and down, then add 7 μL of the mixture into a hemocytometer.
    c. Count the cells using a microscope, then determine cell concentration.
3. Aspirate the supernatant and resuspend the cells at a concentration of 5 million cells/mL.
    a. Note: The cell concentration in the molds should be 0.5million per 100 μL.
4. After resuspending the centrifuged cells, pipet the suspension dropwise onto the agarose wells.
    a. Use 75uL cell suspension for a small mold (24 series) and 190uL for a large mold (12 series).
5. Allow them to sit about 10 mins in the hood to settle.
6. If the agarose wells are not filled completely, add some media to the top of the well once the cells have settled.
7. Add about 1 mL (2 for longer lasting) media to the dish to surround the agarose cell-filled wells. Want the bottom of the plate to be evenly covered with media – use a pipette to encourage even coating.
8. Incubate at 37 C, at least overnight, to allow the spheroids to form in the wells before harvesting.

Harvesting Spheroids from Agarose Molds:

1. In a new cell culture plate add fresh media. The media should form a diameter about the same size as the mold.

2. Use sterile tweezers to carefully flip the agarose mold upside down onto the media bubble taking care not to introduce air-bubbles.
3. Carefully, lift the plate and drop it on the biohood surface to force the spheroids down.
4. If needed, use a micropipette to carefully squirt culture medium into the seeding chamber to dislodge any remaining spheroids out.

Appendix G

Materials and Protocol for the Formation of Rat Smooth Muscle Cell Rings

Materials:

- Autoclaved 2% (w/v) agarose solution
- Complete Media with 10% FBS
- Autoclaved PDMS well molds and spatula
- 6-well plate(s)
- 10% FBS Complete Media

- Dulbecco's Phosphate Buffered Saline without calcium and magnesium (DPBS-)
- 0.25% Trypsin-EDTA
- Trypan Blue and hemocytometer
- 15 mL conical tube

Protocol:

Making the Agarose Molds:

1. Make a 2% (w/v) agarose solution in Complete Media with 10% FBS and autoclave on a liquid cycle ONLY.
   a. Note: Dry cycles may cause evaporation and change the concentration of agarose.
   b. Note: Make sure to make enough for 4 mL per mold, plus >25% extra because agarose will cool quickly if only small amounts are in the bottle.
2. Pipet 4 mL of molten agarose into an autoclaved PDMS negative well mold. Pipette agarose directly into the posts of the PDMS negatives. Remove any air bubbles with a pipet tip. Do not overfill molds.
3. After the agarose cools (approximately 10 minutes for 4 ml agarose), carefully separate agarose wells from PDMS negatives using a spatula and transfer into a well of a 6-well plate. Do not drop molds directly into the well to preserve sterility.
4. Submerge agarose wells in 10% FBS complete culture medium and equilibrate overnight in a 37 °C incubator prior to use.

Seed the rings:

1. After molds are equilibrated, prepare the cells by following the protocol from Appendix B until step 8c.
2. Resuspend RaSMCs at a concentration of 10 million cells/mL.
3. Aspirate all media from the agarose mold. Be careful to remove all medium from individual wells, but to not puncture the bottoms of the wells.
4. Pipet 50µL of cell suspension into each well.
5. Carefully add 2 mL of fresh medium around the outside of the agarose mold. Be careful not to let medium overflow into the wells of the agarose. Place plates in the incubator overnight.
6. After overnight incubation, aspirate the medium from outside the molds, and add 4.5 mL fresh medium to each well so molds and rings are completely submerged. Change medium daily for the duration of culture.

Appendix H
Protocol for Cell Encapsulation in Alginate Beads

Use aseptic techniques:
1. Determine # of cells (X) that are required to obtain desired cell density. EQN: X cells/mL x 1 mL/30 beads = cell density (cells/bead) .
2. Pellet cells from cell culture.
3. Resuspend cell pellet with desired alginate concentration using an electric pipette.
4. Now follow the 'Formation of Alginate Beads and Alginate-Gelatin Crosslinking' procedure.
5. Incubate cell-beads with ~2mL of media (+ 10% FBS) in 12 well plate.
6. Change media every 2 days.

To remove cells from alginate bead:
1. Aspirate media from well plates.
2. Pipette 2 mL of 100mM EDTA (pH 7.4) to each well for ~25-30 minutes in the incubator.
3. Put total solution volume in a 15mL centrifuge tube.
4. Rinse well plates with 1 mL of PBS.
5. Add in additional PBS (~4mL) to make the solution less viscous.
6. Centrifuge cells and solution at 1000 xg for 8 minutes at a level of 2 increase and 9 decrease.
7. Isolate cells by removing supernatant and blot tubes dry.
8. Resuspend cell pellet with 10uL of PBS.
9. Aliquot into microcentrifuge tubes.

Appendix I
Protocol for Degradation Study of Alginate Beads

Degradation of alginate beads is often measured by recording the diameter over time:

1. Beads should be placed in a 96 well plate with 1 bead per well to be measured effectively.
2. Orient beads with sterilized tweezers or measuring spatulas (sterilize in autoclave pouches).
3. Measure at least 30 beads for diameter and input into excel.
4. Calculate the mean and standard deviation.
5. Ideally the microscope in CERES will be used to improve efficiency of the bead measuring process to image multiple wells at one time
6. Bead diameter will be measured with Zen or ImageJ software.
7. Take measurements at desired intervals.
8. Replace media every 2 days if there are cells embedded.

Appendix J
Protocol for CellTiter Viability Assay

1. Remove the spheroids from the wells following the protocol from Appendix F.
2. Trypsinize the spheroids with 5 mL trypsin. Incubate them for 10 minutes at 37℃.
3. After the 10 minutes, the cells will be trypsinized, but will remain in their spheroid formation. Pipette the cells up and down several times in order to break up the spheroids.
4. Add 5 mL of media to neutralize the tripsin.
5. Perform a cell count.
6. Centrifuge the spheroids.
7. Resuspend the cells at 200,000 cells/mL.
8. Add 100 μL of cell suspension to a 96 well plate. Make sure to make replicates.
9. Allow the 96 well plate to sit in a 37℃ incubator overnight.
10. Thaw the CellTiter 96® AQ$_{ueous}$ One Solution Reagent. It should take approximately 90 minutes at room temperature, or 10 minutes in a water bath at 37°C, to completely thaw the 20 mL size.
11. Pipet 20µl of CellTiter 96® AQ$_{ueous}$ One Solution Reagent into each well of the 96-well assay plate containing the samples in 100µl of culture medium.
12. Incubate the plate at 37°C for 1–4 hours in a humidified, 5% CO_2 atmosphere.
13. Record the absorbance at 490 nm using a 96-well plate reader.

Appendix K
Materials and Protocols for Maintenance and Passaging of Uterine Smooth Muscle Cells
Adopted from the Whittington Lab Protocol for these cells

Materials:
- Supplemented Vascular Basal Media
- 0.25% Trypsin-EDTA
- Trypan Blue and hemocytometer
- 15 mL conical tube
- (micro)Pipettes and their tips
- 100 mm tissue culture dish(es)

Protocol:
Culture Maintenance:
1. Check cells for confluency (they should reach 80% confluence before passaging).
2. Change the media every 48 hrs until they are ready to passage.
   a. Pre-warm media in a 37°C water bath for 15 minutes.
   b. Remove flask from incubator and aspirate spent media.
   c. Add 5mL of fresh media per 25 cm2 of surface area (15 mL for a T75).
   d. Return flask to the incubator.

Passaging:
1. Pre-warm media and Trypsin in a 37°C water bath for 15 minutes.
2. For each flask, aspirate spent media.
3. Add 1-2 mL of Trypsin for every 25 cm2 (4 mL for T75) and gently rock to cover the surface.
4. Let sit for 3-5 minutes and then gently tap the sides to detach the cells.
   a. Check under a microscope to see if cells are fully detached.
5. Add double the volume of media to the flask to neutralize the trypsin.
6. Transfer the cells to a sterile conical tube.
7. Centrifuge the cells at 150 x g for 5 minutes.
8. Aspirate the solution without disturbing the cell pellet.
9. Resuspend in 2-8 mL of fresh media.
10. Count the cells and seed new flasks at 2,500 – 5,000 cells/cm^2 (~200,000 – 400,000 cells for a T75).
11. Move flask to an incubator at 37°C and 5% CO_2.

Appendix L
Materials and Protocols for Gomori's One Step Trichrome Staining
Adopted from the University of Rochester Department of Pathology and Laboratory Medicine

<u>Materials</u>:
- Paraffin sections cut at 5 µm
- Bouin's Solution
  - Picric acid
  - Formalin
  - Acetic acid
- Modified Weigert's Iron Hematoxylin
  - Solution A
    - Hematoxylin crystals
    - 90% ethyl alcohol
  - Solution B
    - Ferric chloride
    - Distilled water
    - Hydrochloric acid
- Trichrome Stain
  - Chromotrope 2R
  - Fast green FCF
  - Acetic acid
  - Phosphotungstic acid
  - Distilled water
- 0.5% Acetic Acid
  - Acetic Acid
  - Distilled water

<u>Protocol</u>:
1. Deparaffinize and hydrate in distilled water.
2. Place in Bouin's solution overnight.
3. Wash in running tap water until the yellow color disappears and then rinse in distilled water.
4. Place in Modified Weigert's Iron Hematoxylin for five minutes.
5. Wash briefly in running water.
6. Place in Trichrome stain for 15-20 minutes.
7. Place in 0.5% Acetic Acid for five minutes.
8. Dehydrate sections.
9. Mount with synthetic resin.

Appendix M

Calculations and Protocol Used to Determine the Amount of each Macromolecular Crowder
to be added to Supplemented Vascular Basal Media
Adopted from the Whittington Lab Protocol

Materials:
- L-Ascorbic Acid
- Ficoll 70
- Ficoll 400

- DI Water
- Sterile Filter
- Supplemented Vascular Basal Media

Protocol:

Cells:
- Viewed under microscope to establish reference point for later experimentation.
- Kept in a sterile incubator.

Preparing reagents:

Ascorbic Acid:
1. Weigh 35 mg (0.0352 g) of L-Ascorbic Acid.
2. Dissolve into 20 mL of deionized and filtered H_2O.
3. Sterile filter.

Ficoll 70:
1. Weigh 0.8 g of Ficoll 70.
2. Dissolve into 8 mL of cell culture medium.
3. Sterile filter.

Ficoll 400:
1. Weigh 0.6 g of Ficoll 400.
2. Dissolve into 6 mL of cell culture medium.
3. Sterile filter.

Combining reagents:

Ascorbic Acid and VGM:
1. Add 200 µL of the Ascorbic Acid dilution to 19.8 mol of media in a 50 mL tube.
   a. Use serological pipettes in a Biosafety Level 2 Cabinet.

Ascorbic Acid, Ficolls and VGM
1. Add 7.5 mL of the Ficoll 70 dilution, 5 mL of Ficoll 400 dilution and 200 µL of the Ascorbic Acid dilution to 7.3 mL of cell culture medium.
   a. Use serological pipettes in a Biosafety Level 2 Cabinet.

Calculations:

Calculations

For L-ascorbic acid → need 20 mL of media

$$20 \; mL \; * \; \frac{1 \, L}{1000 \; mL} \; * \; \frac{.0001 \; mol}{L} \; = \; 2 \; * \; 10^{-6} \; mol$$

$$2 \; * \; 10^{-6} \; mol \; * \; \frac{176.12 \; g}{1 \; mol} \; =. \, 00035 \; g \; of \; Ascorbic \; Acid \; for \; 100 \; \mu M$$

$$10 \; mM \; (V_1) \; = \; 100 \; \mu M \; * \; 20 mL$$

$$V_1 \; = \; 200 \; \mu L \; = \; .2 \; mL$$

For Ficoll 70 → 70 g/mol and 37.5 mg/mL

$$100 \; mg/mL \; * \; V_1 \; = \; 37.5 \; mg/mL \; * \; 20 \; mL$$

$$V_1 \; = \; 7.5 \; mL$$

If using 20 mL media, use 2 g of Ficoll 70 when preparing reagent

For Ficoll 400 → 400 g/mol and 25 mg/mL

$$100 \; mg/mL \; * \; V_1 \; = \; 25 \; mg/mL \; * \; 20 \; mL$$

$$V_1 \; = \; 5 \; mL$$

If using 20 mL media, use 2 g of Ficoll 400 when preparing reagent